

Old Dominion University

ODU Digital Commons

Mechanical & Aerospace Engineering Theses & Dissertations

Mechanical & Aerospace Engineering

Spring 2024

Effect of Lunar Magnetic Field and Lunar Regolith Simulant on the Growth and Bioactive Compounds Production of *Chlorella Vulgaris* Microalgae

Jeries Philip Butros Abedrabbo
Old Dominion University, jeriesabedrabbo955@msn.com

Follow this and additional works at: https://digitalcommons.odu.edu/mae_etds



Part of the [Aerospace Engineering Commons](#), [Biology Commons](#), and the [Microbiology Commons](#)

Recommended Citation

Abedrabbo, Jeries P. "Effect of Lunar Magnetic Field and Lunar Regolith Simulant on the Growth and Bioactive Compounds Production of *Chlorella Vulgaris* Microalgae" (2024). Master of Science (MS), Thesis, Mechanical & Aerospace Engineering, Old Dominion University, DOI: 10.25777/m4xy-zw97 https://digitalcommons.odu.edu/mae_etds/378

This Thesis is brought to you for free and open access by the Mechanical & Aerospace Engineering at ODU Digital Commons. It has been accepted for inclusion in Mechanical & Aerospace Engineering Theses & Dissertations by an authorized administrator of ODU Digital Commons. For more information, please contact digitalcommons@odu.edu.

EFFECT OF LUNAR MAGNETIC FIELD AND LUNAR REGOLITH SIMULANT ON THE GROWTH
AND BIOACTIVE COMPOUNDS PRODUCTION OF *CHLORELLA VULGARIS* MICROALGAE

by

Jeries Philip Butros Abedrabbo
B.Sc. June 2017, Birzeit University, Palestine

Thesis Submitted to the Faculty of
Old Dominion University in Partial Fulfillment of the
Requirements for the Degree of

MASTER OF SCIENCE

AEROSPACE ENGINEERING

OLD DOMINION UNIVERSITY
May 2024

Approved by:

Sharana Basaweshwara Asundi (Director)

Drew Landman (Member)

Sandeep Kumar (Member)

ABSTRACT

EFFECT OF LUNAR MAGNETIC FIELD AND LUNAR REGOLITH SIMULANT ON THE GROWTH AND BIOACTIVE COMPOUNDS PRODUCTION OF *CHLORELLA VULGARIS* MICROALGAE

Jeries Philip Butros Abedrabbo
Old Dominion University, 2024
Director: Dr. Sharana Asundi

Since humans last went to the moon on the Apollo missions, there has been a fascination with inhabiting and colonizing other planetary objects, starting with the Earth's Moon, Mars, and recently Jupiter's moon, Europa. However, there is still lack of knowledge and science behind many of the extraterrestrial environmental effects on biological organisms living on Earth. Therefore, there is a need to study how such environments would affect these organisms. Moreover, how can we attain sustainable living in such environments as well through self-providing life support systems (LSS), without the need to provide for additional necessities back and forth from and to earth? Among the many biological organisms that offer such sustainable capabilities is the *Chlorella vulgaris* microalgae. In this research work, we focus on investigating the combined effects of a simulated Lunar magnetic field and simulated Lunar regolith embedded nutrition medium on the growth and bioactive compounds of the *Chlorella Vulgaris* microalgae. To achieve this, a tri-dimensional magnetic field of $0.02\mu\text{T}$ was produced using a Helmholtz cage. Three different sets of four exposures, each set mixed in a different nutrition medium, were exposed in the produced field. Exposures are characterized by time and the nutrition medium they are cultured in, with an exposure time of 0 minutes for control, then 60 minutes, 120 minutes, and 240 minutes for the most prolonged exposure, for the three mediums of BBM, BBM

+ 100 grams of Lunar regolith, and MilliQ Water + 100 grams of Lunar regolith. Experimental work was done in two blocks to follow a Design of Experiments (DOE) statistical approach. Each block was 21 days. Samples within a block were exposed for 6 days and were analyzed every 3rd and 4th day for their carotenoids and bioactive compounds. Their growth rate was checked periodically. Mixed responses of enhancement and stressing effects were noticed in the results of all samples. Most notable were trends of fluctuating peaks and troughs usually central to specific days. No markers were found to correlate specific exposure time values to specific responses. The same goes for nutrition mediums. MilliQ water + lunar regolith-based nutrition medium was found to be least nurturing of growth, generating of carotenoids, and bioactive compounds. Peculiarly some EMF exposures tended to enhance these responses within the same MilliQ medium. ANOVA carried out on both blocks provided identifiers for complex interactions between EMF exposure times and the different nutrition mediums.

©Copyright, 2024, by Jeries Philip Butros Abedrabbo. All Rights Reserved.

First and foremost, I dedicate this work to my beautiful country Palestine, and its beautiful people. Furthermore, I dedicate this work to: my parents Carol and Philip, who were always there throughout my educational journey and life; my sister Clara, my other half and soul twin, my partner in everything, and my refuge; my brother-in-law Jacob, who always saw the best in me and gave me much of his wisdom; and my nephew George, my favorite person, the little guy that made me an uncle for the first time, a brilliant, curious little mind with a wonderful personality.

To them all I dedicate my work, and to my little George, I would say "I love you Khalo."

ACKNOWLEDGMENTS

First of all, I would like to thank my advisor for my master's degree, Dr. Sharan Asundi. His help, guidance, suggestions, and the many, many conversations were invaluable. Moreover, his efforts in keeping me involved with interesting research were very much appreciated.

Additionally, I would like to thank Dr. Sandeep Kumar for allowing us to work in his Environmental Engineering Lab at Kaufman Hall and use all its facilities without any hesitation. Without all the equipment, chemicals, and commodities, this research would not have been possible. A thank you to Dr. Venkat Maurthamathu for allowing us to use his lab as well.

I would also like to thank Dr. Drew Landman, who I consider my mentor. His work in providing the experimental design for this experiment, and his insightful and invaluable suggestions on the analysis of data were crucial for producing this work.

A tremendous amount of appreciation and thanks to the Fulbright Program, and the US Department of State. I wouldn't be here without them; thank you so much for this opportunity!

A huge thank you to Ujjwal Pokharel for facilitating and accommodating our needs in the lab and guiding us throughout lab procedures. Same goes to McKenzie, Lauren, Angela, and Branson for their help in doing experimental work. You were an amazing team.

Most importantly, and to which I fathom my sincerest, dearest, and utmost words of appreciation are my parents Carol and Philip, my sister Clara, her husband Jacob, and the loveliest nephew of all, George, El batal! I would not have been who I am, and where I am without your love, direction, wisdom, advice, appreciation, discipline, motivation, hard work, and undoubtedly many immense sacrifices. I love you and thank you for everything.

NOMENCLATURE

Oe	Oersted (Unit of Magnetic Field Strength)
uT	Micro Tesla (Unit of Magnetic Flux Density)
G	Gauss (Unit of Magnetic Flux Density)
O.D	Optical Density
OD	Optical Density
DC	Direct Current
EMF	Electromagnetic Field
HHC	Helmholtz Cage
A_λ	Absorbance at Wavelength lambda (λ)
T_λ	Transmittance at Wavelength lambda (λ)
λ	Wavelength of light

TABLE OF CONTENTS

	Page
LIST OF TABLES.....	ix
LIST OF FIGURES.....	xiii
Chapter	
I. INTRODUCTION AND METHODS.....	1
ALGAE CULTURE CULTIVATION.....	2
THE <i>CHLORELLA VULGARIS</i> MICROALGAE.....	4
II. ALGAE, PLANTS, AND SPACE ENVIRONMENT RESEARCH.....	15
MAGNETIC FIELDS EFFECT.....	15
EXTRATERRESTRIAL REGOLITH.....	18
III. EXPERIMENTAL PROCEDURE AND DESIGN.....	23
DESCRIPTION OF THE EXPERIMENT AND MOTIVATION.....	23
STATISTICAL DESIGN OF THE EXPERIMENT.....	24
CULTIVATION OF <i>CHLORELLA VULGARIS</i>	27
MIXING AND OPTICAL DENSITY MEASUREMENT.....	37
OPTICAL DENSITY MEASUREMENT.....	42
HELMHOLTZ CAGE OPERATION AND MAGNETIC FIELD EXPOSURE.....	45
CAROTENOID (BETA CAROTENE) EXTRACTION.....	59
PROTEIN EXTRACTION.....	64
IV. RESULTS AND DISCUSSION.....	68
EXPERIMENTAL BLOCK 1.....	68
EXPERIMENTAL BLOCK 2.....	93
BLOCKING AND STATISTICAL ANALYSIS.....	109
V. CONCLUSIONS AND FUTURE WORK.....	136
VI. REFERENCES.....	139
VII. VITA.....	145

LIST OF TABLES

Table	Page
1. Biochemical composition of <i>C. vulgaris</i> [29].	8
2. Statistical Design Factors showing their values, categories, and levels.	25
3. Randomized block runs design.	26
4. List of chemical elements utilized in nutrients by <i>Chlorella v.</i>	28
5. Composition of BBM (Bold's Basal Medium) [50], [51].	29
6. Medium volume to regolith ratio respective to each set of treatments.	38
7. Ratios of medium to regolith per exposure.	38
8. Technical Specifications of 1500 Square HHC Helmholtz coil cage [63].	46
9. Beta-Carotene standard Dilutions Chart.	62
10. BSA Protein standard Dilutions Chart.	67
11. Optical Density Measurements for <i>Chlorella V.</i> growth in BBM only.	69
12. Optical Density Measurements for <i>Chlorella V.</i> growth in BBM + 100g lunar regolith.	69
13. Optical Density Measurements for <i>Chlorella V.</i> growth in MilliQ + 100g lunar regolith.	69
14. Trendlines produced for the two parts before and after abrupt change points for each exposure.	76
15. Overall trendlines produced for the whole curve for each exposure.	76
16. Extracted Beta-Carotene Optical Density Measurements for <i>Chlorella V.</i> growth in BBM only (Blanked with Hexane).	77

17. Extracted Beta-Carotene Optical Density Measurements for <i>Chlorella V.</i> growth in BBM +100g lunar regolith (Blanked with Hexane).	77
18. Extracted Beta-Carotene Optical Density Measurements for <i>Chlorella V.</i> growth in MilliQ +100g lunar regolith (Blanked with Hexane).	78
19. Average OD for Beta-Carotene Concentrations in BBM Nutrition Medium.	81
20. Extracted Protein Optical Density Measurements for <i>Chlorella V.</i> growth in BBM only (Blanked with NaOH).....	85
21. Extracted Protein Optical Density Measurements for <i>Chlorella V.</i> growth in BBM + 100g lunar regolith (Blanked with NaOH).	86
22. Extracted Protein Optical Density Measurements for <i>Chlorella V.</i> growth in MilliQ + 100g lunar regolith (Blanked with NaOH).....	86
23. Extracted Protein Concentration Measurements for <i>Chlorella V.</i> growth in BBM only (Blanked with NaOH).....	86
24. Extracted Protein Concentration Measurements for <i>Chlorella V.</i> growth in BBM + 100g lunar regolith (Blanked with NaOH).	87
25. Extracted Protein Concentration Measurements for <i>Chlorella V.</i> growth in MilliQ + 100g lunar regolith (Blanked with NaOH).....	87
26. Averaged values for protein concentrations over the timeline of the experiment for each exposure.....	93
27. Optical Density Measurements for <i>Chlorella V.</i> growth in BBM only (Block 2).	93
28. Optical Density Measurements for <i>Chlorella V.</i> growth in BBM + 100g lunar regolith (Block 2).	94

29. Optical Density Measurements for <i>Chlorella V.</i> growth in MilliQ + 100g lunar regolith (Block 2).	94
30. Extracted Beta-Carotene Optical Density Measurements for <i>Chlorella V.</i> growth in BBM only (Block 2 - Blanked with Hexane).	97
31. Extracted Beta-Carotene Optical Density Measurements for <i>Chlorella V.</i> growth in BBM + 100g lunar regolith (Block 2 - Blanked with Hexane).....	98
32. Extracted Beta-Carotene Optical Density Measurements for <i>Chlorella V.</i> growth in MilliQ + 100g lunar regolith (Block 2 - Blanked with Hexane).....	98
33. Extracted Protein Optical Density Measurements for <i>Chlorella V.</i> growth in BBM only (Blanked with NaOH).....	102
34. Extracted Protein Optical Density Measurements for <i>Chlorella V.</i> growth in BBM + 100g lunar regolith (Blanked with NaOH).	103
35. Extracted Protein Optical Density Measurements for <i>Chlorella V.</i> growth in MilliQ + 100g lunar regolith (Blanked with NaOH).....	103
36. Extracted Protein Concentration Measurements for <i>Chlorella V.</i> growth in BBM only (Blanked with NaOH - Block 2).	103
37. Extracted Protein Concentration Measurements for <i>Chlorella V.</i> growth in BBM + 100g lunar regolith (Blanked with NaOH - Block 2).	104
38. Extracted Protein Concentration Measurements for <i>Chlorella V.</i> growth in MilliQ + 100g lunar regolith (Blanked with NaOH - Block 2).	104
39. ANOVA for Protein Concentration on Day 3.	110
40. ANOVA for Protein Concentration on Day 7.	111

41. ANOVA for Protein Concentration on Day 10.	112
42. ANOVA for Protein Concentration on Day 14.	113
43. ANOVA for Protein Concentration on Day 17.	114
44. ANOVA for Beta-Carotene Concentration on Day 3.....	118
45. ANOVA for Beta-Carotene Concentration on Day 7.....	119
46. ANOVA for Beta-Carotene Concentration on Day 10.....	120
47. ANOVA for Beta-Carotene Concentration on Day 14.....	121
48. ANOVA for Beta-Carotene Concentration on Day 17.....	122
49. ANOVA for Beta-Carotene Concentration on Day 21.....	123
50. ANOVA for Beta-Carotene Concentration in Global Model.	126
51. Fit Summary Statistics of Global Beta-Carotene Concentration Model.....	126
52. ANOVA for Protein Concentration in Global Model.....	131
53. Fit Summary Statistics of Global Protein Concentration Model.	131

LIST OF FIGURES

Figure	Page
1. Ultrastructure of a <i>C. vulgaris</i> cell showing different organelles [8].....	7
2. Summary of operation of light reactions and dark reactions and their relationship [32].....	12
3. Summary of the light reactions within photosynthesis. PSII extracts electrons and evolves Oxygen, it further pushes the electrons towards PSI, which produces NADPH from NADP. ATP Synthase is triggered after a pH difference occurs.	13
4. The Calvin-Benson Cycle, photosynthetic carbon fixation pathways [32].....	14
5. Yamato SM300 Autoclave.	31
6. <i>Chlorella vulgaris</i> beakers in the cultivation chamber.	34
7. Flowchart of the microalgae and nutrition medium mixing process.....	41
8. Optical System Schematic [60].....	44
9. Dispersing a uL volume sample using a pipette [61].	44
10. Upper and lower cylinders of the sampling compartment shutting, forming a sampling column [62].	45
11. Sampling compartment with formed sampling column [62].....	45
12. 1500 Square HHC Helmholtz cage used for exposing microalgae to a magnetic field.	47
13. Microalgae samples (Nine Samples) placed in cardboard box inside the Helmholtz Cage.	49
14. Sliding carriages for X and Y directions showing slider ruler for centering Y-Direction.....	50
15. Z-Encoder motor connected to worm gear.....	51
16. Lower part of worm gear connected to Z-direction carriage.....	52

17. Vertical Motor Switch Inside Power Supply Cabinet [63].	53
18. Linear motion motor control parameters section in LabView application.	53
19. Toggle button for measuring earth's field before running application [63].	54
20. Sleeving of magnetometer using zero-gauss chamber to measure ambient field [63].	55
21. Magnetic Field Strength Input Panel with toggle for cancelling earth field [63].	55
22. Button to stop DC controller while keeping DC field turned on [63].	55
23. Rotary motor control parameters configuration LabView interface [63].	58
24. Tubes showing a yellow layer of extracted Beta-Carotene from samples.	61
25. Samples containing dilutions of Beta-Carotene standard.	63
26. Resulting protein samples after adding Bradford reagent.	66
27. Measured Optical Density timeline for <i>Chlorella V.</i> exposures growth in BBM (Block 1).	70
28. Measured Optical Density timeline for <i>Chlorella V.</i> exposures growth in BBM + 100g lunar regolith (Block 1).	72
29. Measured Optical Density timeline for <i>Chlorella V.</i> exposures growth in MilliQ + 100g lunar regolith (Block 1).	74
30. Measured Optical Density timeline for extracted Beta-carotene from exposures in BBM (Block 1).	78
31. Measured Optical Density timeline for extracted Beta-carotene from exposures in BBM + 100g lunar regolith (Block 1).	79
32. Measured Optical Density timeline for extracted Beta-carotene from exposures in MilliQ + 100g lunar regolith (Block 1).	79
33. Measured Optical Density timeline for extracted Protein from exposures in BBM (Block 1).	88

34. Measured Optical Density timeline for extracted Protein from exposures in BBM + 100g lunar regolith (Block 1).....	88
35. Measured Optical Density timeline for extracted Protein from exposures in MilliQ + 100g lunar regolith (Block 1).....	89
36. Timeline of extracted protein concentration in mg/ml for BBM only exposures (Block 1)....	89
37. Timeline of extracted protein concentration in mg/ml for BBM + 100g lunar regolith exposures (Block 1).	90
38. Timeline of extracted protein concentration in mg/ml for MilliQ + 100g lunar regolith exposures (Block 1).	92
39. Measured Optical Density timeline for <i>Chlorella V.</i> exposures growth in BBM (Block 2).	94
40. Measured Optical Density timeline for <i>Chlorella V.</i> exposures growth in BBM + 100g lunar regolith (Block 2).....	95
41. Measured Optical Density timeline for <i>Chlorella V.</i> exposures growth in MilliQ + 100g lunar regolith (Block 2).	96
42. Measured Optical Density timeline for extracted Beta-carotene from exposures in BBM (Block 2).	99
43. Measured Optical Density timeline for extracted Beta-carotene from exposures in BBM + 100g lunar regolith (Block 2).....	100
44. Measured Optical Density timeline for extracted Beta-carotene from exposures in MilliQ + 100g lunar regolith (Block 2).....	101
45. Measured Optical Density timeline for extracted Protein from exposures in BBM (Block 2).	105

46. Measured Optical Density timeline for extracted Protein from exposures in BBM + 100g lunar regolith (Block 2).....	105
47. Measured Optical Density timeline for extracted Protein from exposures in MilliQ + 100g lunar regolith (Block 2).....	106
48. Timeline of extracted protein concentration in mg/ml for BBM only exposures (Block 2)..	106
49. Timeline of extracted protein concentration in mg/ml for BBM + 100g lunar regolith exposures (Block 2).	107
50. Timeline of extracted protein concentration in mg/ml for MilliQ + 100g lunar regolith exposures (Block 2).	108
51. Interactions between factors for protein concentration analysis on Day 3.....	111
52. Interactions between factors for protein concentration analysis on Day 7.....	112
53. Interactions between factors for protein concentration analysis on Day 10.....	113
54. Interactions between factors for protein concentration analysis on Day 14.....	114
55. Interactions between factors for protein concentration analysis on Day 17.....	115
56. Interactions between factors for Beta-Carotene concentration analysis on Day 3.....	118
57. Interactions between factors for Beta-Carotene concentration analysis on Day 7.....	119
58. Interactions between factors for Beta-Carotene concentration analysis on Day 10.....	120
59. Interactions between factors for Beta-Carotene concentration analysis on Day 14.....	121
60. Interactions between factors for Beta-Carotene concentration analysis on Day 17.....	122
61. Interactions between factors for Beta-Carotene concentration analysis on Day 21.....	123
62. Global Model Response Surface for Beta-Carotene Concentration in BBM Medium.	127

63. Global Model Response Surface for Beta-Carotene Concentration in BBM + 100g Medium.
..... 128

64. Global Model Response Surface for Beta-Carotene Concentration in MilliQ + 100g Medium.
..... 129

65. Global Model Response Surface for Protein Concentration in BBM Medium..... 132

66. Global Model Response Surface for Protein Concentration in BBM + 100g Medium..... 133

67. Global Model Response Surface for Protein Concentration in MilliQ + 100g Medium..... 134

CHAPTER I

INTRODUCTION AND METHODS

As humans are intending to reach further in space, they are affected by multiple factors such as radiation, extreme temperature gradients, and sustainable resources. While science has provided many advancements in preventing radiation and handling extreme temperatures, the matter of sustainability remains an open question, and a barely answered one.

The Artemis mission [1] is one of the nearest future missions to go to the Moon. As humans, we intend to colonize the Moon and make it a habitable place. However, lacking the tools to build a sustainable life makes it very difficult, as it is very costly to keep on transporting resources whenever needed. For example, carrying a ton of water from the Earth to the Moon would cost millions if not billions of dollars in building rockets and sustaining rocket fuel to do so.

Biological organisms could provide the required mechanisms to produce or extract elements in space that might be expensive to bring otherwise. One group of such biological organisms are microalgae, which could be critical for a sustainable future in space, as they produce protein, vitamins, needed nutritional pigments, and edible biomass. Now, despite the existence of many species of microalgae, *Chlorella vulgaris* could be an ideal candidate due to its unicellular construction and known health benefits.

In this thesis work, experimental research is performed to study the effects of the lunar magnetic field and lunar regolith on the growth and bioactive compounds production of the *Chlorella v.* microalgae. It begins by providing an introduction on the biology of *Chlorella v.*, then it moves to review existing literature about magnetic field effects and space effects on microalgae

in general and *Chlorella v.* specifically. The experimental design, its approach and motivation behind selecting the design, and its details are discussed. Subsequently, the procedure performed in the lab for sample preparation, introducing the lunar effects, extracting bioactive compounds, and measuring growth and compounds concentrations is described in detail provided with any needed steps and figures to clarify instructions. Results are then stated and discussed providing noticed trends and raising possible hypothesis. Finally, a short conclusion is provided summarizing the perceived outcomes and suggesting potential directions for future work.

ALGAE CULTURE CULTIVATION

Microalgae classification and species

While the science of biology studies different species discovered, and tries to understand their internal operations, it also manages to try and implicitly classify organisms based on similarity. In a general sense, when we talk about an animal, plant, or any other organism, including microorganisms, we tend to try and provide an organization for these organisms. A reason for that could stem from our self-tendency to cast ourselves as humans under hierarchies [2], [3, p. 3]. Furthermore, classification of organisms tends to provide an easier way to navigate species based on similarity in the internal and external ongoing biological processes, construction, intakes, and excess outputs. Nonetheless, some organisms tend to not fall under a single classification, as observations concluded them of improper nature to be classified under the plant or animal kingdom. Based off this inability, the new kingdom of Protista was formed. This kingdom represents organisms that are unrelated and of harder potential for classification [4]. As microalgae is our main concern, we focus on listing its main classes, and we aim to list some of the common species falling under each list. However, for simplicity and reduced technical

biological jargon, it is important to mention that the decision of scientists to classify microalgae was alternating and still is, as it considered some types of algae to fall under Protista, while others such as green, red, and macroscopic green algae were still to be classified under the plantae kingdom. Eventually, the classification of algae into a single kingdom has not been satisfactory, yet [3, p. 3].

Microalgae comprise a large diversity of species. They are found in many different kinds of environments. In a most general manner, microalgae can be classified into different categories of phytas as follows: Chlorophyta, Rhodophyta, Haptophyta, and Stramenopiles [3], [5], [6]. Each has subclassifications. Many distinct types of microalgae are put under one of these groupings. One general grouping of microalgae is based on pigment composition. Such grouping categorizes algae into nine different classes as follows: Chlorophyceae (green algae), which is the largest group, Phaeophyceae (brown algae), Pyrrophyceae (dinoflagellates), Chrysophyceae (golden brown algae), Bacillariophyceae (diatoms), and Rhodophyceae (red algae) [5]. These classifications fall under the main Phytas yet contain other subgroups. Despite the presence of many species of microalgae, however, some are more common, due to abundance, and due to applications and generated products. Of the most common species useful for commercial applications are *Spirulina*, *Chlorella*, *Haematococcus*, *Dunaliella*, *Botryococcus*, *Phaeodactylum*, *Porphyridium*, *Chaetoceros*, *Cryptocodinium*, *Isochrysis*, *Nannochloris*, *Nitzschia*, *Schizochytrium*, *Tetraselmis*, and *Skeletonema* [5].

THE *CHLORELLA VULGARIS* MICROALGAE

Chlorella Vulgaris, a microalga with a well-defined nucleus was first discovered in 1890 by the Dutch researcher Martinus Willem Beijerinck [7]. Its name originates in a mix of both Greek and Latin languages, where the first part of *Chlorella* refers to the Greek word chloros, meaning green, and the suffix 'ella', is a Latin word referring to its macroscopic size [8]. This microalga is unicellular and has preserved its genetic integrity since its estimated presence in the pre-Cambrian period. Moreover, it can grow in multiple habitats of salt water, forests, freshwater, and different marine and terrestrial environments. Its photosynthetic ability is high, additionally, it is easy to grow, and has rapid growth capability in a variety of mediums under autotrophic, mixotrophic, and heterotrophic conditions and in photobioreactors [6], [8], [9], [10].

Chlorella Vulgaris and Space Environment

Space flight and exploration has been an endeavor pursued daily. Therefore, more missions are being planned to understand more about the scientific nature of the universe, and to further push for our aim in colonizing other planets. Nonetheless, as technology is on a pedestal of advancement, missions are now becoming more sophisticated, and are reaching further into space. One aspect of such missions is the increased distance and duration away from Earth, thus requirements of life support systems become elevated. Life support systems (LSS) are present to provide a habitable environment for humans, by providing oxygen, drinking water, and other bodily needs. A current example of such technology is present on the International Space Station (ISS). However, as efficient as one can hope this system to be, it can still only recycle 90% of water, and reclaim 42% of the O₂ present in the CO₂ exhaled by astronauts aboard the station [11]. Such technologies are based on a combination of physical and chemical reactions to process

and recycle waste on board missions. Additionally, current technologies are limited to recycling human, and other waste only. The outlook is to consider food production to accompany the previous activities within the floating space habitat. Microalgae, with its varieties, and more specifically, *Chlorella Vulgaris*, seem to provide a refreshing potential towards augmenting a better LSS.

The earliest research on *Chlorella* strains goes back to the 1960s, in which a variety of strains were launched aboard the Vostro 5 and 6 missions by Russian scientists. Macro and microcolony analysis methods were conducted post flight, to reveal that both control strains and those in flight had no dissimilarity in survival or mutation frequency [12], [13]. In the years 1968 and 1969, the Zond 5-8 missions took *Chlorella V.* cells with them [14], [15]. The cells were on agar and were flown for six or seven days, in darkness. The Zond missions exposed the algae to a unique environment, as their trajectory around the moon subjected the algae to deep-space radiation. Furthermore, with the mission going beyond the radiation protecting Van Allen belts, the algae were also exposed to trapped radiation in the Van Allen belts. Nonetheless, no statistically significant differences were found between ground and flight cultures in the post-flight analysis. Survival and mutability trends were contradictory in the different mission experiments. Similar other trends were found in later missions studied by the same group [14], [15], [16], [17]. An experiment done in 1970 on the Soyuz 9 mission found only one difference in productivity and sporulation; it was seen that these were slightly decreased in flight. This is attributed to the space environment causing the death of cells. This result was deduced after attempting to grow multiple *Chlorella* cultures for 1, 6, and 14 days, in addition to a four day cultivation period post flight [18]. Other experiments and studies were conducted on the *Chlorella*

genus in general, and on *Chlorella Vulgaris* specifically. However, some of these experiments never had any published results, and the remaining experiments reached a similar conclusion of no difference between control and flight cultures [12]. Moskvitin et al. explored the potential effects of dynamic factors of space flight on this strain of algae. In the article, the author studied the effects of vibrations, and irradiance on microalgae; two effects present in space flight conditions. From the results, it is concluded that vibrational tests did not incur any statistically significant difference between experiment and control cultures. Nevertheless, an experiment exposing the algae to pre- and post-vibrational γ radiation, showed a weak tendency towards mutability of the cells [19]. In recent years, some more work has been done relating *Chlorella Vulgaris* to space. Mostly, the focus is on making useful applications of the algae in space environments through photobioreactors. A German experiment employed such application of a photobioreactor on board the ISS. The aim was to demonstrate functionalities of carbon dioxide absorption and evolving of oxygen [20]. Lots of other reports and research efforts were conducted on *Chlorella Vulgaris*, and *Chlorella* strains. This shows the potential expected from this microalga. Moreover, microalgae in general were, and are still actively researched for space applications due to the facilitation of photobiosynthesis. Additionally, algae were found to have the exact needed rate of CO₂ to O₂ conversion required to support humans in space environments [21]. All these factors contributed to considering microalgae as the missing piece of biological support systems for space environments.

Morphology of *Chlorella Vulgaris*

In terms of construction, *Chlorella Vulgaris* is a microscopic cell with a spherical shape. The diameter of the cells range from 2 to 10 micrometers [22], [23], [24]. It carries lots of similarities to plants in terms of structural elements [8].

Mainly, this microalga is composed of the following general elements:

1. Cell Wall
2. Cytoplasm
3. Mitochondrion
4. Chloroplast

Figure 1 displays the ultrastructure of the *Chlorella Vulgaris* microalgae.

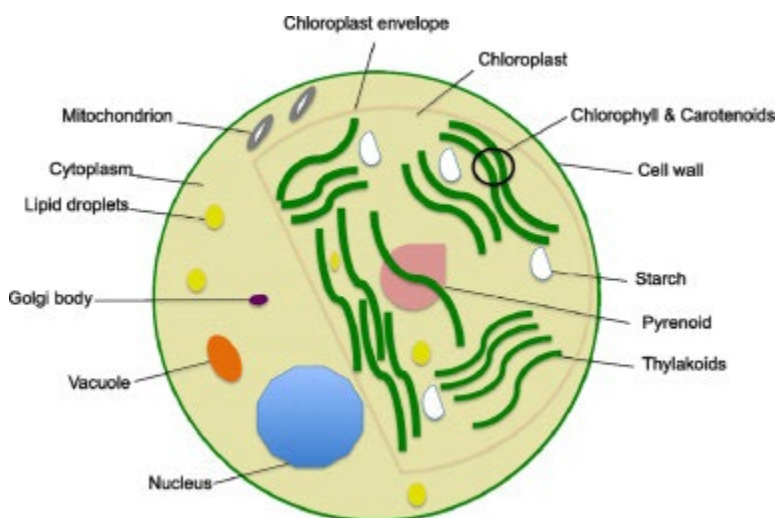


Figure 1. Ultrastructure of a *C. vulgaris* cell showing different organelles [8].

Biochemical components

In addition to the generic elements of the *C. vulgaris* cell, this microalga is made up of many biochemical components that represent elements needed for the operation of the cell, in addition to outcomes resulting from the biological processes happening inside the cell. *C. vulgaris* has a biochemical makeup of proteins, lipids, carbohydrates, pigments, minerals, and vitamins. According to Maruyama et al. a more detailed composition of the biochemical components can be found in Table 1.

Table 1. Biochemical composition of *C. vulgaris* [25].

Overall Composition (% dry matter)	Value
Protein	55.0
Lipid	10.2
Ash	5.8
Carbohydrate	23.2
Fiber	5.8
Amino Acids (% total amino acids)	Value
Isoleucine	4.44
Leucine	9.38
Methionine	1.24
Phenylalanine	5.51
Tyrosine	3.14
Threonine	5.15
Valine	6.61
Lysine	6.68
Arginine	6.22
Histidine	1.97
Alanine	8.33
Aspartic acid	9.80
Glutamic Acid	12.66
Glycine	6.07
Proline	4.90
Serine	4.32
Cystine	1.28
Tryptophan	2.30

Fatty acids (% total fatty acids)	Value
Palmitic acid	13.9
Palmitoleic acid	5.7
Stearic acid	3.1
Oleic acid	2.2
Linolenic acid	25.3
Linolenic acid	24.2
Arachidonic acid	0
Eicosapentaenoic acid	0
Docosahexaenoic acid	0
Minerals (mg g⁻¹ dry matter)	Value
Ca	1.6
Mg	3.6
K	11.3
Fe	2.0
Vitamins (μg g⁻¹ dry matter)	Value
Vitamin B ₁	24
Vitamin B ₂	60
Vitamin B ₆	10
Vitamin B ₁₂	0.001 (2-6) ²
Vitamin C	1000
Vitamin E	200

Growth and nutrients utilization of *Chlorella v.*

Based on research, the growth of *chlorella vulgaris* has been found to be possible in multiple ways. This microalga can be grown using autotrophic, heterotrophic, and mixotrophic techniques. For autotrophic growth, microalgae are grown by providing nutrients and light stimulus to initiate photosynthesis. The technique can be further subdivided into two methods: open pond systems, and closed photo-bioreactors. For the former, *C. vulgaris* is generally grown in open ponds that interact with the environment. This method offers the following benefits as declared by Safi et al. and Masojidek et al. [8], [26]:

- Cheap, as it can utilize any open natural water systems (Lakes, Lagoons, Ponds), wastewater systems, or artificial ponds.
- Offers the capability of large-scale biomass production.
- Easy exposure to sunlight due to their open nature
- Absorbance of Nitrogen from the atmosphere

Nonetheless, open pond systems force limits on culture depth $\sim(10-50\text{cm})$, as deeper ponds could result in an inadequate exposure of the cells to sunlight and a low volumetric density of the culture. Moreover, such systems present difficulty in controlling pollution, water, evaporation, contamination, bacteria, and the growth of different algae species within the same system. They also require constant stirring to verify that all cells are getting enough sunlight exposure.

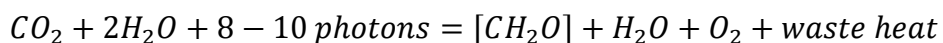
For closed photo-bioreactor systems, the aim is to provide a well-controlled environment. This would result in higher cell concentrations. In closed systems, gas tubes are fed inside closed vessels containing biomass. These bubble inside the vessels to deliver CO_2 . Additionally, artificial lights are used around the vessels to provide enough light absorption within the biomass [8], [26]. However, despite the dual approach possibility for autotrophic growth, the main aim is to utilize the photosynthesis cycle within the microalgae and to utilize the nutrients within the culture medium.

Photosynthesis

The process of photosynthesis is a process that all species on earth are directly or indirectly dependent on [26], and microalgae is no exception. Nonetheless, this process is

dependent on certain biochemical molecules present within the microalgae to carry out the process. Such molecules are made up of certain elements, usually provided through nutrition mediums. Microalgae depends on multiple nutrients such as (N, C, P, S, K, Fe, etc.) as nutrient elements to carry out its growth process and synthesize its biomass compounds. Furthermore, these elements need to be present in specific quantities to render the microalgae capable of biomass production [27].

Photosynthesis, also known as Oxygenic Photosynthesis, is based on the following equation:



This mechanism is driven by light energy and can be expressed as a redox reaction. Within this mechanism, chlorophyll pigment molecules harvest light energy, for which the mechanism would then utilize this energy to convert carbon dioxide and water into carbohydrates and oxygen. Our focus of study (*Chlorella Vulgaris*) falls under the Chlorophyta division of light harvesting pigments. Within these cells, the chloroplasts house the photosynthetic apparatus needed to carry out the process [28].

Hence the name, the light reactions convert light energy to chemical energy. This conversion results in $NADPH_2$ and ATP. A biochemical reductant, and a high energy compound, respectively, made up of needed nutrients mentioned earlier. Subsequently, the resulting $NADPH_2$ and ATP are utilized to reduce carbon dioxide to carbohydrates. This is done in a sequential biochemical reduction [28]. Figure 2 summarizes the relationship between light and dark reactions.

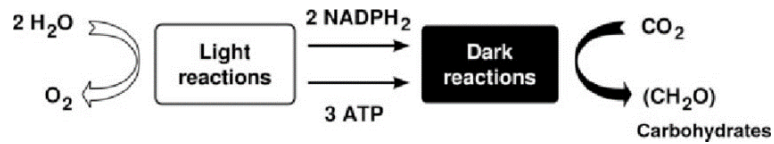
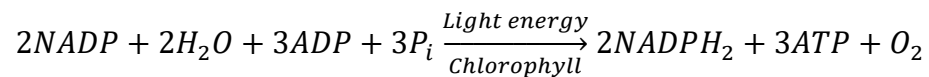


Figure 2. Summary of operation of light reactions and dark reactions and their relationship [28].

The thylakoid of the chloroplast is the location of the light reactions. Five major complexes are housed within the thylakoid membranes. These carry the key role of assimilating inorganic carbon, by providing NADPH_2 and ATP .

The operation of the light reactions follows a sequential process to synthesize NADPH, and ATP. The whole photoreactive activity can be summarized in Figure 3. It is further expressed in the following equation [28], [29]:



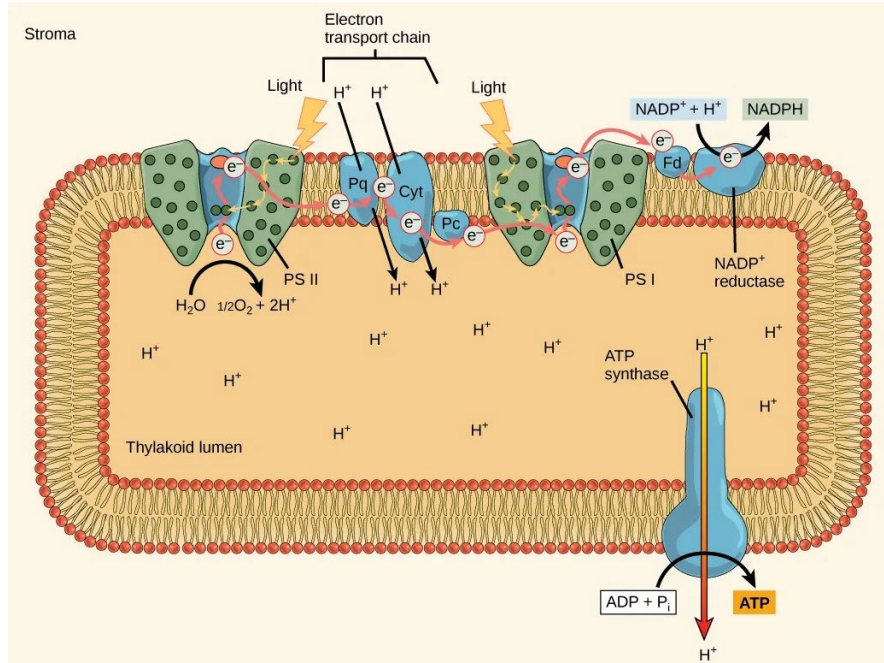


Figure 3. Summary of the light reactions within photosynthesis. PSII extracts electrons and evolves Oxygen, it further pushes the electrons towards PSI, which produces NADPH from NADP. ATP Synthase is triggered after a pH difference occurs [29].

The dark reactions, otherwise more commonly known as the Calvin cycle, utilize the resultants of the light reaction. They use the resulting NADPH and ATP to assimilate inorganic carbon and create carbohydrates. There are two main processes that occur in these reactions: Carbon assimilation, and Photorespiration. Focusing more on the former, we can summarize the process with the following reaction [28]:

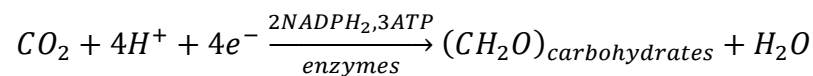


Figure 4 displays the stages of the Calvin cycle.

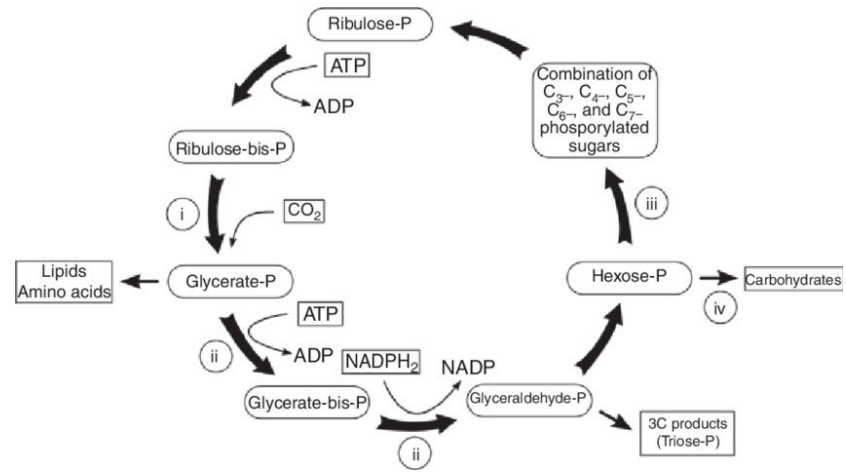


Figure 4. The Calvin-Benson Cycle, photosynthetic carbon fixation pathways [28].

CHAPTER II

ALGAE, PLANTS, AND SPACE ENVIRONMENT RESEARCH

As mentioned in a previous section, *Chlorella vulgaris* has been studied for its potential utility in space. Some of this research was actually held in a real space environment. Nonetheless, the aim in previous mentioned research is to verify the validity of *Chlorella v.* in this proposed route. However, other research has been done, which considered certain factors that could correlate to space. Most of this research was not done to study the effects of space, but rather for Earth applications. Yet, the results could translate into anticipated effects if similar experiments were done on space missions. Moreover, studied effects considered isolated factors and their interactions, rather than a combined effect of a space environment. The former exemplifies the possible influences of each factor, and some of the non-anticipated interaction effects, while the latter shows the total effect from a macro lens. Most uncovered research mentioned here involves the effects of magnetic fields, and lunar regolith on *C. vulgaris*, and some other algae and plants.

MAGNETIC FIELDS EFFECT

The magnetic field of Earth is a crucial example of a prominent effect on all life forms. Many organisms utilize the existence of such field in their daily operational mechanisms. Nonetheless, the nature of earth's magnetic field is correlated to its internal construction [30], [31], [32]]. Therefore, it is expected for other planets within our universe to have different forms of magnetic fields. This variation in magnetic fields within our universe introduces the need to study the effects of changing these fields on the internal mechanisms of living organisms.

Studying the effects of a static magnetic field on the proliferation of *C. vulgaris* cells, Luo et al. cultured the microalgae in media containing bacteria, in addition to other nutrients, and exposed this culture to a static magnetic field. From the research, it was found that the Static magnetic field (SMF) accelerated the division and proliferation of *C. vulgaris* with the presence of sufficient nutrients. The study speculated that the effects on the synthesis and accumulation of proteins within the microalgae, was due to the SMF altering the activity of some protein synthesis involved enzymes. Nonetheless, it was also found that the SMF restricted protein synthesis and accumulation at a later stage of experimentation. The researchers concluded that although the SMF affected protein synthesis and accumulation, yet the effect is still limited and non-obvious. On the other hand, studying the effects of SMF on photosynthesis, it was concluded that the efficiency of light energy conversion increased. However, the second day of the experiment held the highest peak in photosynthesis efficiency value for all *C. vulgaris* groups. According to the researchers, the results of this experiment show the ability of *C. vulgaris* to adapt to relatively low strength SMF, while suffering high stress effect at higher SMF. Additionally, the study also concludes that the *C. vulgaris* microalgae tends to endorse an anti-oxidative stress when exposed to high intensity magnetic fields, in comparison to the low intensity magnetic fields growth and reproduction promoting effects. Eventually, the researchers settle on the impact of higher SMF in promoting faster algal growth rates [33]. Focusing more on the amount of biomass produced, Luo et al. had another study in which *C. vulgaris* was also exposed to a varying SMFs. From the results, it was found that algae grew fastest when treated with a 800G field. Also, it was seen that the SMF had a significant effect on biomass. It was also inferred that SMF treatment could promote

proliferation and biomass formation for fields of adequate strength. However, extended periods of exposure for excessive field strengths inhibits growth [34].

A study targeting an environmental application of water tried to inactivate algae by magnetic treatment of water. Water was to be treated separately before it is used to grow algae. Treatment was done using two different systems. The first was an electronic water treatment system that had capabilities for a variable magnetic field, the other consisted of a set of ferrous magnets for creating a constant (static) magnetic field. Four experiments were done. For the first experiment, algal medium was pumped once through the electronic variable magnetic field (VMF) treatment system. Some of the medium was pumped again for the second experiment, thus exposed twice. The third experiment involved inoculating the *C. glomerata* alga within the medium, the algae – medium mix was then circulated through the VMF. The fourth experiment was done to compare the VMF with the SMF of the second system. The results of the first experiment showed normal growth, whereas significant declination in biomass was seen in the second experiment. However, transferring the algae back to an untreated medium reverted it to normal growth. For the third experiment, the continuous exposure to the VMF prevented growth of *C. glomerata* and caused discoloration and necrosis. The algae did not grow when transferred back to fresh untreated medium. Experimenting with the SMF did not affect the growth of the alga, in comparison to the VMF inhibiting growth by 17% [35]. This study seems to show that algae expect a coherent predefined environment, while still being resilient enough to adapt and grow in a new environment.

Reciting summaries of multiple different studies, Deamici et al. mentioned their concluded effects on the content of microalgae. The review mentioned the positive influence of

magnetic fields on pigment content (chlorophyll α , chlorophyll β , carotenoids, phycocyanin). It also mentioned that protein content of different microalgae is affected by static magnetic fields. Moreover, the presence of more noticeable changes in *Spirulina* sp. over *Chlorella* Sp. is also mentioned. Nonetheless, studies mentioned in the review amount to show that MFs have the slightest effects on lipid contents of microalgae. Additionally, studies mentioned that some additional energy might be necessary for the algae to counteract oxidative stress due to MF exposure [36].

EXTRATERRESTRIAL REGOLITH

Another studied aspect focuses on the factor of sustainability. Microalgae, plants, and other organisms require the presence of nutrients, usually obtained from solid media like soil, or aqueous media containing dissolved essential elements. To understand nutrition in the sense of space, multiple studies attempted to understand the effects of using extraterrestrial media such as Lunar, and Martian regolith as nutritional sources.

Reviewing the potential roles of cyanobacteria on Mars, Verseux et al. mentioned that all elements needed for growth seem to be found in Martian regolith. Yet, these nutrients might be in poor availability for organisms with no leaching abilities. Furthermore, physiochemical/biological treatment of regolith is needed before becoming usable as a growth substrate. Such limitations are contributed by the low nutrient availability, and poor water holding capacity. One approach the review mentioned as a way of overcoming these limitations is by planting plants that can withstand harsh environments in the regolith while introducing bioleaching bacteria. According to this approach, the bacteria would help extract nutrients from

the regolith, thus becoming usable for the plant. Biomass resulting from the grown plants can then be used to fertilize the soil through microorganisms. More demanding plants can then be grown in this fertilized soil [37].

Assessing cell survival and the preservation of potential biomarkers, Baqué et al. conducted a study on *Chroococcidopsis* cells exposed to a simulated Martian atmosphere. Persistence of the β -carotene signature and chlorophyll fluorescence were measured. As a result, it was found that unexposed β -carotene and chlorophyll were the dominant signals present and were similar in value to the control measurements. The same pattern persisted even after exposure to a simulated Martian atmosphere. However, it was after the cells were mixed with S-MRS and P-MRS Martian regolith simulants, that a 2-5% drop in β -carotene signal was seen [38].

With a focus on the moon, Ming and Henninger studied the potential of using Lunar regolith as a substrate for plant growth. In their study, Lunar regolith was considered to supply essential elements needed for growth, thus used as an agricultural soil. However, Lunar regolith is found to be poorly sorted, and has no soil structure. The study, however, considers improving various properties, as a possible means towards transforming it into a useful soil. These properties include composition, particle size, exchange properties, and hydraulic properties. Other factors seem to render Lunar regolith of low stability; chemical weathering is one. Nutrients of the Lunar regolith would be released due to the weathering. Additionally, Lunar regolith might suffer from proper aeration, and water movement problems due to its poor physical structure. Nonetheless, sieving and sizing could salvage both potential problems. From the nutrition perspective, there might also arise a need for amending the regolith with other elements, due to the limited capacity of growth provided by its prevalent materials and minerals. Moreover, the regolith might have

some unknown potential toxicity. This study suggested another potential use for the regolith as a solid support-substrate in nutriculture systems, but for self-sufficiency of the regolith on the moon, there still exists the need to extract all needed elements to prepare nutrient solutions for nutriculture systems and soil fertilizers [39].

Another review by Ellery compared the viability between Martian and Lunar regolith. The review favored former over the latter. It mentioned the possibility of combining Lunar regolith with plant parts to give it a more humus factor, however, toxicity still exists with the presence of metals such as Ni and Cr in its makeup. Thus soil-less hydroponics were suggested in place of lunar soil, where direct delivery of nutrient solution is exploited through the exposed root system. Other experiments mentioned by the review have attempted the cultivation of plants such as tomatoes, wheat, and crest in regolith simulants. Superior growth was found in Martian simulant in comparison to Lunar, yet both were still able to support plant cultivation. The presence of aluminum is to be blamed for the degraded performance of the lunar regolith according to the experiment [40]. The same approach of direct nutrient solution delivery is reiterated by Salisbury. However, instead of hydroponics, he suggested the utilization of regolith as a solid plant substrate, while watering it with a solution of plant essential minerals [41].

With an attempt to show the ability of plants to grow on Lunar regolith, Paul et al. tried to grow *Arabidopsis thaliana* on samples from the Apollo missions 11, 12, and 17. In this study, plants were potted in ventilated terrarium boxes that simulated an open laboratory environment, similar to a human occupied lunar habitat. Germination occurred in all samples 48 to 60 hours after planting. A single plant per planting well was left for each regolith sample in the 6th to 8th day. In lunar regolith, roots of the plants inhibited in comparison to the lunar simulant, thus

indicating growth inhibition in the actual lunar samples. Beyond the 8th day, the growth became slower, it took longer to develop extended leaves, rosettes were smaller, and plant stress reaction was apparent with the presence of pigmentation. Apollo 11 was inferior to Apollo 12, and 17 samples. Simulant plants always maintained a higher rate of growth. However, despite the degraded growth performance, yet the experiments demonstrated the capability of terrestrial plants to grow on lunar regolith as a primary support matrix. However, the data still shows it to not be a benign growth substrate. As a discerning conclusion, plants seem to struggle more to grow on regolith from the Apollo 11 location in comparison to 12, and 17. This suggests that the more mature a regolith is, the poorer it would be to act as a substrate for plant growth [42]. Other studies involving plants have also been done on both Lunar regolith and Martian regolith. Nonetheless, Lunar regolith marks a higher priority in this thesis. Mentioned by Duri et al. in his review, regolith and its simulant should possess certain characteristics to be able to integrate with crop production. The simulant should have optimal water holding capacity to maintain an effective level of humidity after irrigation. It should also have optimal air circulation to allow gas exchange and root and microbial respiration in the porous medium. The same review included a study that attempted to grow a variety of plants under lunar experimental conditions and using lunar regolith as a growth substrate. The conclusion of the experiment pointed towards the potential for regolith to support growth, most specifically the growth of ferns, liverworts, and tobacco. In addition to this general conclusion, the study found an interaction between the species of plants grown and the uptake of iron, aluminum, and titanium. To further understand effects, another experiment was done, utilizing recovered lunar material from the initial study. The second experiment found higher sterol concentration in tissue grown in contact with lunar

material, differences between relative and absolute fatty acid concentrations were found as well. Also, higher concentrations of chlorophyll and carotenoid were found, where chlorophyll α was the major pigment present [43].

An additional study about growing plants was conducted by Wamelink et al. The study investigated both Martian and Lunar regolith simulants for the possibility of growing plants, in comparison to a control from the river Rhine. This study used the JSC-1A Martian and Lunar simulant. The results of this study showed that all plants that were grown on all soils were able to germinate, except the Common vetch plant. It was also found that Lunar soil had the lowest germination, in comparison to Martian, which had highest. The percentage of leaf forming plants were sometimes considerably lower than germination percentages. This might cause some of the plants to stop developing or die, as it is thought that having no leaves might render the plants incapable of photosynthesis operation, hence the death of the plant. Martian soil tended to have the highest leaf forming rates, while Lunar regolith had lowest. The biomass results of the study seem to fare better for the Martian simulant to the Lunar as it seemed inferior. Reasons were speculated, like higher pH, moisture holding capacity, and/or free Aluminum in the soil [44].

Although the multitude of research that has been attempted on biological organisms in space or under simulated space environments, not much research has been done on the interaction of multiple environmental effects of space. Usually, single factors are studied. Moreover, despite the existence of research on the effects of magnetic fields on microalgae, very little research has studied *Chlorella vulgaris* specifically. Additionally, until now there has been no research on the effects of the Lunar regolith on *Chlorella vulgaris*, despite the existence of some research on the effects of Martian regolith.

CHAPTER III

EXPERIMENTAL PROCEDURE AND DESIGN

In this thesis, the research focuses on the effects of lunar regolith on microalgae, more specifically, the *Chlorella vulgaris* microalga strain. The research and the experiment also focus on studying the effect of the magnetic field of the Moon on microalgae. Therefore, the focus of this academic work is on the combined effects and interactions of simulated lunar magnetic fields and lunar regolith on the *Chlorella Vulgaris* microalgae.

DESCRIPTION OF THE EXPERIMENT AND MOTIVATION

The experiment done in this study exposes the *Chlorella vulgaris* microalgae to an uncharacterized magnetic field that simulates the magnetic field of the moon. The magnetic field is generated by three coils in the X, Y, Z axis using a Helmholtz cage. In addition to the magnetic field, the experiment attempts growing *Chlorella vulgaris* in multiple nutrition mediums. The microalgae are grown in BBM, BBM and Lunar regolith, and MilliQ Water and Lunar regolith. A hundred grams of Lunar regolith is used in each nutrition medium; such an amount of regolith was chosen to simulate an attempt to grow the algae on the moon, where the nutrition medium could be contaminated with this approximate amount of regolith. The *Chlorella vulgaris* grown in the mentioned Lunar regolith contaminated mediums are put on a rotating plate, which rotates with a very slow speed that simulates that of the moon, and they are exposed under the lunar simulated magnetic fields for predetermined periods of 0, 1, 2, and 4 hours. After the experiment is done, the exposed microalgae are analyzed for its growth, and for the quantity of protein, and β -carotene pigment. The motivation behind this experiment is to understand the interaction

between these factors of medium and magnetic field, and to understand their effects on the microalgae and its constituents. From there, results could be deduced, allowing for a better understanding of space environmental effects on biological species.

Putting the general stages of the experiment in an eloquent set of steps, we can list them as follows:

1. Cultivate microalgae for an approximate period of one month in multiple flasks to provide quantity and redundancy of algae.
2. Sterilize and prepare flasks for each growth medium and exposure duration.
3. Mix algae with growth medium to achieve a predefined optical density range.
4. Randomly spread flasks within borders of magnetic field.
5. Start exposure for proposed durations, eliminating each flask related with each duration time from within the field.
6. Perform exposure procedure over a set period of days.
7. Every certain number of days, attempt to do analysis of microalgae growth, and protein, and β -Carotene content, until the pre-set total duration of the experiment.

STATISTICAL DESIGN OF THE EXPERIMENT

The statistical experimental design of the experiment follows a general factorial design conducted as a full replicate in each block format [45]. In this design, both factors of magnetic field exposure time, and growth medium are considered. This approach towards blocks verifies that each block contains a complete replication of all factor combinations. At a 5% level of significance, using an effect size of 2 (*Signal to noise ratio*, $\frac{\delta}{\sigma} = 2$) power is 98% for all factors

and 86% for interaction factors. All terms of calculated power associate with a full quadratic model. Orthogonality exists between all blocks and all regression model terms. In an alternative definition, no block effect is confounded with a factor effect. Blocks can be added to the design to improve the total statistical power. This shows the flexibility allowed within such a statistical approach. Furthermore, albeit not recommended, blocks can still be omitted for the reason of depleted resources, such as lunar regolith or micro algae. Omitting blocks, however, is at the expense of statistical power.

Per the aim of this thesis research to study the effects of the lunar magnetic field and lunar regolith on the growth and change in the constituents of *Chlorella vulgaris*, and per the statistical design approach, the following factors were chosen for the statistical design as seen in Table 2. Factors have a maximum of four levels per appropriate design in accordance with appropriate scientific literature, and with acceptable statistical power.

Table 2. Statistical Design Factors showing their values, categories, and levels.

Factor	ID	Unit	Type	Level 1	Level 2	Level 3	Level 4
Magnetic Field Exposure Duration	A	Minutes	Numeric	0 m	60 m	120 m	240 m
Growth Medium	B	-	Categoric	BBM	BBM+JSC-1A	MilliQ+JSC-1A	

The completely randomized block design can be seen in Table 3. Each replicated factorial block is represented by its specifier, where each block is a simple factorial design. Per block, sufficient degrees of freedom exist in the design, which allows for outlier removal. Nonetheless, in the sense of error evaluation, there exists no additional replicates. The absence of these replicates affects the evaluation of pure error, and lack of fit testing. In other words, replications allow for detection of variance, and thus error, therefore, lack of these would render the incapability of doing so. Considering blocks, it is possible to render block results towards error evaluation if the effect of a block is negligible. Design model adequacy will be judged utilizing fit statistics, specifically the R^2 statistical indicators.

Table 3. Randomized block runs design.

Block	Run	Factor: A	Factor: B	Block	Run	Factor: A	Factor: B
Block 1	1	240	BBM + 100	Block 2	19	60	BBM
Block 1	2	0	BBM + 100	Block 2	20	0	BBM + 100
Block 1	3	0	MilliQ + 100	Block 2	21	60	BBM + 100
Block 1	4	240	BBM	Block 2	22	240	BBM
Block 1	5	120	BBM + 100	Block 2	23	0	MilliQ + 100
Block 1	6	0	BBM	Block 2	24	0	BBM
Block 1	7	60	BBM + 100	Block 3	25	240	MilliQ + 100
Block 1	8	120	BBM	Block 3	26	240	BBM
Block 1	9	60	MilliQ + 100	Block 3	27	120	BBM
Block 1	10	60	BBM	Block 3	28	0	MilliQ + 100
Block 1	11	120	MilliQ + 100	Block 3	29	60	BBM + 100
Block 1	12	240	MilliQ + 100	Block 3	30	0	BBM
Block 2	13	120	BBM	Block 3	31	0	BBM + 100
Block 2	14	240	MilliQ + 100	Block 3	32	120	MilliQ + 100
Block 2	15	60	MilliQ + 100	Block 3	33	120	BBM + 100
Block 2	16	240	BBM + 100	Block 3	34	60	BBM
Block 2	17	120	BBM + 100	Block 3	35	240	BBM + 100
Block 2	18	120	MilliQ + 100	Block 3	36	60	MilliQ + 100

Now, although we have factors representing different mediums and exposure time, the experimental procedure considers the parallel exposure of all runs to save run time. In each block, each medium iteration is exposed in all duration iterations within the same run. Elaborating further on the actual implementation of iterations, for medium, each iteration entry resembles a separate physical entity placed within the same magnetic field. However, for duration, an iteration is realized by removing the related entity from the magnetic field when exposure time is achieved.

CULTIVATION OF *CHLORELLA VULGARIS*

Forming the main focus of our research, the *Chlorella vulgaris* microalgae was chosen for its many health benefits, growth, and robustness. For this experiment, an adequate amount of *C. vulgaris* needed to be cultivated to be able to carry out the total exposure and growth media requirements.

Despite the robustness of the *Chlorella vulgaris* microalgae, and its ability to thrive in many environments, however, its ability to do so depends on the presence of certain nutrients that the algae use to perform internal cellular operations. Additionally, despite the harsh environments, these environments need to offer some living potential for the algae to adapt to, and thrive in.

Nutrient requirements and utilization

As with other living species, and specifically ones that fall under the plantae kingdom, microalgae tend to utilize photosynthesis for energy production through ATP. This being a biochemical process explains the nutritional need; of these chemicals, Phosphorus, Nitrogen, Potassium, and Carbon are needed. All nutrition mediums need to have these elements in certain

ratios for the perfect growth of *C. vulgaris*. However, some other ratios of these elements will still suffice, despite microalgae having to react and adapt.

Based on literature, microalgae (of which *C. vulgaris* is part), utilize nutrients as listed in Table 4.

Table 4. List of chemical elements utilized in nutrients by *Chlorella v.*

Chemical Element	Nutritional Utilization
Carbon	Main microalgal biomass element. Contributes to the photosynthesis process by being transformed from its inorganic state to useful organic matter [27]
Nitrogen	Can be taken up in both organic (urea, amino acids) and inorganic forms (NO_3^- , NO_2^- , NO , NH_4^+ , N_2). It takes part in the formation of biochemical compounds such as nucleic acids (RNA, DNA), amino acids (proteins), and pigments such as chlorophylls and phycocyanin.
Phosphorus	Critical to the formation of ATP. It is further a component in organic molecules essential to metabolism such as nucleic acids (RNA, DNA), and membrane phospholipids.
Potassium	Affects synthesis of protein and carbohydrates, it also regulates the cells osmotic potential. Furthermore, it is an activator for some enzymes involved in photosynthesis and respiration.

Composition of BBM (Bold's Basal Medium)

Many nutrition mediums exist for microalgae cultivation where each medium provides a different mix of elements. However, for the cultivation of *Chlorella vulgaris*, BBM was found to have all the nutrients the microalgae need, and it can be transformed into an aqueous form, and hence provides an adequate cultivation approach. Additionally, as the discrepancy of the growth from a known baseline is the main objective, a well-known growth medium provides the best

choice. Moreover, BBM is commercially available in large quantities, and it can also be mixed in a lab from its basic components. The basic contents of BBM are presented in Table 5.

Table 5. Composition of BBM (Bold's Basal Medium) [46], [47].

Component	Stock Solution ($g \cdot L^{-1} H_2O$)	Quantity Used
Macronutrients		
NaNO₃	25.00	10ml
CaCl₂ · 2H₂O	2.50	10ml
MgSO₄ · 7H₂O	7.50	10ml
K₂HPO₄	7.50	10ml
KH₂PO₄	17.50	10ml
NaCl	2.50	10ml
Alkaline EDTA Solution		
EDTA	50.00	
KOH	31.00	
Acidified Iron Solution		
FeSO₄ · 7H₂O	4.98	1ml
H₂SO₄		
Boron Solution		
H₃BO₃	11.42	1ml
Trace Metals Solution		
ZnSO₄ · 7H₂O	8.82	
MnCl₂ · 4H₂O	1.44	
MoO₃	0.71	
CuSO₄ · 5H₂O	1.57	
Co(NO₃)₂ · 6H₂O	0.49	

Preparation of BBM (Bold's Basal Medium)

For this work, BBM was bought from PhytoTech Labs as a powder [48]. Preparation of BBM was done according to the information document supplied on the manufacturer's website [49], in addition to instructions provided on the bottle package. To prepare an aqueous BBM solution, one liter of MilliQ Water was measured in a volumetric flask, in the meantime, 0.73 grams of the BBM powder is weighed. After that, the powder was mixed with the MilliQ water in a 1 Liter Pyrex

bottle with a sterilizable plastic cap that can handle up to 125 degrees in the autoclave. The mixing was done by hand in increments of 250 ml. The powder was first added to the bottle, then around 250 milliliters of MQ water were added. The bottle was then mixed by hand until the powder was very well distributed within the water. The powder was yet to dissolve and mix due to oversaturation. Increments of 250 milliliter additions followed the initial spill, with hand mixing in between. Eventually, when all of the water was added, the mix was thoroughly hand shaken, until no large chunks or largely visible traces of the powder were present. A small trace of fine particulates could be seen floating when the mix is shaken. After the powder is mixed, 0.1% sulfuric acid (H₂SO₄) solution was prepared from concentrate. 1ml of the diluted acid was added to the mix to adjust the pH of the solution. The mix was hand shaken very well after the addition of the acid. The ready BBM solution was sealed tight with the plastic cap and was then placed in the autoclave to be sterilized at a temperature of 121 degrees Celsius for 40 minutes. The sterilized solution was then used to cultivate the *C. vulgaris* microalgae.

Medium Sterilization Equipment

The autoclave used for sterilization at the lab is a Yamato SM300 with a capacity of 32 liters. It supports temperatures up to 128°C for sterilization and 180°C for drying. Furthermore, it supports two modes, one for sterilization, and another for sterilization and drying. Moreover, it is equipped with a HiTec IV CR Microprocessor controller and a control interface to set the sterilization mode, temperature, and total time. The measured temperature inside the sterilization chamber is shown on the control interface screen. The autoclave is equipped with an analog pressure gauge to show the internal sterilization chamber pressure. Additionally, an electronic button is provided to exhaust chamber pressure. In terms of construction, the

sterilization chamber utilizes two heating coils, which provide 1.7kW, and 1.5kW of thermal power for sterilization, and drying, respectively. Both steam and excess water drainage systems are present, they externally attach to a drainage valve, and to cooled steam water drainage tank. Whenever the autoclave is to be utilized, three liters of water is dumped over the heating coil inside the chamber. Subsequently, all samples are put in a solid net metal basket with long metal handles and lowered into the sterilization chamber. The lid is then tightened securely. A large one-liter beaker is placed beneath the exhaust in case of cooled water dripping. Mode, temperature, and time are set as desired according to application (For this study it was sterilization and drying at 121 degrees, for 40 minutes). Picture of the autoclave can be seen in Figure 5 below.



Figure 5. Yamato SM300 Autoclave.

Cultivation Process

To carry out the cultivation, multiple tubes of live *Chlorella vulgaris* were bought from the commercial provider Carolina Biological Supply and brought to the lab, where they were further grown to a larger quantity. Having the microalgae sourced from a vendor ensures consistency of the strain and confirms the absence of any form of bacterial contamination, moreover, it ensures the history of the specific *chlorella vulgaris* strain obtained and the type of nutrient in which it is grown. Hence, this route provides an overall well controlled research subject.

The process of cultivating *Chlorella Vulgaris* follows a cycle of provision, nutrition, propagation, and maintenance, and is done in the following order:

1. Sourcing the micro algae to the lab: *Chlorella Vulgaris* could be found in open ponds or in laboratories. Usually, the source of the algae is determined based on what factors need to be considered for the study. In this thesis research, consistency and contamination factors are of utmost importance.
2. Determining, and exposing the microalgae to an adequate nutrient solution: Based on the cellular makeup of the specific microalgae strain, there can exist multiple nutrient sources based on their absorption; it is important to choose a solution that will reflect the desired growth characteristics.
3. Maintain growth preferred environmental factors, such as: temperature, and illumination: Temperature cycles can introduce changes in the biomass and growth characteristics of the *chlorella vulgaris* microalgae [50], [51], [52]. Illumination introduces a similar effect.
4. The propagation of microalgae and increase in biomass, indicating healthy growth: It is important to monitor the changes in culture over time. Indicators of healthy growth in

Chlorella vulgaris include color change, flocculation, and volume change. Such indicators provide a sense of how well algae is performing under current set environments.

5. Maintenance of cultivated microalgae through nutritional and environmental sufficiency:

It is important to maintain the *Chlorella vulgaris* culture while it is growing, and once it reaches a certain level of growth. This requires constant supplementation of culture nutrition medium and ensuring a safe limit for the variation of environmental effects.

Nonetheless, each step in the process of cultivation embodies many different procedures for achieving the same objective.

Cultivation Chamber Design

To accommodate and ensure the *Chlorella vulgaris* microalgae is of consistent characteristics throughout this research, it was important to set the cultivation environmental factors constant. To achieve this, the microalgae was grown in a cultivation chamber that accommodates the required level of control. This chamber offers constant illumination, helps keep the cultivating algae shielded from temperature variations, and allows passing oxygen tube feeds. A picture of the algae in the cultivation chamber can be seen in Figure 6:



Figure 6. *Chlorella vulgaris* beakers in the cultivation chamber.

This chamber is made up of two levels. Each level is used for a different purpose in experimentation. The algae is cultivated in the first level of the chamber, and the second level is used to incubate the *Chlorella vulgaris* flasks after adding lunar regolith to the medium and lunar magnetic field exposure. To accommodate illumination requirements, the chamber is equipped with 3 sets of LED tube lights resting on a set of rails above each level. These lights are removable. Furthermore, additional lights can be added. The chamber does not have an illumination control knob, but rather depends on the number of LED tubes present during incubation. However, the tubes are connected to an analog intensity controller. Moreover, the chamber is covered using white curtains, reflecting light inside. No set temperature point is specified inside the chamber, the temperature is specified through the thermostat of the room hosting this chamber, also, the LED lights emit enough heat to compensate for any heat lost to the external surroundings, and the curtains keep the air inside at a low circulation rate, conserving temperature.

Cultivation Procedure and Cultivation Containers

Despite the simple unicellular composition of the *Chlorella Vulgaris* microalgae, it still manages to provide much potential to discover a plethora of methods for how it can be cultivated and the different media in which it can grow. Multiple research papers investigate the different environments and mediums used to grow the algae [33], [34], [53]. Furthermore, microalgae, not falling into categorization within the plant kingdom, proves to show a high level of photosynthetic performance [54]. On actual grounds, this was apparent from rapid growth witnessed within the vessels used to cultivate the repository of algae within the lab. Nonetheless, the approach taken to cultivate the algae for this research was very simple. The algae needed nutritional elements, and it can extract these nutrients from an aqueous medium. BBM was found to have all the nutrients the microalgae need, and it can be transformed into an aqueous form, and hence provides an adequate cultivation approach. Additionally, as the discrepancy of the growth from a known baseline is the main objective, a well-known growth medium provides the best choice.

BBM Medium [48], [55] was used to cultivate the *Chlorella Vulgaris* microalgae. The microalgae were cultivated at room temperature (72.5°F or 22.5°C), and it was under (add lux amount) Lux illumination. Four 1L Erlenmeyer flasks were used for the cultivation process. Furthermore, air was provided using clear rubber tubes. The flasks were sealed with a cork that had two openings to circulate the air. One opening provided a path for the clear rubber tube to enter the flask and provide air, while the other opening provided a filtered vent; a pipette tip filled with cotton was used as the vent.

As mentioned before, I sourced two 50ml *Chlorella V.* microalgae tubes from a provider rather than directly acquire it from a natural source. These contained *Chlorella Vulgaris* culture in

BBM medium. To start the cultivation procedure, we cleaned the four 1L Erlenmeyer flasks with detergent, washed them, and drained the excess water. We then covered the top of the flasks with a piece of aluminum wrap and transferred them to be sterilized in the Autoclave at a temperature of 121°C for a period of 40 minutes. The autoclave was set to the “sterilize and dry mode,” ensuring the flasks are dry upon finishing.

When the sterilization was done, we emptied each of the tubes in a separate 1L Erlenmeyer flask. Previously prepared BBM medium was used to top up the flasks. In the initial stage, we transferred 250 ml from each flask to a smaller 500ml flask for each. The reason for this procedure is to allow for a quicker, more flexible utilization of the algae as backup in the case of contamination or death of any of the larger cultures.

After the culture is distributed into the flasks, we shook them to ensure proper mixing of the cells with the nutrition medium. In addition to the nutrition medium, it was particularly important to deliver oxygen to the microalgae. Thin clear rubber tubes of 5 mm diameter were used for this purpose. To ensure the cultivating *Chlorella V.* does not get contaminated, I prepared a 70% Ethanol alcohol solution, and we pushed the solution through the tubes. The ethanol was left inside the tubes for a period of 5 minutes, we then proceeded to drain and leave them to dry. Further eliminating any risks of contamination and ensuring no dust particulate exposure, we equipped the connector ends of the tubes with a micro porosity air filter. We proceeded to equip the outlet ends of the tubes with pipette tips to ensure higher air velocity, and less algae entanglement. Needing to tightly seal the tops of the flasks, we resorted to using rubber stoppers. However, having to pass the tube inside the flask, we drilled a hole of the same diameter as the tube, ensuring a tight seal. We proceeded to drill another hole for venting and filled it with a

pipette tip stuffed with cotton. We topped up the remaining available volume of each flask with BBM and eventually sealed the tops of the flasks with the rubber stoppers then further wrapped them with Parafilm. We shook the flasks one more time to ensure mixing with the added BBM. They were left for a total of 2 weeks while topping with BBM every few days to keep the algae growth process ongoing.

After a period of two weeks, we could notice the increase in the opacity and darkening in color of the cultivating algae, hence indicating growth, and letting us know that we could start utilizing the microalgae for the experiment. Every time we used the algae, we used to top-up the flasks with BBM to keep the cultivation cycle continuous. After completing the first experimental block, we moved the algae from the smaller 500ml flasks to larger 1L flasks due to needing a large volume of algae in the regolith mixing process.

MIXING AND OPTICAL DENSITY MEASUREMENT

To study the effect of lunar regolith and lunar magnetic field, 12 total samples were prepared. These included three different sets of treatments, each set included four treatments. The first set is BBM only, the second is BBM + 100g lunar regolith, and the third set includes MilliQ Water + 100g lunar regolith. Preparing each set requires the careful mixing of Lunar regolith with each nutrition medium, furthermore, mixing these enhanced mediums with *Chlorella Vulgaris* to investigate the question of lunar effects.

As per the design of the experiment, the aim is to mix 100g of lunar regolith with 1L of each nutrition medium, later adding the algae. Table 6 shows a list of the ingredients ratio as

determined appropriate considering the aspect of spillage, where we multiply the amount of each ingredient with a 1.1 factor.

Table 6. Medium volume to regolith ratio respective to each set of treatments.

Treatment	Medium Volume	Medium:Regolith
BBM: 0m, 60 m, 120 m, 240 m	1000 ml	1100 ml:110 g
BBM + 100g: 0m, 60m, 120m, 240m	1000 ml	1100 ml:110 g
MilliQ + 100g: 0m, 60m, 120m, 240m	1000 ml	1100 ml:110g
Total	3000 ml	3300 ml:330g

Therefore, dividing the mixed ratio of ingredients per exposure would result in the following ratios per exposure:

Table 7. Ratios of medium to regolith per exposure.

Exposure	Medium Volume	Medium:Regolith
0m	250ml	275ml:27.5g
60m	250ml	275ml:27.5g
120m	250ml	275ml:27.5g
240m	250ml	275ml:27.5g
Total	1000ml	1100ml:110g

Researching the lunar effects on *Chlorella v.*, it is important for the results to be comparable. This is done by starting the experiment with the same initial *Chlorella V.* density for

all treatments. We measure the optical density (OD) of the microalgae to provide a quantification for the density, which is affirmed to be constant by considering setting a constant baseline for the OD of the microalgae. In this experiment, we set the base line value to be between 0.2 ~ 0.5. The reason for setting a range is due to the nature of the algae culture not being isotropic, which is related to irregularities in the sizes of its unicells.

After previously mixing in the regolith, we mixed in the microalgae with each type of culture medium to arrive at the base line OD. For the first block of treatments in the experiment, we approached the process by measuring the initial OD of the pure *Chlorella V.* in BBM culture and proportionally adding the required nutrition medium starting with BBM. Our approach is based on diluting the *Chlorella V.* culture gradually rather than pre-calculating the required dilution volume; this is referred to the anisotropic density distribution of the culture, as different volumes of the same culture sample could have varying densities, moreover, having multiple cultivating algae samples would render some samples having higher or lower density based on their growth rate and present biomass.

To measure the OD, we used the NanoDrop 2000 spectrophotometer. After measuring the initial OD (~5.2), we shook the culture very well, took a sample of 200ml, and measured OD again. Luckily, the OD was still at (~5). We then proceeded to dilute by pipetting 10ml of BBM, adding it to the culture then shaking and measuring the OD, not budging from its initial measured value. We continued the process of adding 10ml and measuring, noticing a slight reduction in the OD value on every addition. We were able to arrive at the required 0.2 OD value after adding 100ml of BBM. We followed this process for all three sets of the first block, each including the four exposure treatments (0m, 60m, 120m, 240m). Moreover, we were able to reach the desired levels

of optical density within a similar range of BBM dilution volume, which spanned from 90ml to 110ml. This indicated quite a similar density profile for the cultivated algae, in addition to well-mixed culture samples used to do the mixing.

The repetitive pipette, dilute, then measure process proved to be exceedingly long and hectic in the long run for preparing the first block treatments. For the subsequent blocks, however, we planned a different approach, based on increasing the dilution BBM volume steps from the initial 10ml increments. In the new approach, we started the mixing by obtaining a well-mixed 50ml sample of the algae culture, subsequently adding 50ml of BBM and mixing them very well. We then measured the OD value three times and took the average value. Depending on the measurement we proceeded to either add more BBM to further dilute and reduce the OD or add more of the algae culture to increase the algae concentration, and subsequently the OD, and repeated the measurement process. The amount of added BBM or algae depended on the closeness of the measurement to the desired value. If the discrepancy was large (> 1), we would add another 50 ml to arrive at 150ml, and measure again. If the discrepancy was still high, we would add another 50ml to arrive at 200ml, we would then add fractions of 50ml until we arrive at the desired OD. The smaller the discrepancy, the smaller the fraction we would add to fine tune the OD measurement. We continued with this process until we arrived at 250ml, however, we ran into some cases where we arrived at a total volume of +300ml. We managed to utilize the remaining excess volume as a starting base for mixing the next treatment; nonetheless, as the excess volume had the correct optical density, we kept adding equal fractions of 50ml of both algae and nutrition medium until we arrived at the total desired volume of 250ml while keeping OD constant. Despite the non-linear mixing process, the process we used attempted linearization

over small increments of fractions of the diluent and the dilute, thus providing a more accurate control on the desired OD measurement. Through this process we were able to arrive at the desired concentration much faster. Figure 7 provides a flowchart describing the process.

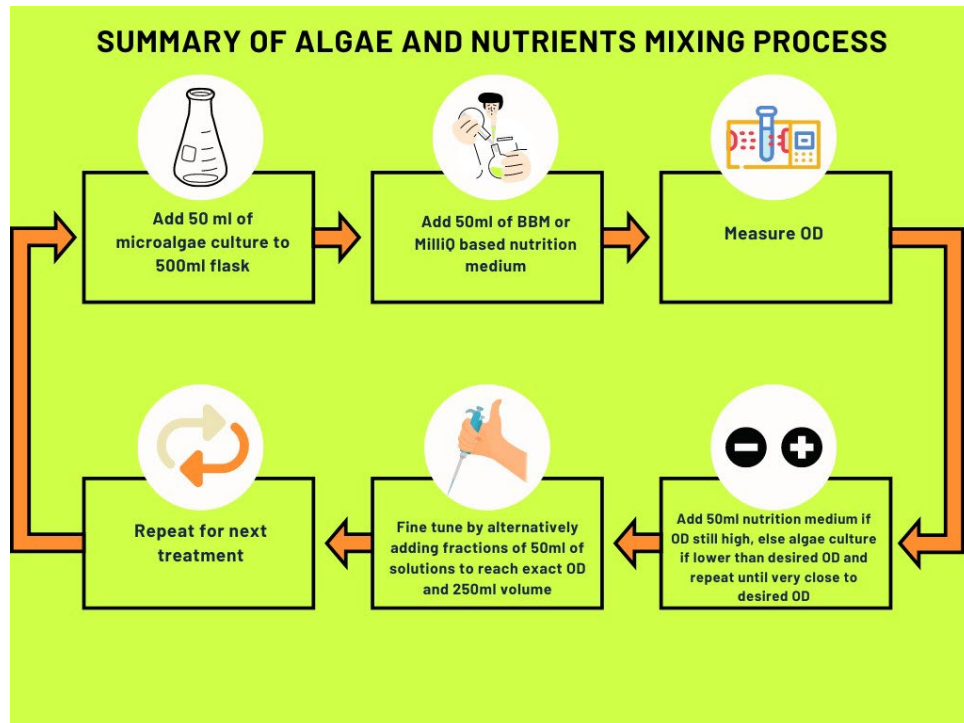


Figure 7. Flowchart of the microalgae and nutrition medium mixing process.

Eventually, of total samples prepared, nine were exposed to a magnetic field simulating that of a lunar environment for different periods of time; that is 60 minutes, 120 minutes, and 240 minutes. Three control samples from each treatment were left unexposed. Magnetic field exposure lasted for 6 days. After that, the samples were monitored for 21 days. Monitoring included growth measurement, beta carotene, and protein content estimation.

OPTICAL DENSITY MEASUREMENT

Having optical density (OD) measurements as part of many of the procedures used throughout this scholarly work, it is worth describing its concept of operation and execution process. The OD process operates on the concept of light absorbance shifting throughout different materials. Depending on how opaque or transparent a material is, the OD measurement value varies.

Optical density is referenced through two opposite identifiers: Absorbance, and transmission. It is mathematically defined as the log to the base 10 of the reciprocal of the transmission, as described by the following equation.

$$A_{\lambda} = \log_{10} \frac{1}{T_{\lambda}}$$

Simplifying, and using the rules of logarithms,

$$A_{\lambda} = \log_{10} 1 - \log_{10} T_{\lambda}$$

Which results in,

$$A_{\lambda} = -\log_{10} T_{\lambda}$$

Where λ is the wavelength of light passing through a material, A_{λ} is the absorbance, and T_{λ} is the transmission. An OD measurement value always refers to absorbance, where absorbance resembles the ratio of the falling intensity of light on a material to the amount of transmitted light through the same material. Hence, higher OD refers to a lesser amount of passing light, and vice versa.

A spectrophotometer is the device used to measure OD. There are many variations of these devices, depending on the actual instrument design, sensitivity, sample size, and supported light wavelength range. Nonetheless, the operational concept remains the same, a light source of predetermined illumination intensity is passed through a sample, a sensor on the opposite end, obstructed by the sample reads the perceived intensity of light. Based on the deviation between the source and the sensor, the amount of transmission is determined and hence the absorbance.

In my work, I utilized two spectrophotometers. The UNICO 1000, and the NanoDrop One. Referenced by its data sheet, Figure 8 illustrates how the UNICO 1000 system is set up. Initially, a halogen bulb (1) emits light through a collecting lens (2), which focuses light through an entrance slit (3). Light passes through a collimating lens (4) onto an analytical grating (5), where it is dispersed into its spectrum, then passes through the exit slit (6), passing through the sample compartment (7) and another collimating lens (8), before it is finally received by a photo detector (9). The sample compartment in this device accepts 3.5mL standard cuvettes. Although similar, the Nanodrop One has a smaller well size, and can measure sub-micro samples of 1-2uL volume and does not need a cuvette despite being capable of accepting one. Its sampling compartment is made up of two opposing closing cylinders with microvolume sized holes hosted on a pedestal. Light is provided through the first hole of the top cylinder attached to the pedestal arm, and the bottom hole allows light to pass to a sensor placed below the hole of the bottom cylinder fixed to the pedestal bed. The hollow volume of the holes is where the desired measurement sample is contained. A microliter pipette is used to disperse the sample into the hole of the bottom cylinder, before lowering the pedestal, where the top cylinder closes creating a sample column.

Figure 9, Figure 10, and Figure 11 show sample dispersion, the sampling compartment, and sample column formation between the cylinders of the NanoDrop One.

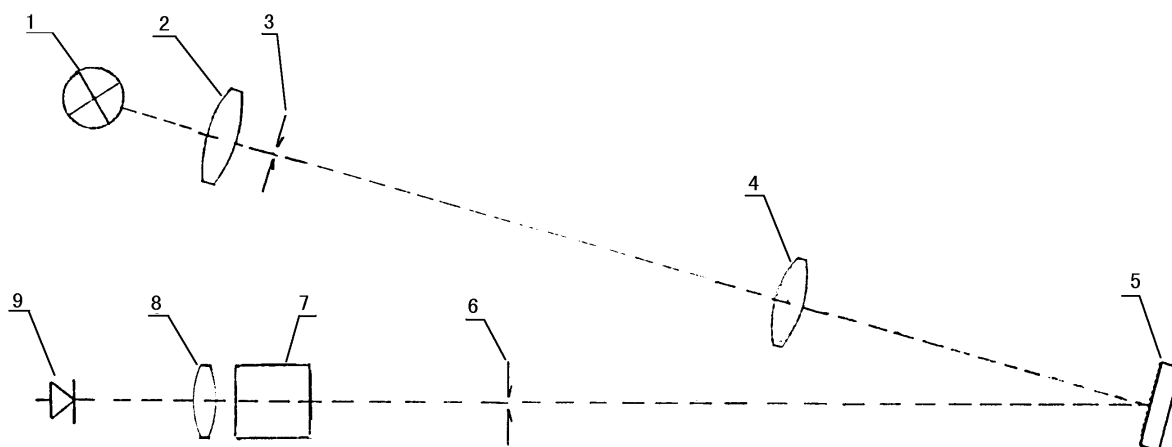


Figure 8. Optical System Schematic [56]



Figure 9. Dispensing a μL volume sample using a pipette [57].

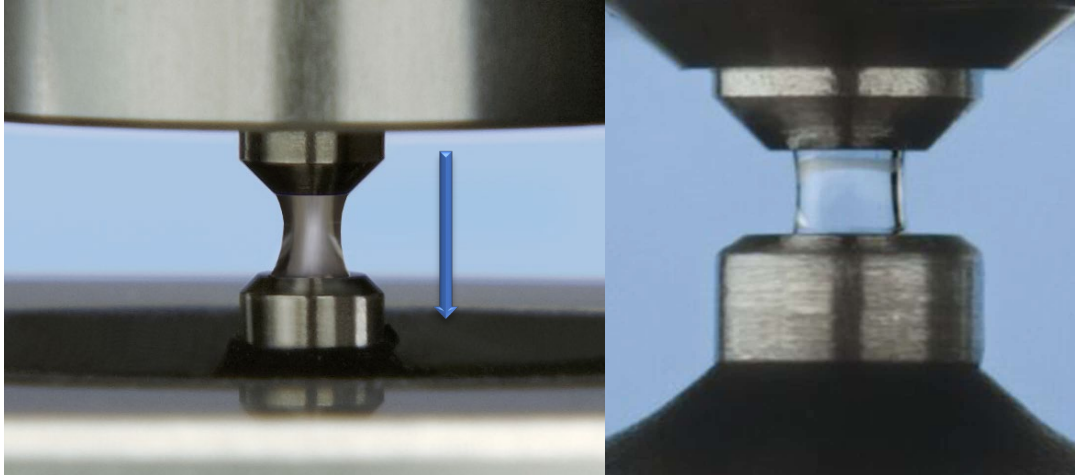


Figure 10. Upper and lower cylinders of the sampling compartment shutting, forming a sampling column [58].



Figure 11. Sampling compartment with formed sampling column [58].

HELMHOLTZ CAGE OPERATION AND MAGNETIC FIELD EXPOSURE

Needing to simulate the Lunar magnetic field on Microalgae as part of the study, the Helmholtz cage provides to be an invaluable tool. Using this device, we can produce different patterns of magnetic fields of controlled strength.

In the experiment done for this thesis, we utilized the Micro Magnetics 1500 Square HHC Triaxial Helmholtz cage with controller, built by Micro Magnetics Inc. shown in Figure 12. This device is capable of producing both AC and DC magnetic fields up to 8 Gauss at 1Hz, and ± 8 Gauss respectively, in the three directions of X, Y, and Z. It is equipped with the capability to measure and cancel the earth's magnetic field to produce fields of absolute magnitude.

In its construction, the cage consists of three sets of coils, two for each direction, moreover, it supports a rotating turn table connected to a stepping motor. Within the boundaries of the cage four magnetometers are connected to a linear traversing worm gear on the Z-axis, a motor rotates the worm gear modifying the height of the sensory elements, this setup sits on a sliding deck in both the X and Y-axis allowing flexibility in the location of the sensing elements. The magnetic field inducing coils are connected to an external accompanying power supply setup, providing the needed power, in addition to a controller interfacing with a custom LabView program. Table 8 lists the Helmholtz cage capabilities. Figure 12 shows the Helmholtz cage, and its accompanying accessories.

Table 8. Technical Specifications of 1500 Square HHC Helmholtz coil cage [59].

Specifications	X-axis	Y-axis	Z-axis
DC Field (Gauss)	± 8.5	± 8.5	± 8.5
Max AC Field (Gauss) @ 1 Hz (max)	8.5	8.5	8.5
Input Voltage	208 VAC, 50/60 Hz, 20A (max)		



Figure 12. 1500 Square HHC Helmholtz cage used for exposing microalgae to a magnetic field.

To control and operate the Helmholtz cage we use a custom designed LabView program. There are three LabView application interfaces used to control the different elements of the device as follows:

1. **3D HHC Magnetic Field Controller:** Measures current magnetic field of the earth, and any other disturbances and cancels them, and generates 3-Dimensional DC, Sinusoidal, or Triangular AC magnetic fields up to 1Hz. We specify desired generated magnetic field type and strength through this window.

2. **MMI Rotation Recorder:** Controls platform turn table rotation, and provides the ability to set stepping speed, direction, location, and homing of the turn table. It monitors all magnetometers.
3. **MMI Linear Motion Z Recorder:** Controls linear Z motion, and sets the direction, speed, and distance of axial worm gear traversal in the Z-axis. It monitors all magnetometers.

For the procedure used in studying the effect of the lunar magnetic field, nine treatments of *Chlorella Vulgaris* were exposed to a lunar magnetic field for three different repetitions. These treatments were exposed to a magnetic field of $0.2\mu\text{T}$ over the three axes of the Helmholtz Cage (HHC). Treatments were exposed for different durations, these varied from 60 minutes to 240 minutes. Each exposure duration is a multiple of the previous. The exposure setup used consisted of a set of cardboard boxes to provide the correct elevation towards the uniform magnetic field, and for holding the samples. The samples were aligned inside the cardboard boxes in sets of three. Furthermore, the samples were rotated throughout the exposure duration, at the slowest possible angular speed of 0.005 rev/s , this is due to the very slow rate of lunar angular rotation. This exposure was repeated for six consecutive days. Furthermore, the six-day exposure was repeated in four different blocks of the experiment. Figure 13 shows all nine microalgae samples placed inside the cardboard box inside the cage.



Figure 13. Microalgae samples (Nine Samples) placed in cardboard box inside the Helmholtz Cage.

Operating the Helmholtz cage to conduct the experimental procedure, we started by aligning magnetometer #1 to the center of the turn table. To do so, we manually slid the carriage holding the magnetometers in the X-direction setting its location to the center of the slider marked ruler, subsequently, we did the same procedure to the Y-direction carriage, centering it to the ruler. We then proceeded to inspect the radial alignment of the first magnetometer and verified that it is aligned above the center of the turn table. The verification was done visually, as we did not need precise center placement due to the uniformity of the induced field. Figure 14 shows sliding carriages for both X and Y directions.

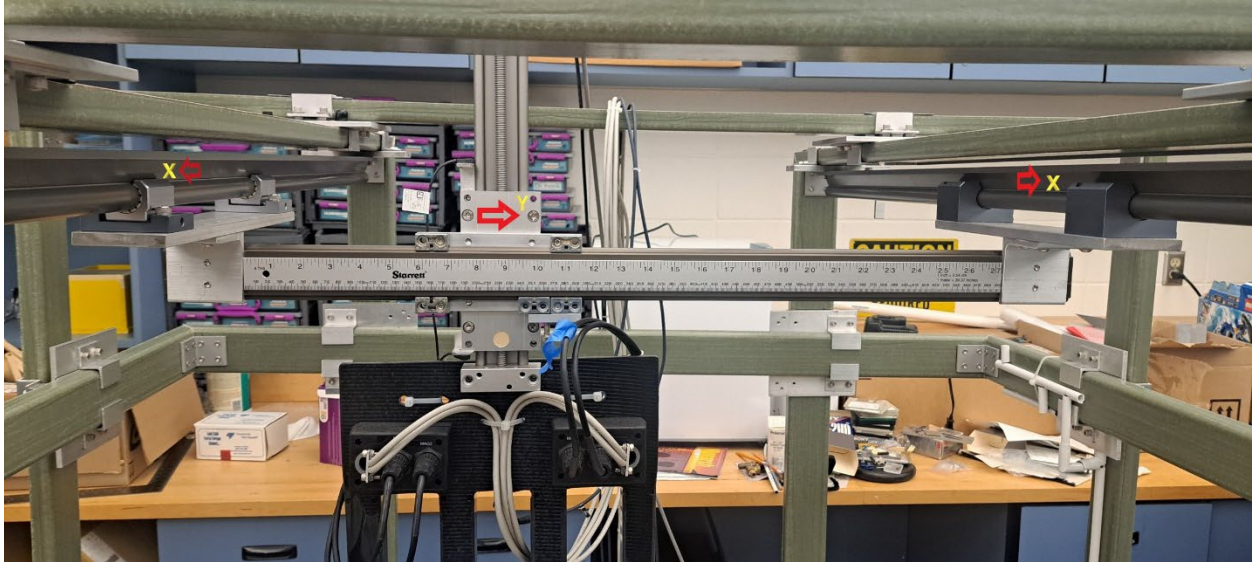


Figure 14. Sliding carriages for X and Y directions showing slider ruler for centering Y-Direction.

After aligning the first magnetometer radially, it was still important to modify the vertical Z-axis distance. However, this distance requires the operation of the vertical worm gear motor setup shown in Figure 15, and Figure 16. To run the motor, we had to do the following:

1. Flip the motors switch found inside the power-supplies chamber as shown in Figure 17.
2. On the connected computer, we ran the “MMI Linear Motion Z Recorder” LabView application.
3. Before triggering any action, we measured the distance from the bottom point of the magnetometer at its current vertical position, to the anticipated top of the microalgae samples, while keeping a clearance distance to reduce the risk of collision with the samples.
4. Inside the application, we entered the required movement distance in millimeters inside of the empty text field next to the “Move to” button as shown in Figure 18.

5. According to the position of the magnetometer, we had to indicate a downward movement direction by clicking on the “Down” button, which is also shown in Figure 18.
6. For accurate movement, we specified the displacement velocity to be half a revolution per second, in the velocity text field next to the “Down” button.
7. To finally trigger motion, we clicked on the “Move To” button, and verified that the worm gear was rotating, and that the magnetometer was moving downward.

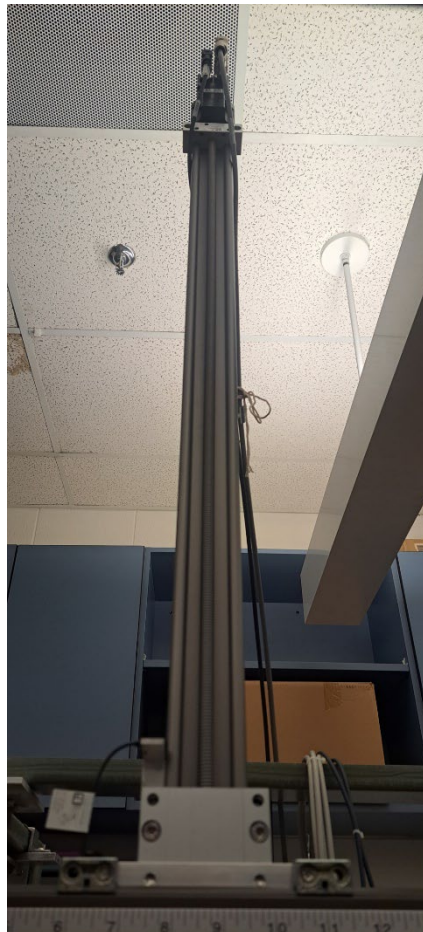


Figure 15. Z-Encoder motor connected to worm gear.



Figure 16. Lower part of worm gear connected to Z-direction carriage.



Figure 17. Vertical Motor Switch Inside Power Supply Cabinet [59].

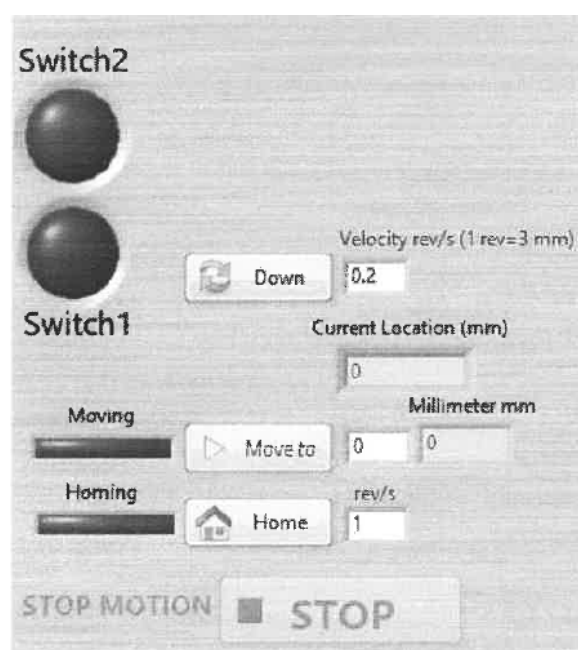


Figure 18. Linear motion motor control parameters section in LabView application.

The next step after alignment was to set the desired DC magnetic field value. For this research, we exposed the samples to a fixed DC magnetic field, while rotating the samples to simulate the changing lunar field. It was possible to achieve the same effect using a rotating AC

magnetic field, nonetheless, it would introduce more complexities in addition to introducing more failure points, hence more factors affecting the experiment. To achieve the intended DC field, we had to follow these steps:

1. Turn on power supply breakers for X, Y, and Z magnetic fields.
2. On the computer, we ran the “3D HHC Magnetic Field Controller” LabView application.
3. It is important to measure and cancel out the earth’s magnetic field, therefore, once the application loaded, we toggled the “Measure Earth Field” toggle button shown in Figure 19, and then proceeded to start execution.
4. Prompted, we used the accompanying zero-gauss chamber provided by the manufacturer as a sleeve over the first magnetometer to specify a zero-gauss field reference reading. The chamber and sleeving process is illustrated in Figure 20.
5. We waited until the application managed to measure the magnetic field of the earth, and then we toggled the “Cancel Earth Field?” button shown in Figure 21 to cancel it.
6. Using the “DC (Oe)” text fields shown in Figure 21, we set the magnetic field in all directions to 0.00158Oe.
7. After the magnetic field was set to the requested field strength, we clicked the “Stop Hold DC” button shown in Figure 22 to stop the DC controller software, while keeping the DC output turned on.

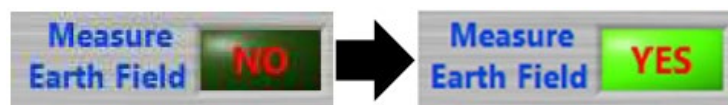


Figure 19. Toggle button for measuring earth’s field before running application [59].



Figure 20. Sleeving of magnetometer using zero-gauss chamber to measure ambient field [59].

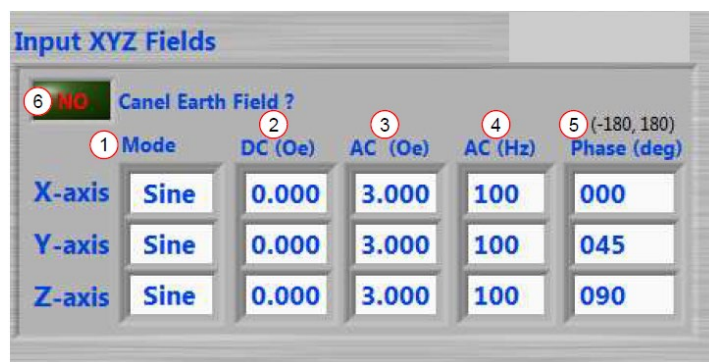


Figure 21. Magnetic Field Strength Input Panel with toggle for cancelling earth field [59].

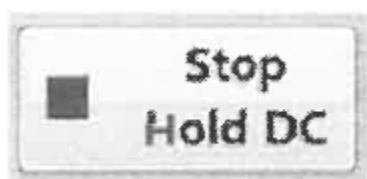


Figure 22. Button to stop DC controller while keeping DC field turned on [59].

Having the magnetic field operational, the only remaining part was to introduce the microalgae samples and start the turn table rotation. This was done by following these steps:

1. We verified that the motors switch previously shown in Figure 17 is correctly flipped to the “On” position.
2. On the computer, we ran the “MMI Rotation Recorder” LabView application.
3. Inside the application, we used the text field next to the “CCW” button to specify the angular velocity of rotation at the lowest possible value of 0.005 rev/s. This is the lowest angular speed of the motor. Figure 23 shows the rotation motor control parameters where we specified velocity.
4. Having the motor support rotation for a specified number of steps and intending to run the experiment for four hours without having an option to do so in the interface, we had to calculate the number of required steps to run for this total time. We were able to do so as follows:
 - a. Determine the smallest angle of rotation per step θ according to the device manual

$$\theta = 0.0074 \frac{Deg}{Step}$$

- b. For a full revolution, calculate the total number of steps

$$\begin{aligned} Steps_{revolution} &= \frac{Full\ Revolution\ in\ Degrees}{Degrees\ per\ Step} \\ &= \frac{360^\circ}{0.0074} \cong 48649\ Step\ per\ one\ revolution \end{aligned}$$

- c. Using the angular velocity, we calculate the number of revolutions for a total of four hours

$$\begin{aligned} \text{Number Revolutions}_{total} &= \text{Velocity} \times \text{Experiment time (seconds)} \\ &= 0.005 \times 14400 \\ &= 72 \text{ Revolutions} \end{aligned}$$

- d. Calculate the total number of steps for the required number of revolutions for the experiment time

$$\begin{aligned} \text{Steps}_{total} &= \text{Number of Revolutions} \times \text{Steps per Revolution} \\ &= 72 \times 48649 \\ &= 3502728 \text{ Steps} \end{aligned}$$

5. Based on the calculations we did in the previous step, we specified the total number of steps to rotate in the text field next to the "Move to" button.
6. Having the turn table rotation system configured correctly, and while the magnetic field is also operational, we introduced nine samples in sets of three, and placed them inside a carton box fitted over the turn table as previously shown in Figure 13.
7. To not let the samples be exposed for longer than intended, we proceeded to immediately start the table rotation by clicking on the "Move to" button shown in Figure 23.

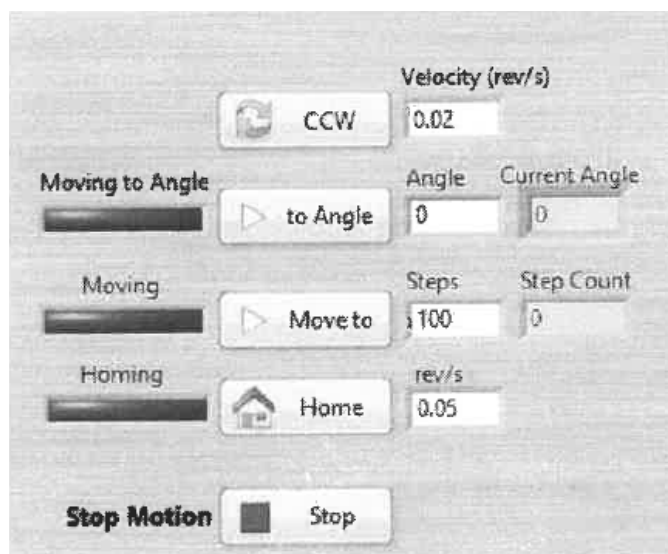


Figure 23. Rotary motor control parameters configuration LabView interface [59].

After configuring and running the Helmholtz cage, all nine samples of microalgae were exposed for a period of 60 minutes. After this time elapsed, three samples labelled for their exposure time, one of each exposure medium, were removed. The exposure resumed for another 60 minutes for a total of 120 minutes. Three additional time labelled samples of each exposure medium were removed after this time elapsed. The remaining samples were left exposed for another 120 minutes for a total of 240 minutes and were then removed.

Ensuring a consistent experimental environment, a special rack was prepared to keep exposure samples after they are exposed for the allotted time. Control samples were placed on the rack before the exposure started. This rack was placed in a room with ample light. Upon finishing the exposure, all samples were transferred from the temporary rack to the algae cultivation chamber and kept under the same temperature and light intensity as the initial algae

cultures. We repeated sample exposures for 6 consecutive days while measuring the Beta-Carotene and Protein content in a schedule of every third and fourth day for twenty-one days.

CAROTENOID (BETA CAROTENE) EXTRACTION

The method of extraction of beta carotene borrows from different processes mentioned in multiple different studies [60], [61], [62], [63], [64]. We had to do some experimental work to verify a process that extracts most of the carotenoid. Sodium hydroxide and potassium hydroxide were tested for their efficacy in facilitating cell lysis. Milli-Q Water, BBM, and BBM plus different weights of lunar regolith were used to dilute these solutions; separate tests were carried out using each of the diluents. Potassium hydroxide turned out to have a better outcome. Diluting medium did not seem to affect the extraction as much, despite that, small variations in color and optical density readings were seen. Nevertheless, both visual and quantitative variances were negligible.

To carry out the extraction process we used 50ml volume plastic tubes, one for each exposure. Having 12 exposures we utilized 12 tubes in total. We did this beta carotene extraction procedure in correlation with the exposure pattern that was done for the microalgae, where not all 12 samples were analyzed for beta carotene in the same day. From each exposure 20 ml of algae was poured into their labelled tubes, and then centrifuged at a speed of 7500 RPM for 15 minutes to separate the biomass from the base medium, allowing the use of a different base medium. After centrifuging, the supernatant was discarded and about 10 grams of green algae biomass was left in each tube. We added 5ml of Milli-Q water to the biomass as a new base medium. This allowed for saving quite a bit on the base mediums of algae that were proposed as diluents. The tubes were slightly shaken by hand to unstick any algae in the bottom, then tubes

were left to agitate for 15 minutes in the incubator shaker. Following that, 0.2 grams of Potassium Hydroxide (KOH) pellets were weighted on a microscale, for each sample. The weighted Potassium Hydroxide pellets, in addition to 2ml of Pure Ethanol were added to each sample tube. Tubes were given a quick shake by hand to mix up the KOH pellets with the Ethanol and Algae-Milli-Q solutions and were put to sonicate in an ultra-high frequency sonicator for 30 minutes to facilitate the degradation of the *Chlorella V.* cell wall. After sonication, the samples were vortexed using the Fisher Scientific Fixed Speed pressure operated Vortex Mixer for about 30 seconds then left to agitate in the shaking table at a table shaking rotation speed of 200 RPMs for a period of 24 hours.

After 24 hours, samples were taken out and we pipetted 6ml of hexane into each tube. The tubes were given a quick shake by hand and were put back in the incubator shaker for 5 minutes. Samples were then transferred to be centrifuged at 7500 RPM for 15 minutes to separate the hexane layer, as it is a hydrophobic non-polar organic solvent, hence its usability to extract beta-carotene, a non-polar molecule. While the centrifuge was running, the Unico-Fisher S-1100 spectrophotometer was turned on and was left to warm up for 15 minutes as per the instructions. After the spectrophotometer was ready, it was configured to measure absorbance at a wavelength of 448nm then blanked with 3ml of hexane. When the centrifuge was done, a very yellow layer of beta carotene pigment was noticed as shown in Figure 24. Samples were then taken to be measured. 3ml of sample size was used to measure the optical density of each exposure beta carotene sample, in accordance with the volume of blank used. Measurement cuvettes were washed with MilliQ water three times between each exposure sample measurement.



Figure 24. Tubes showing a yellow layer of extracted Beta-Carotene from samples.

For quantifying the amount of beta carotene present within the samples, we had to utilize a beta-carotene standard to plot a standard curve, which would allow us to convert the optical density measurements into actual beta-carotene concentrations. In our work, we utilized a synthetic $\geq 93\%$ purity standard produced by Sigma-Aldrich [65], which comes in powder form of dark red to brown color. The powder has a hexane solubility of 1.1 mg/mL.

Preparing the standard curve, we created multiple dilutions of the initial concentration of the standard. Anticipating having at least three different O.D measurements per diluted sample, we proposed a 12ml sample for each dilution, as each O.D measurement would utilize around 3ml in the cuvette. Six different dilutions were proposed as shown in Table 9. Initial dilution concentration is based on the hexane solubility of the standard. Therefore, the amount of beta-carotene present in the non-diluted standard for 12 mL of hexane was calculated according to the following:

$$\text{Beta - Carotene amount}_{12 \text{ mL}} = \text{Volume of Hexane Medium} \times \text{Hexane Solubility}$$

$$= 12 \text{ mL} \times 1.1 \frac{\text{mg}}{\text{mL}} = 13.2 \text{ mg}$$

Table 9. Beta-Carotene standard Dilutions Chart.

Dilution Factor	Concentration	Beta-Carotene Amount (12ml)	Dilution
1x	1.1 mg/mL	13.2 mg	12 mL Hexane
2x	0.55 mg/mL	6.6 mg	(6mL 1x) + 6 mL Hexane
4x	0.275 mg/mL	3.3 mg	(3mL 1x) + 9 mL Hexane
8x	0.1375 mg/mL	1.65 mg	(1.5 mL 1x) + 10.5 mL Hexane
16x	68.75 ug/mL	825 ug	(750 uL 1x) + 11.25 mL Hexane
32x	34.375 ug/mL	412.5 ug	(375 uL 1x) + 11.625 mL Hexane

To prepare the initial concentrated solution and having to accommodate for dilutions made from the 1x solution, we mixed 25ml of Hexane with the beta-carotene powder mixture by dispensing 27.5 mg (25 ml * 1.1 mg/mL) of the powder into a 50 ml plastic tube with a cover, and then added the hexane. We then replaced the cover of the tube and gave it a robust shake to ensure that the powder was dissolved. To further ensure the dissolution of the powder, we vortexed the solution for 30 seconds. From this solute the dilutions were made by adding specific volumes of hexane to the concentrated standard solute as shown in the previous Table 9. Figure 25 shows the resulting dilutions of the Beta-Carotene standard.

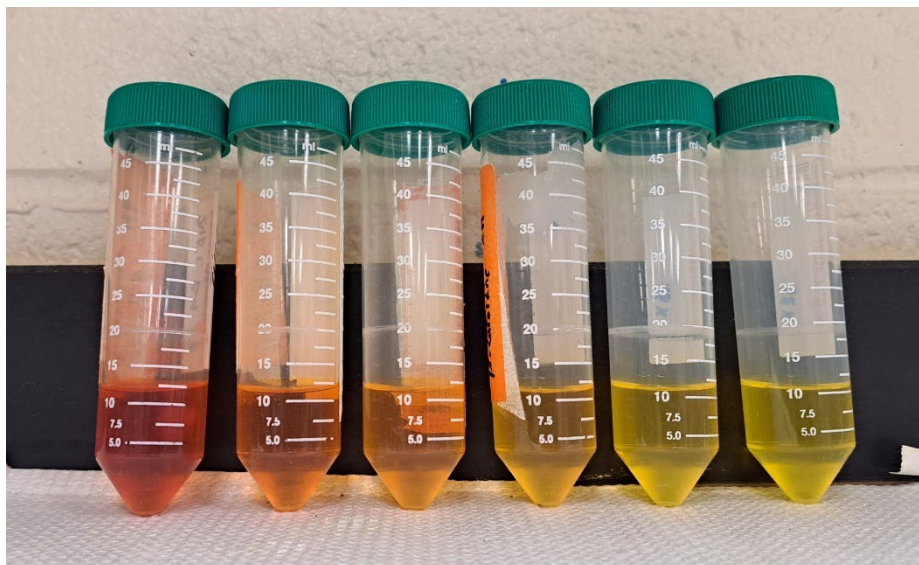


Figure 25. Samples containing dilutions of Beta-Carotene standard.

To plot the standard curve, we measured the optical density for each dilution proposed using the Unico spectrophotometer. We used the same blanking procedure by using 3 ml of hexane as a blank in the cuvette. After blanking, the cuvette was washed three times using MilliQ water and then dried with compressed air and laboratory tissues. For each sample, we would use 3 ml in the cuvette, place it inside the measurement chamber of the UNICO device, and measure the O.D. We made sure to wash the cuvette three times with MilliQ water between each measurement attempt. For each sample, we took three measurements by putting the cuvette in the chamber, closing the chamber door, reading the value, taking the sample out, and then repeating the process with the same sample. The average for each sample O.D measurements was then associated with the amount of beta-carotene concentration per sample by plotting them as points on a graph, where the X-axis is the beta-carotene concentration in mg/mL, and the Y-axis corresponds to the O.D measurement value. A curve was then fitted for the plotted

points forming a reference for determining any unknown sample concentration. Based on the produced standard curve, the concentration of unknown samples measured in each block were then determined. We determined the concentration by taking the measured O.D for each exposure in each nutrition medium sample and interpolated the corresponding beta-carotene amount.

PROTEIN EXTRACTION

Protein produced by microalgae specimens was extracted and analyzed. The process was done by centrifuging 10 ml of microalgae of each exposure sample of every medium in a 50 ml plastic tube for 15 mins at 7500 RPM. In some of the analysis days, we had to put two different batches in the centrifuge, because it can only support up to six tubes, where we had to do the analysis for twelve tubes. Post centrifuging the supernatant was discarded, leaving around 10mg of dry biomass. Two milliliters of 0.5M Sodium Hydroxide (NaOH) was added to the dry biomass in each sample tube to induce breaking of the cell wall. The tubes were given a shake to mix the contents and were put to sonicate in the ultra-high frequency sonicator for 30 minutes. After sonication, samples were centrifuged for 15 minutes at a speed of 7500 RPM. This was done to separate the protein extract from cell wall and biomass leftovers. The resulting supernatant was green in color.

To quantify the amount of protein present within each sample. The Bradford method was used [66], [67], [68], [69], [70], [71], [72], [73], [74], [75], [76]. This method is a way to obtain the concentration of protein present in a sample based on the concept of shifting in absorbance from 465nm to 595nm established through the binding of the Coomassie blue dye to the protein.

Following this method, we started the analysis by transferring the previously obtained supernatant to clean chemical ware; that is in plastic tubes of 50 ml volume for each exposure sample. To achieve a protein concentration analysis value that is in the linear Bradford reagent response range, we had to dilute our samples. The supernatant was diluted to 60x its concentration by adding 2.95ml of Sodium Hydroxide (NaOH) to 50uL of the supernatant. 1ml of Bradford Reagent from Millipore Sigma was added to the diluted samples using a pipette. Immediately, the samples gave a blue hue. Figure 26 shows our samples. Yet, according to the Bradford method, they should be incubated for at least five minutes before proceeding with any measurements. The samples were inverted five times to avoid foaming and left for ten minutes to allow for the complete binding of the assay to the protein [66]. Optical Density was then measured using a NanoDrop One [77] spectrophotometer at a wavelength of 595nm. The spectrophotometer was blanked with a 1.8uL drop of NaOH. A standard protein reference was needed to be able to estimate the amount of protein present in our unknown samples.

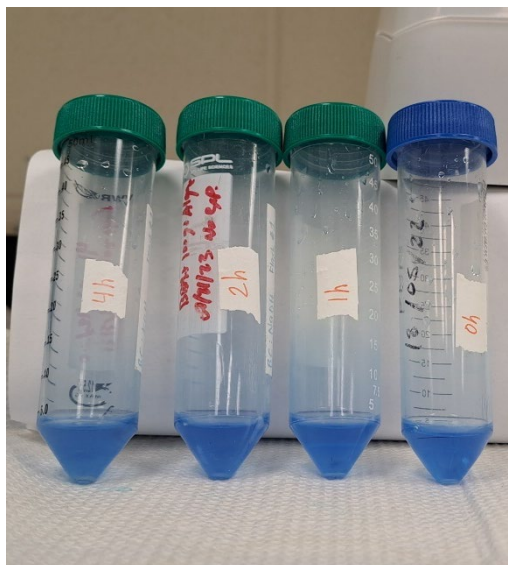


Figure 26. Resulting protein samples after adding Bradford reagent.

For the standard protein reference, the BSA protein standard from Sigma-Aldrich is used [78]. This standard comes as a set of 10 glass ampules with the protein solution. The use of this protein to carry out the quantification is very well accepted due to its superb binding to the Bradford reagent assay. A similar Bradford process is carried out on a standard solution, where the optical density of a range of different concentrations of the standard are measured. This results in a standardized curve that can be used to quantify and estimate the amount of protein per sample.

The preparation of the standard reference is done by diluting the initial standard concentration of the reference. Table 10 shows the set of proposed dilutions. 10 mL of the initial standard concentration is prepared to ensure an adequate amount for successfully performing serial dilutions. NaOH is used as a dilution buffer. Proposed concentrations are achieved by pipetting the specified amount of NaOH for each concentration level according to Table 10 and

adding it to separate plastic tubes with the specified volume of the initial standard concentration for a total volume of 3 ml. In each of the dilution tubes 1 ml of the Bradford reagent dye is added to the 3 mL of the protein, resulting in a total volume of 4 mL. Upon adding the Bradford reagent, a blue hue develops. After adding the reagent, the tubes are inverted 5 times to avoid any foaming, and they are left for 10 minutes to incubate, as previously done with the experiment samples. The optical density of prepared standards is then measured using the NanoDrop One spectrophotometer. NaOH is used as a blanking buffer, where a 1.8 uL drop is used. A set of three measurements is taken per sample to produce an average. Measured optical density averages are then correlated to the concentration of protein present per sample. For each measurement value a point is plotted on a graph, where the X-axis corresponds to the concentration of protein present per sample in mg/mL, and the Y-axis corresponds to its measured O.D. A curve is fitted according to the resulting points, and a relation is developed. Through the resulting curve, measured optical densities of the samples are interpolated for their respective protein concentration in mg/mL.

Table 10. BSA Protein standard Dilutions Chart.

BSA Concentration	Dilution
0.25 mg/mL	(375 uL of 2mg/mL) + 2.625 mL NaOH
0.5 mg/mL	(0.75 mL of 2mg/mL) + 2.25 mL NaOH
1.0 mg/mL	(1.5 mL of 2mg/mL) + 1.5 mL NaOH
1.4 mg/mL	(2.1 mL of 2mg/mL) + 0.9 mL NaOH
2 mg/mL	(3 mL of 2mg/mL) + 0 mL NaOH

CHAPTER IV

RESULTS AND DISCUSSION

Carrying out the experimental work described in the procedure, it is important to investigate the resulting data for the purpose of discussing the question of effects of the Lunar environment, and how the different experimental factors examined affect the *Chlorella Vulgaris* microalgae. In this section, the results of the experimental works are laid out in tables and figures to provide a visual and quantitative representation. Moreover, this section discusses these results, and attempts to infer their meaning for further understanding. The results shown in this section correspond to two experimental blocks executed subsequently following the experimental design. Each block is listed in its own subsection, nonetheless, a section discussing the results based on both blocks is provided.

EXPERIMENTAL BLOCK 1

This section lists results obtained in the first experimental block.

Growth as optical density values

To determine growth of microalgae over the period of 21 days of the experiment, and after the 6 days of exposure, we attempted to measure the optical density for each exposure sample over a few days for the whole period. It was not possible to do the measurement every third day due to the excessive amount of time needed to do the beta carotene and protein extraction procedures. Moreover, not having a spectrophotometer within the same lab, and having to carry the samples to another lab without the presence of other team members deemed the process to be difficult to do frequently. The following tables, Table 11, Table 12, and Table 13

list the data resulting from measuring the optical density of the *Chlorella Vulgaris* microalgae in different nutrition mediums to assess its growth, where the first measurement day resembles the initial optical density achieved when mixing the algae with the nutrition mediums before exposure. Later measurements correspond to days during and after exposure. Error measurements provided resemble standard deviation obtained from three measurements of the same value. Figure 27, Figure 28, and Figure 29 illustrate the timeline of growth of the microalgae.

Table 11. Optical Density Measurements for *Chlorella V.* growth in BBM only.

Exposure	Day 1	Day 3	Day 9	Day 15	Day 21
0 m	0.180 ± 0.000	0.208 ± 0.045	0.261 ± 0.033	0.216 ± 0.014	0.210 ± 0.020
60 m	0.208 ± 0.003	0.187 ± 0.014	0.206 ± 0.027	0.196 ± 0.007	0.153 ± 0.003
120 m	0.186 ± 0.012	0.200 ± 0.033	0.202 ± 0.010	0.165 ± 0.007	0.121 ± 0.008
240 m	0.171 ± 0.012	0.215 ± 0.019	0.233 ± 0.026	0.121 ± 0.005	0.115 ± 0.006

Table 12. Optical Density Measurements for *Chlorella V.* growth in BBM + 100g lunar regolith.

Exposure	Day 1	Day 3	Day 9	Day 15	Day 21
0 m	0.204 ± 0.017	0.187 ± 0.038	0.238 ± 0.038	0.237 ± 0.036	0.151 ± 0.016
60 m	0.186 ± 0.008	0.217 ± 0.007	0.257 ± 0.039	0.187 ± 0.004	0.195 ± 0.014
120 m	0.206 ± 0.010	0.188 ± 0.004	0.275 ± 0.031	0.189 ± 0.007	0.123 ± 0.003
240 m	0.177 ± 0.013	0.192 ± 0.016	0.192 ± 0.013	0.152 ± 0.004	0.148 ± 0.005

Table 13. Optical Density Measurements for *Chlorella V.* growth in MilliQ + 100g lunar regolith.

Exposure	Day 1	Day 3	Day 9	Day 15	Day 21
0 m	0.196 ± 0.003	0.160 ± 0.021	0.179 ± 0.026	0.120 ± 0.012	0.099 ± 0.013
60 m	0.183 ± 0.014	0.149 ± 0.024	0.135 ± 0.022	0.139 ± 0.008	0.101 ± 0.017
120 m	0.183 ± 0.008	0.175 ± 0.013	0.125 ± 0.010	0.085 ± 0.006	0.055 ± 0.005
240 m	0.180 ± 0.005	0.180 ± 0.006	0.110 ± 0.006	0.077 ± 0.002	0.082 ± 0.007

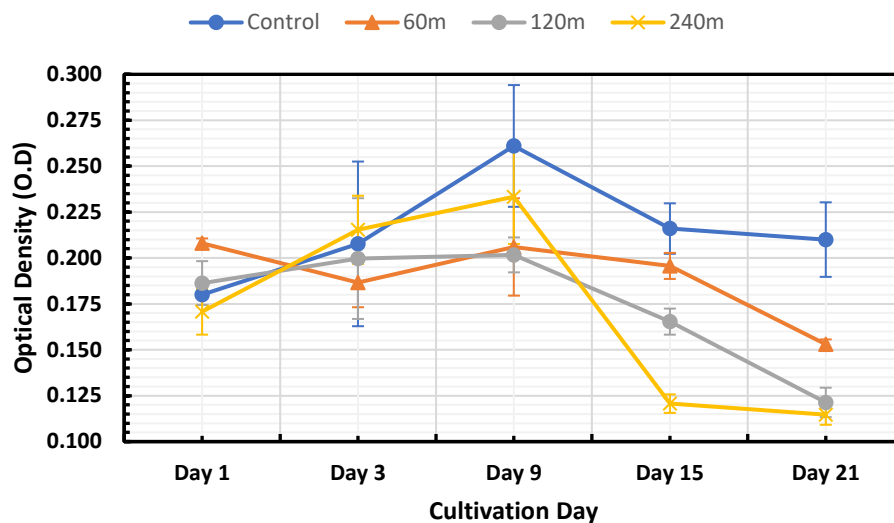


Figure 27. Measured Optical Density timeline for *Chlorella V.* exposures growth in BBM (Block 1).

Looking at the BBM medium growth graph shown in Figure 27, it is noticed that albeit all cultures starting from approximately the same optical density, their growth tends to peak at different values. Based on the graph, all samples tend to peak at the 9th day of cultivation, nonetheless, it can be seen that both the Control samples, and the samples exposed to the magnetic field for the longest time of 240 minutes, tend to have the highest growth amount as reflected by their measured optical density. In comparison, the 60 minutes exposure culture, and the 120 minutes exposure samples peak at lower growth values. Having all exposures peak at the same day is an indicator of a consistent growth cycle performed by *Chlorella Vulgaris*. The control culture nonetheless is superior to others, as it sits at a discrepancy of between ~ 0.025 to ~ 0.060 from its closest and furthest exposure samples measurements, respectively. Another observation is the almost equal peak value for both the 60 minutes and 120 minutes culture. Such superiority from the control culture can be simply referred to the growth capability of the microalgae in its

natural state with no reactions to external affecters, as both the required medium and conditions are met. However, for the case of the prolonged exposure of four hours (240 minutes), the magnetic field seems to introduce a stressing agent. Now, in comparison to both the 60-, and 120-minutes exposures, the latter seem to be severely affected. This discrepancy between prolonged exposure samples and less exposed samples tend to provide a clue. It could be hypothesized that a stress adaptation response is undergoing effect, where the prolonged exposure (240 minutes) sample has eventually adapted with the magnetic field, but the 60- and 120-minutes samples have still yet to manage to do so, their growth value equality indicates a non-linear relationship for the adaptation effect. Another indicator of such effect could be inferred from later growth stages, where at day 15 optical density measurements, and hence growth amount, are ordered based on exposure time from highest at control to lowest at 240 minutes. A possible occurrence due to a negative external effect. This extends further until Day 21.

A striking similarity in growth degradation slope from Day 15 to Day 21 exists between Control and 240 minutes solely, and between 60 minutes and 120 minutes. The last average measured value for the 120 minutes exposure at Day 21 seems to be equal to one measured for 240 minutes. Having such similarity in slope resembles another lurking factor, which seems to be the amount of nutrients exhausted and available for each sample, and it seems that this factor is interrelated to the stress response hypothesized earlier. A strong supporting evidence resides in the steep drop in the 240 minutes exposure OD from Day 9 to Day 15, which could refer to an attempted compensation of nutrients to the adapted growth stress response, as such extreme drops do not exist for all other exposure samples, albeit the increase drop in slope for each exposure from the 60 minutes to the 240 minutes samples. Moreover, the almost horizontal

constant slope for the 240 minutes exposure between Day 15 to 21 seems to resemble stability in growth due to the earlier nutrient exhaustion caused by the stress response, in addition to the already established adaptability, which does not seem to hold for the 60- and 120-minutes exposures as they are still exhausting more nutrients in their adaptation attempts. Also, the increasing slope steepness for each exposure time respectively enhances the idea of increased nutrients exhaustion due to increased adaptability to stress in relation to increasing magnetic field exposure times. Where the most prolonged exposure managed to reflect a growth enhancement response at the expense of nutrients, and the not exposed enough samples were affected negatively from the stress as they are not given enough time to adapt before the exposure ends and they are relieved from stress before being exposed and stressed again, hence having an increasing but not a similar nutrient exhaustion rate.

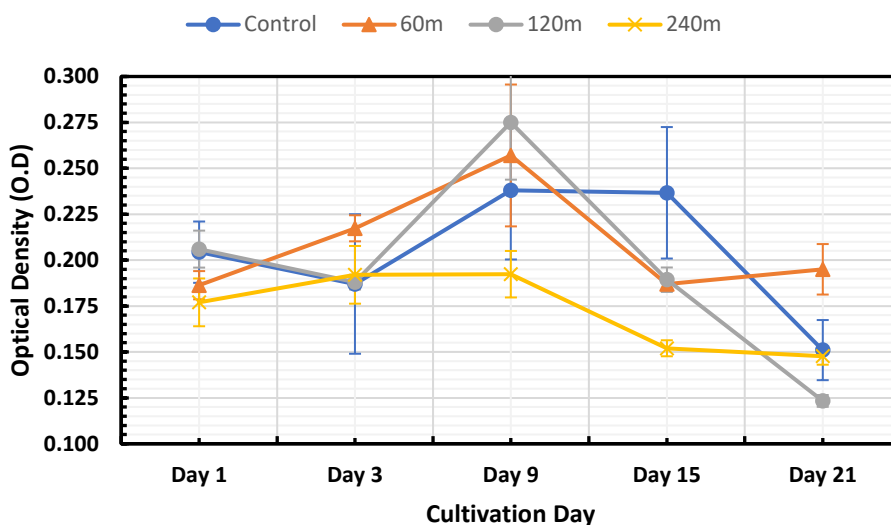


Figure 28. Measured Optical Density timeline for *Chlorella V.* exposures growth in BBM + 100g lunar regolith (Block 1).

In regard to the case of BBM nutrition medium augmented with 100g of lunar regolith simulant, all samples are still peaking at Day 9. However, the less exposed samples tend to have higher peak values than both the control and prolonged exposure (240 minutes) samples. This is peculiar since in the BBM only case these two samples had highest growth. Considering that the only changing factor is the presence of the lunar regolith, it could be understood to be an affecter. One can think of the existence of an interaction between the regolith and the field exposure; however, the nature of that relation cannot be inferred. It seems that the higher the exposure time, the higher the yield until to a certain point, where the yield degrades drastically. More exposure points need to be studied for determining this relation: both extensively prolonged, and barely exposing. Referring to the proposed idea of nutrition exhaustion in relation to growth peak, we can see that it still holds. This can be understood from the decreasing slopes of the exposures ordered by highest yielding (120 minutes).

Now, the constant slope part of the control samples from day 9 to day 15, might indicate growth stagnation, and then death of microalgae culture after that time until day 21 because of the presence of the regolith. This was the same for Day 15 to Day 21 for all other exposure samples.

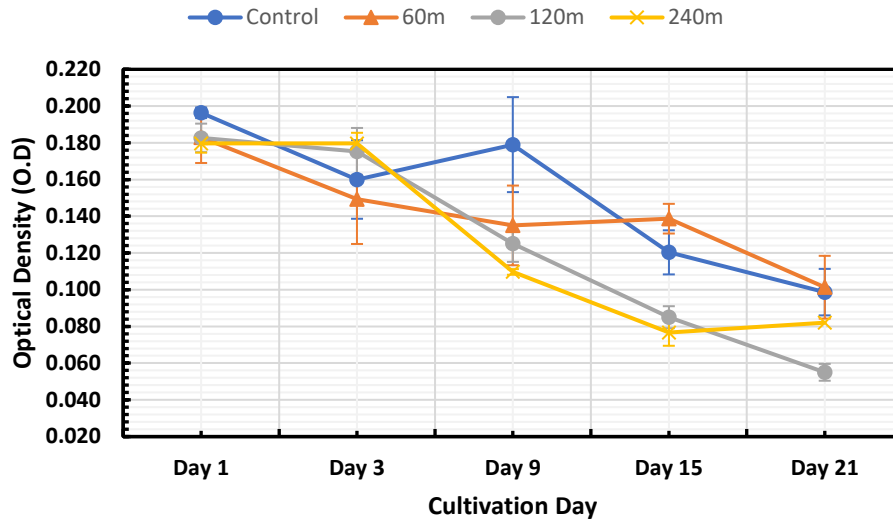


Figure 29. Measured Optical Density timeline for *Chlorella V.* exposures growth in MilliQ + 100g lunar regolith (Block 1).

For the MilliQ case, all trends are shown to be decreasing. Such a result is expected, as there is no nutrition medium for the microalgae to use, which would provide us an understanding of how capable the lunar regolith of providing enough nutrients, and until now it seems to not be capable of providing any, as all trends are down.

However, examining the graph carefully, one could notice a growth bump, or an abrupt change in growth slope at certain cultivation days of each algae exposure. This bump seems to start in the middle at Day 9 with the control and then moves to the right and is delayed until Day 15 for the 60 minutes exposure, then it moves to the left to be triggered earlier for more exposed samples. This bump might indicate the potential of the algae to attempt growth regardless of the medium and the environment. Moreover, relating this abrupt change to EMF exposure times, it seems that low exposure (resembled by the 60 minutes samples) delays this abrupt change, whereas at a certain point, more exposure leads to this abrupt change earlier. Testing with

intermediate levels of exposure times would allow us to determine the validity of this inference. A higher granularity experiment in terms of both days and exposures would be able to determine the validity of this inference.

Noticing a decay pattern, it struck me the potential of trying to reason the presence of multiple affecting factors mathematically by trying to find out what type of curve would fit. A logarithmic or exponential curve might not be especially useful. However, polynomial relations higher than the 2nd degree could possibly point towards other factors involved. A cubic relation can possibly indicate that instead of having one variable cubed, one variable could be of 2nd degree, and is multiplied with a different variable. Attempting to produce a fitting trendline for each of the curves using Microsoft Excel™, all exposures turned out to truly follow a polynomial decay pattern either before or after the abrupt change in growth. I considered two approaches for producing these trendlines, the first is by separating parts before and after the abrupt change and fitting each with an independent trendline; this resulted in different quadratic polynomials for each of the parts for all exposures. For the second approach, I included the whole growth curve from Day 1 to Day 21. The only polynomials that would fit such a curve were of fourth degree. While this could possibly hold true, it seems most unlikely, and it would be more logical to consider a multivariable trendline, hence a varying response plane, which in turn hints towards the effect of the medium and the exposure. Logarithmic and exponential trendlines were found to be very close fits in the first approach, yet polynomials had superior adequacy. Resulting trendlines are described in Table 14, and Table 15 based on each approach taken. Overall, it seems that both nutrients and magnetic field exposure play a role in determining growth.

Table 14. Trendlines produced for the two parts before and after abrupt change points for each exposure.

Exposure	Abrupt change point	Trendline Before	Trendline After
0	Day 9	$0.0277x^2 - 0.1193x + 0.288$	$-0.0205x^2 + 0.0652x + 0.0903$
60	Day 15	$0.0093x^2 - 0.0614x + 0.285$	$-0.0373x + 0.176$
120	Day 3	$-0.0073x + 0.19$	$0.0051x^2 - 0.0655x + 0.2358$
240	Day 3	0.1797 (<i>constant</i>)	$0.0188x^2 - 0.1268x + 0.2877$

Table 15. Overall trendlines produced for the whole curve for each exposure.

Exposure	Abrupt change point	Trendline
0	Day 9	$0.0103x^4 - 0.1254x^3 + 0.5218x^2 - 0.8791x + 0.6687$
60	Day 15	$-0.0024x^4 + 0.0238x^3 - 0.0731x^2 + 0.055x + 0.1797$
120	Day 3	$-0.0022x^4 + 0.0313x^3 - 0.1531x^2 + 0.2668x + 0.04$
240	Day 3	$-0.0044x^4 + 0.0619x^3 - 0.2961x^2 + 0.5213x - 0.103$

Effects on Beta-Carotene

Interested in the effect of the lunar environment on the *Chlorella Vulgaris* microalgae, it is important to investigate results affecting its growth. Nonetheless, although the microalgae might be growing, its internal elements might be affected, such as its pigments and bio-active compounds (protein). The following results demonstrate the measured optical density of extracted beta-carotene pigment for block 1. Table 16 provides optical densities measured for the extracted beta-carotene from exposures cultivating in BBM only nutrition medium, Table 17 provides optical densities for BBM + 100g lunar regolith nutrition medium, and Table 18 provides optical densities for MilliQ + 100g lunar regolith nutrition medium. Error measurements provided in tables resemble standard deviation obtained from three measurements of the same value.

Visually, Figure 30 illustrates measured O.D for extracted Beta-carotene from BBM only exposures, Figure 31 illustrates these measurements for BBM + 100g lunar regolith exposures, and Figure 32 illustrates these measurements for the MilliQ + 100g lunar regolith exposures.

Table 16. Extracted Beta-Carotene Optical Density Measurements for *Chlorella V.* growth in BBM only (Blanked with Hexane).

Exposure	Day 3	Day 7	Day 10	Day 14	Day 17	Day 21
0 m	0.015	0.042	0.037	0.025	0.030	0.023
	± 0.001	± 0.001	± 0.001	± 0.003	± 0.001	± 0.001
60 m	0.008	0.035	0.052	0.017	0.019	0.017
	± 0.001	± 0.001	± 0.001	± 0.002	± 0.001	± 0.001
120 m	0.006	0.036	0.042	0.012	0.007	0.004
	± 0.001	± 0.001	± 0.000	± 0.002	± 0.001	± 0.001
240 m	0.008	0.042	0.029	0.016	0.008	0.000
	± 0.001	± 0.000	± 0.000	± 0.000	± 0.001	± 0.000

Table 17. Extracted Beta-Carotene Optical Density Measurements for *Chlorella V.* growth in BBM +100g lunar regolith (Blanked with Hexane).

Exposure	Day 3	Day 7	Day 10	Day 14	Day 17	Day 21
0 m	0.038	0.037	0.043	0.023	0.023	0.023
	± 0.001	± 0.001	± 0.000	± 0.002	± 0.001	± 0.001
60 m	0.036	0.042	0.050	0.019	0.016	0.014
	± 0.001	± 0.001	± 0.000	± 0.000	± 0.001	± 0.001
120 m	0.051	0.014	0.036	0.013	0.011	0.011
	± 0.001	± 0.001	± 0.001	± 0.002	± 0.001	± 0.001
240 m	0.037	0.020	0.034	0.011	0.010	0.005
	± 0.001	± 0.001	± 0.000	± 0.001	± 0.001	± 0.001

Table 18. Extracted Beta-Carotene Optical Density Measurements for *Chlorella V.* growth in MilliQ +100g lunar regolith (Blanked with Hexane).

Exposure	Day 3	Day 7	Day 10	Day 14	Day 17	Day 21
0 m	0.018 ± 0.001	0.013 ± 0.001	0.010 ± 0.001	0.014 ± 0.000	0.016 ± 0.001	0.017 ± 0.001
60 m	0.017 ± 0.002	0.018 ± 0.001	0.011 ± 0.000	0.012 ± 0.000	0.012 ± 0.001	0.017 ± 0.001
120 m	0.016 ± 0.001	0.014 ± 0.001	0.008 ± 0.000	0.011 ± 0.000	0.010 ± 0.001	0.011 ± 0.000
240 m	0.019 ± 0.001	0.015 ± 0.001	0.007 ± 0.000	0.009 ± 0.001	0.008 ± 0.001	0.008 ± 0.001

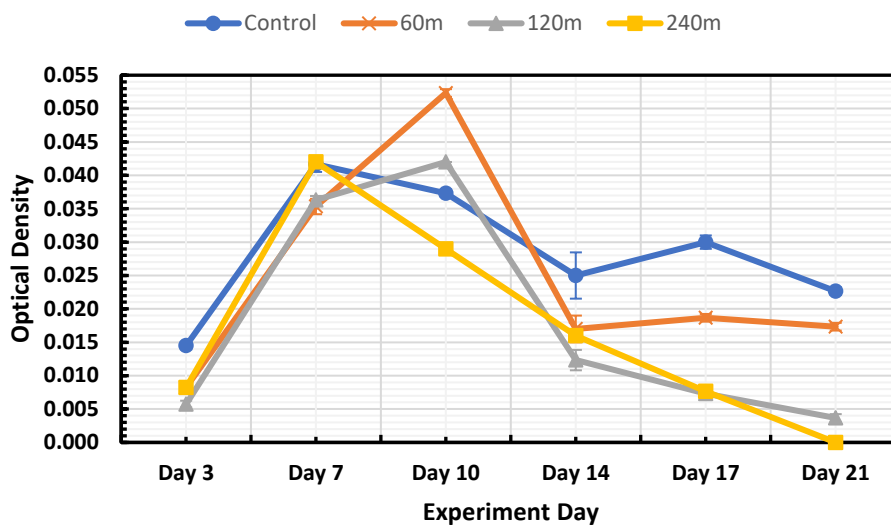


Figure 30. Measured Optical Density timeline for extracted Beta-carotene from exposures in BBM (Block 1).

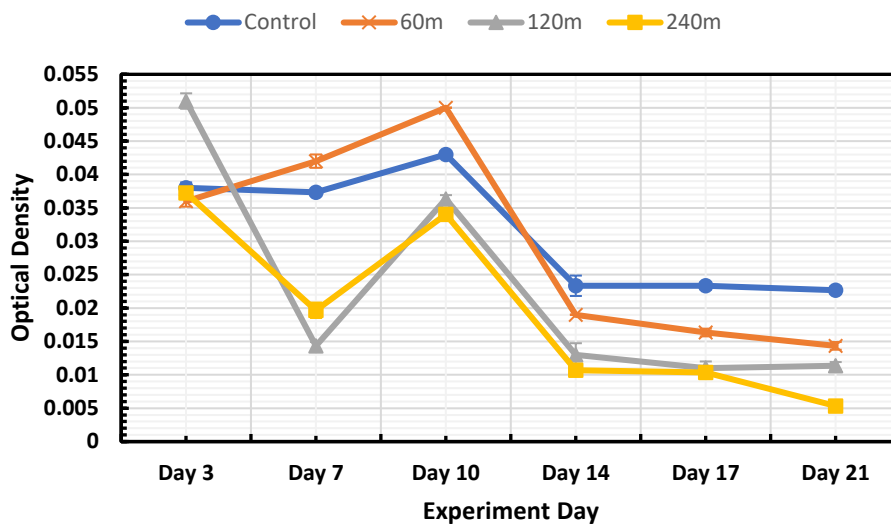


Figure 31. Measured Optical Density timeline for extracted Beta-carotene from exposures in BBM + 100g lunar regolith (Block 1).

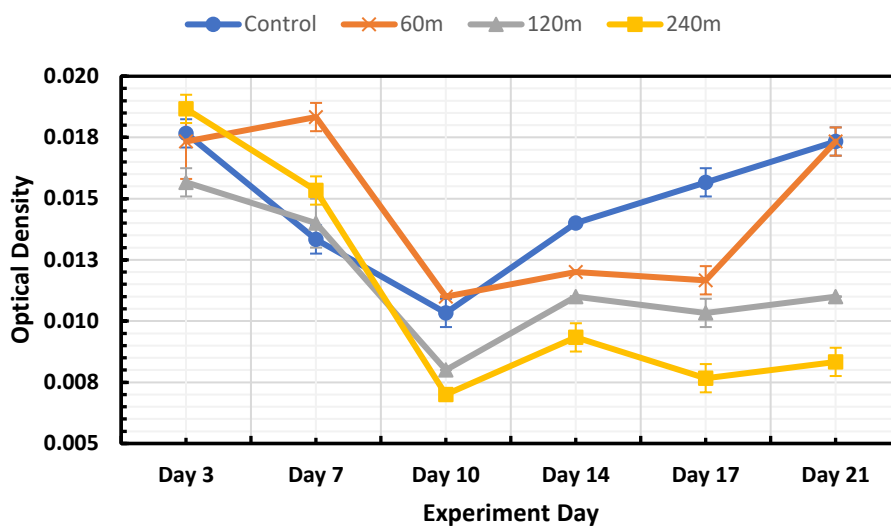


Figure 32. Measured Optical Density timeline for extracted Beta-carotene from exposures in MilliQ + 100g lunar regolith (Block 1).

In the case of Beta-carotene presence and concentration, the results are generally consistent regardless of exposure time or nutrition medium. Looking at Figure 30, Figure 31, and Figure 32, all lines follow the same path despite the change in their levels.

Similar to what was seen in the BBM growth graphs, the Control and 240 minutes exposures tend to have their peak beta-carotene concentrations on Day 7, where the 60 minutes and 120 minutes exposures tend to have their peaks on Day 10. From such a grouping, which was also present in the growth graphs, we can hypothesize that no exposure (control) and prolonged exposure (240 minutes) might be similar. Because the no exposure case, for which was never exposed to EMF is peaking at Day 7, the 240 minutes prolonged exposure sample could have adapted to the EMF and went back to its natural pattern of peaking at Day 7. Now, for the 60 minutes and 120 minutes cases, and because they are neither prolonged nor not exposed, they seem to be peaking at a delayed stage. Relating it to the proposed idea of magnetic field stress response mentioned earlier, and the effects seen on growth in the previous section, the exposure could possibly be affecting the growth mechanism of the algae, and hence the beta-carotene concentration. Nevertheless, the 60 minutes exposure tends to have the highest Beta-Carotene yield. It could also possibly be that the stress response on the algae is causing a growth spurt in lower exposure values. Both 60- and 120-minutes exposures suffer sharper dips in Beta-Carotene concentration after peaking. This is not the case for other exposures (Control and 240 minutes) as their beta-carotene concentration values decrease at a lower rate and over more time. Moreover, for the 120 minutes exposure case, although the highest beta-carotene value is delayed until day 10, yet it is still equal or slightly less than other peak beta-carotene concentrations for control and 240 minutes exposures. This might be another indication towards

the stress response and the starting phase of adaptation to the magnetic field. It seems that the more time the *Chlorella V.* algae is exposed, the more elaborate it becomes in responding to the EMF. Later stages of the experiment (Day 14 to Day 21) seem to push towards that more EMF exposure might affect the beta-carotene concentrations eventually, as beta-carotene values during that period is ordered with control samples having highest concentration during that time, and the concentrations get lower in order of increasing exposure time values. Nonetheless, the experiment day might play a factor in the current growth phase of the microalgae. However, having the 240 minutes exposure concentration decrease slope steeper than the 120 minutes exposure slope might relate to higher exposure time causing faster nutrition exhaustion due to EMF induced stress.

A final observation is that the control and 60 minutes exposure curves seem to be at a higher beta-carotene concentration average over the total days of the experiment. These averages are shown in Table 19. They also seem to be decreasing by a factor of 10 for each increasing exposure. Such an observation might be a supporting point for the argued idea of higher nutrition medium exhaustion earlier on in more exposed samples (120 minutes, and 240 minutes), and thus higher beta-carotene concentrations earlier, but lower concentrations later in the experiment.

Table 19. Average OD for Beta-Carotene Concentrations in BBM Nutrition Medium.

Exposure	Average
0 m	0.029
60 m	0.019
120 m	0.018
240 m	0.017

In the case of augmenting BBM with 100 grams of lunar regolith shown in Figure 31, not much difference could be seen in the general pattern of Beta-carotene concentrations. However, all exposures tend to peak in their beta-carotene concentrations on Day 10, compared to the earlier peaking of some exposures in the previous case of BBM. For this medium, it seems that the 60 minutes exposures have the highest beta-carotene concentration, followed by the control samples. Longer exposures at 120- and 240- minutes have the lowest pigment concentration.

Pigment concentration starts from a similar value for all samples, except the 240 minutes exposure, which starts higher, nonetheless, longer exposed samples seem to dip in concentration values from Day 3 to Day 7 before picking up, this is not the case for the control and 60 minutes exposures. This seems to hint at the adaptation of the microalgae to the EMF after a few days, as the control samples beta-carotene concentration seems to stay fairly constant. Although such dipping does not exist in the case of BBM, the existence of the lunar regolith in the nutrition medium from which these measurements were taken could be a contributing factor. For the 60 minutes exposure samples, Beta-carotene concentrations are increasing from the start, which could be due to an enhancing effect introduced by the EMF. Surprisingly, after Day 10, all samples decrease in their concentration with a very similar slope. Eventually, all samples seem to be holding consistent concentration values over the last few days of the experiment, where concentrations seem to be decreasing in value in order from lowest exposure to highest. Although concentration for the 60 minutes exposures was higher, it became less than the control between Day 10 and Day 14. This might be due to more nutrient exhaustion from the medium due to the EMF, which could also explain why the 120- and 240- minutes samples are also low. There does

not seem to be too much of an effect because of the lunar regolith, apart from all samples peaking on the same day.

For the nutrition medium consisting of MilliQ water augmented with 100 grams of lunar regolith, it is apparent from Figure 32 that beta-carotene concentrations are dipping for the first few days (Day 3 to Day 10) in comparison to the other nutrition mediums responses. However, they seem to be increasing later in the timeline of the experiment near the end. Following up to the hypothesis of stress response, and nutrition medium exhaustion, the graph seems to make sense. In this specific medium, nutrients are only coming from regolith as there is no BBM, which might explain why the beta-carotene concentration drops in the first few days, until the *Chlorella V.* microalgae was able to adapt and increase in production again. It seems that the lunar regolith does not contribute enough nutrients to allow for adequate beta-carotene production.

Because *Chlorella V.* was not able to utilize the present regolith nutrients from the beginning as it would BBM, it was able to compensate increasing its beta-carotene content later in the experiment, as nutrients in the regolith might have not been exhausted yet, and it might have been able to utilize them again after adapting to the environment. Nonetheless, if one pays attention to the control and 60 minutes exposure graphs, they tend to go back to almost the initial concentration. This might also be an indication of the EMF response effect on the microalgae, as 60 minutes of exposure is not much compared to 120 and 240 minutes of exposure. Hence, the microalgae is compensating for its lack of nutrition rather than a stress from the EMF, as the 60 minutes of exposure rather introduced enhancing effects previously, and in this case no enhancing effects were seen initially. However, the EMF effect looks to be substantial for the 120- and 240-minutes exposures. Both of these exposures become steady in their beta-carotene

content in the last days of the experiment, yet they are much lower than their starting points. This might indicate that the algae is being stressed from the EMF and is trying to adapt, and through this adaptation it is exhausting nutrients, which are less than the other cases of BBM and BBM augmented with lunar regolith thus it is not capable of going back to its initial beta-carotene concentration. Also, the control and the 60 minutes exposures are higher after Day 10 of the experiment, which the day that all samples in other mediums peaked in. Conducting deeper research into the concentration dipping rate might indicate the amount of nutrients needed to have the beta-carotene concentration increase throughout the cultivation process. Because the microalgae needed nutrients in this phase of its growth that it could not find, it decreased in concentration and compensated later.

Explaining the slight increase in concentration for the 60 minutes exposure samples in Day 7 of the experiment, there exists a heavily diluted amount of BBM still present in the MilliQ nutrient mix that might have been used in that day. The longer exposure samples seem to have decreased from Day 3 to Day 7 because this diluted amount nutrients could not keep up with the demand of the microalgae cells in their response to the EMF. The steeper decline in the control samples might indicate that this is not actually the case, but it could also indicate that the EMF response seems to be of an enhancing effect in the first few days of the experiment before it become stressful, as the nutrients might not be enough for the control anyways, and because it is not under exposure it did not have any enhancing effect that eases its drop in beta-carotene concentration. Moreover, the fact that past Day 7, longer exposures drop at lower beta-carotene concentrations than the control seems to indicate the evolution of the EMF response between an enhancing and stressful effect on the microalgae.

Effects on Protein Concentration

For extracted protein measurements over the different exposures in block 1, resulting data is listed in terms of optical density in Table 20 for BBM nutrition medium, Table 21 for BBM + 100g lunar regolith nutrition medium, and Table 22 for MilliQ + 100g lunar regolith nutrition medium. Visually, the same data is represented as graphs in Figure 33, Figure 34, and Figure 35, respectively. Similarly, data in terms of protein concentration is found in Table 23 for BBM nutrition medium, Table 24 for BBM + 100g lunar regolith nutrition medium, and Table 25 for MilliQ + 100g lunar regolith nutrition medium. Visually, the same data is also represented as graphs in Figure 36, Figure 37, and Figure 38, respectively. Error measurements provided in tables resemble standard deviation obtained from three measurements of the same value.

Table 20. Extracted Protein Optical Density Measurements for *Chlorella V.* growth in BBM only (Blanked with NaOH).

Exposure	Day 3	Day 7	Day 10	Day 14	Day 17	Day 21
0 m	0.47 ± 0.01	0.50 ± 0.04	0.51 ± 0.02	0.38 ± 0.02	0.50 ± 0.02	0.56 ± 0.04
60 m	0.51 ± 0.02	0.54 ± 0.06	0.31 ± 0.06	0.43 ± 0.05	0.60 ± 0.02	0.50 ± 0.04
120 m	0.53 ± 0.02	0.66 ± 0.04	0.49 ± 0.03	0.38 ± 0.01	0.57 ± 0.06	0.45 ± 0.02
240 m	0.57 ± 0.02	0.49 ± 0.03	0.46 ± 0.05	0.36 ± 0.05	0.51 ± 0.01	0.47 ± 0.03

Table 21. Extracted Protein Optical Density Measurements for *Chlorella V.* growth in BBM + 100g lunar regolith (Blanked with NaOH).

Exposure	Day 3	Day 7	Day 10	Day 14	Day 17	Day 21
0 m	0.66 ± 0.05	0.30 ± 0.05	0.44 ± 0.03	0.37 ± 0.03	0.58 ± 0.03	0.39 ± 0.01
60 m	0.50 ± 0.02	0.46 ± 0.02	0.46 ± 0.04	0.35 ± 0.02	0.55 ± 0.06	0.40 ± 0.04
120 m	0.53 ± 0.01	0.34 ± 0.03	0.48 ± 0.03	0.35 ± 0.04	0.51 ± 0.02	0.47 ± 0.04
240 m	0.59 ± 0.02	0.50 ± 0.02	0.58 ± 0.03	0.35 ± 0.03	0.51 ± 0.03	0.37 ± 0.01

Table 22. Extracted Protein Optical Density Measurements for *Chlorella V.* growth in MilliQ + 100g lunar regolith (Blanked with NaOH).

Exposure	Day 3	Day 7	Day 10	Day 14	Day 17	Day 21
0 m	0.65 ± 0.04	0.49 ± 0.08	0.47 ± 0.03	0.45 ± 0.04	0.51 ± 0.04	0.53 ± 0.02
60 m	1.02 ± 0.02	0.41 ± 0.04	0.62 ± 0.08	0.39 ± 0.05	0.36 ± 0.03	0.51 ± 0.01
120 m	0.68 ± 0.05	0.55 ± 0.04	0.54 ± 0.04	0.58 ± 0.03	0.37 ± 0.01	0.62 ± 0.03
240 m	0.69 ± 0.09	0.44 ± 0.02	0.54 ± 0.03	0.52 ± 0.03	0.39 ± 0.05	0.50 ± 0.02

Table 23. Extracted Protein Concentration Measurements for *Chlorella V.* growth in BBM only (Blanked with NaOH).

Exposure	Day 3	Day 7	Day 10	Day 14	Day 17	Day 21
0 m	12.65 ± 0.96	15.42 ± 3.00	16.53 ± 1.73	5.72 ± 1.27	15.42 ± 1.66	20.69 ± 3.46
60 m	15.98 ± 1.27	18.47 ± 4.80	0.00 ± 1.92	9.88 ± 4.19	23.74 ± 1.66	15.70 ± 3.15
120 m	18.20 ± 1.73	28.46 ± 3.15	14.59 ± 2.50	5.72 ± 0.96	21.25 ± 4.63	11.54 ± 1.92
240 m	21.53 ± 1.27	14.32 ± 2.40	11.82 ± 3.84	3.78 ± 3.97	16.53 ± 0.48	12.93 ± 2.50

Table 24. Extracted Protein Concentration Measurements for *Chlorella V.* growth in BBM + 100g lunar regolith (Blanked with NaOH).

Exposure	Day 3	Day 7	Day 10	Day 14	Day 17	Day 21
0 m	28.74 ± 3.81	0.00 ± 1.70	10.43 ± 2.20	4.89 ± 2.09	22.36 ± 2.09	6.00 ± 0.48
60 m	15.15 ± 1.92	12.37 ± 1.73	12.10 ± 3.00	2.67 ± 1.73	19.86 ± 5.08	6.83 ± 3.36
120 m	17.92 ± 0.83	2.11 ± 2.31	13.48 ± 2.40	2.95 ± 3.00	16.53 ± 1.27	13.21 ± 3.15
240 m	22.91 ± 1.44	15.70 ± 1.27	22.08 ± 2.88	2.67 ± 2.46	15.98 ± 2.09	4.33 ± 0.96

Table 25. Extracted Protein Concentration Measurements for *Chlorella V.* growth in MilliQ + 100g lunar regolith (Blanked with NaOH).

Exposure	Day 3	Day 7	Day 10	Day 14	Day 17	Day 21
0 m	27.90 ± 3.63	14.87 ± 6.72	13.21 ± 2.67	11.26 ± 3.00	15.98 ± 2.92	17.92 ± 1.44
60 m	58.69 ± 1.66	8.21 ± 3.46	25.13 ± 6.98	6.55 ± 3.75	3.50 ± 2.40	16.53 ± 0.96
120 m	30.12 ± 4.27	19.86 ± 3.36	18.75 ± 3.00	22.08 ± 2.20	4.89 ± 0.96	25.41 ± 2.50
240 m	31.51 ± 7.08	10.43 ± 1.44	18.47 ± 2.67	17.37 ± 2.54	6.27 ± 3.81	15.42 ± 1.66

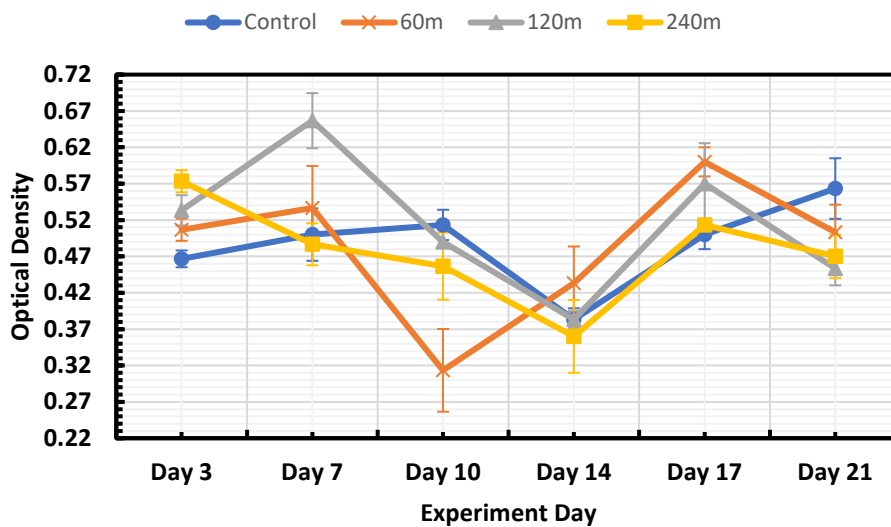


Figure 33. Measured Optical Density timeline for extracted Protein from exposures in BBM (Block 1).

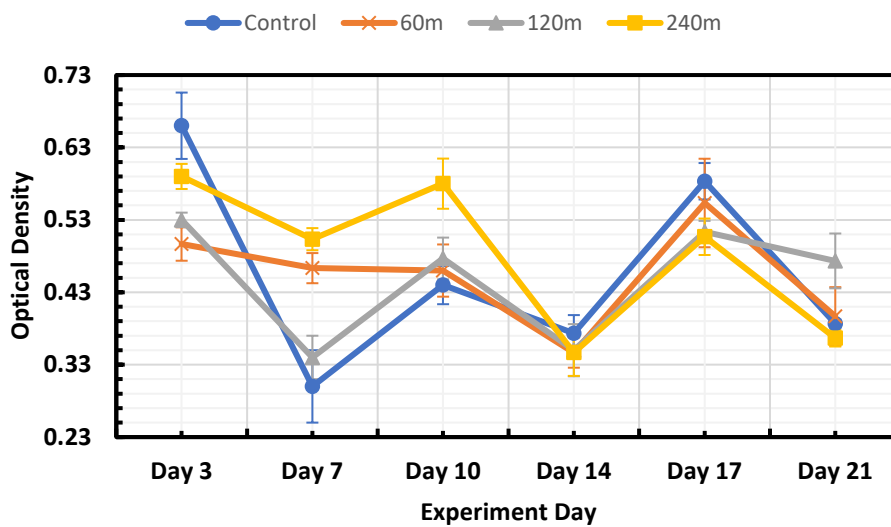


Figure 34. Measured Optical Density timeline for extracted Protein from exposures in BBM + 100g lunar regolith (Block 1).

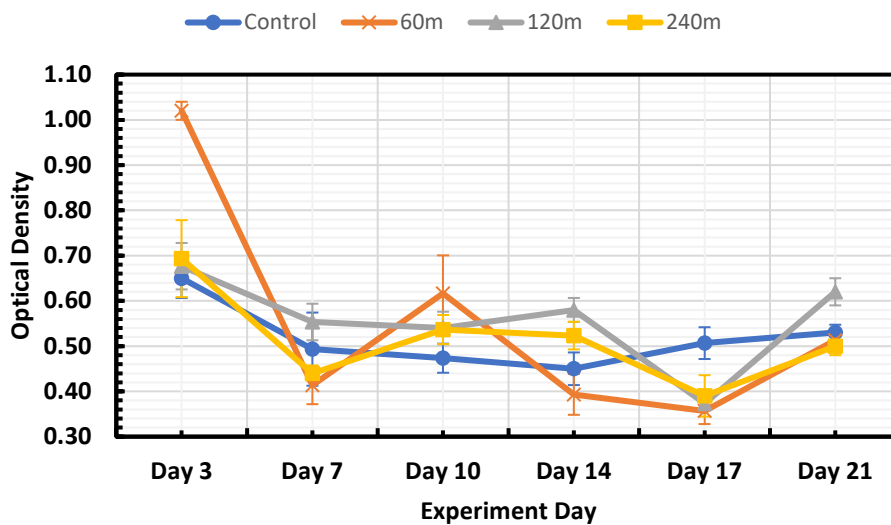


Figure 35. Measured Optical Density timeline for extracted Protein from exposures in MilliQ + 100g lunar regolith (Block 1).

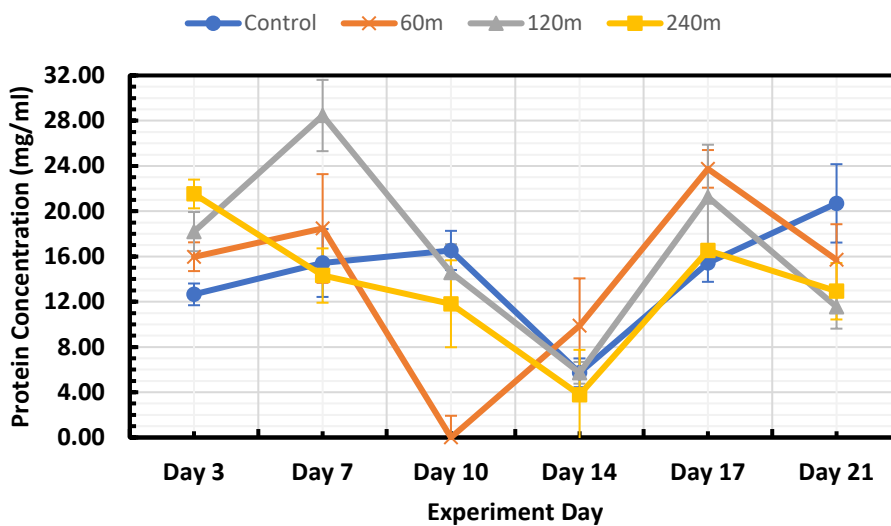


Figure 36. Timeline of extracted protein concentration in mg/ml for BBM only exposures (Block 1).

Investigating protein concentration trends for the BBM medium as shown in Figure 36, it looks like the increase in protein happens at a later phase of the experiment. Magnetic field exposure tends to provide higher protein concentrations initially, as the concentration increases with increasing exposure time. The 60- and 120-minutes samples increase even more on Day 7 but tend to drop rapidly after. The 240 minutes exposure samples start dropping in concentration after Day 3. The control does not increase much but falls in concentration eventually. All samples pick up and increase their protein concentration past Day 14, except the 60 minutes exposure, which starts increasing in concentration at Day 10 from almost no concentration. The amount of protein seems to be enhanced by the EMF later in the experiment, because all exposed samples sit at higher concentration values at Day 17. On Day 21 however, the control samples tend to become superior. This might be due to nutrients exhaustion as mentioned repeatedly in the discussions.

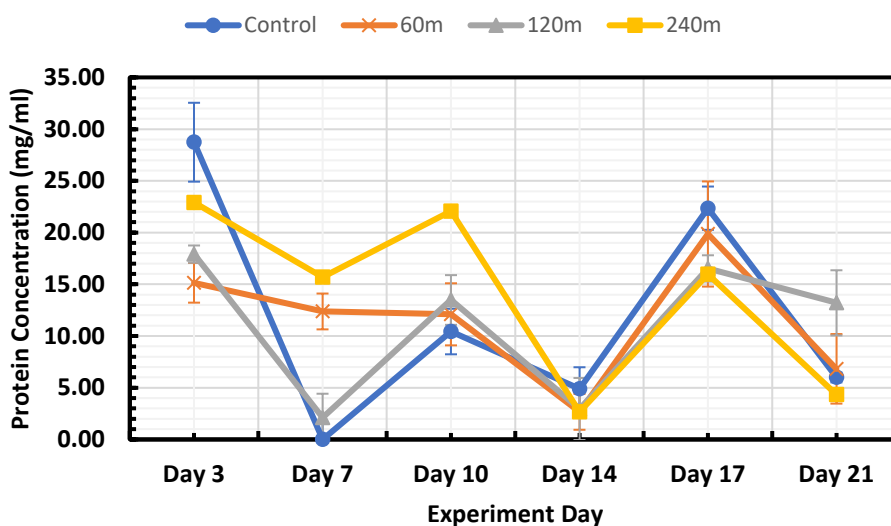


Figure 37. Timeline of extracted protein concentration in mg/ml for BBM + 100g lunar regolith exposures (Block 1).

The same pattern seems to repeat for the BBM augmented with the 100 grams of lunar regolith, however, protein concentrations decrease initially compared to the increase seen in the BBM only graph. This can be seen in Figure 37 Protein peaks again at Day 10, and drops again until Day 14, where another peak cycle happens on Day 17.

Control samples have the highest measured protein in the early part of the experiment on Day 3, followed by the 240-, 120-, and 60-minutes samples, respectively. This might indicate that the EMF has no initial effect on protein production, as neither the highest exposure has more protein than control, nor the lowest exposure does. In subsequent days, the EMF starts to take an enhancing effect around Day 10, as all exposed samples are higher in protein concentration. For the second peaking cycle, however, the opposite is happening, as control and lower exposures tend to have higher protein. Overall, deviations in following the same trend between the samples, which could be noticed for the 60- and 240-minutes samples on Day 7, could be a result of a better cell lysis process that happened in the lab due to chance.

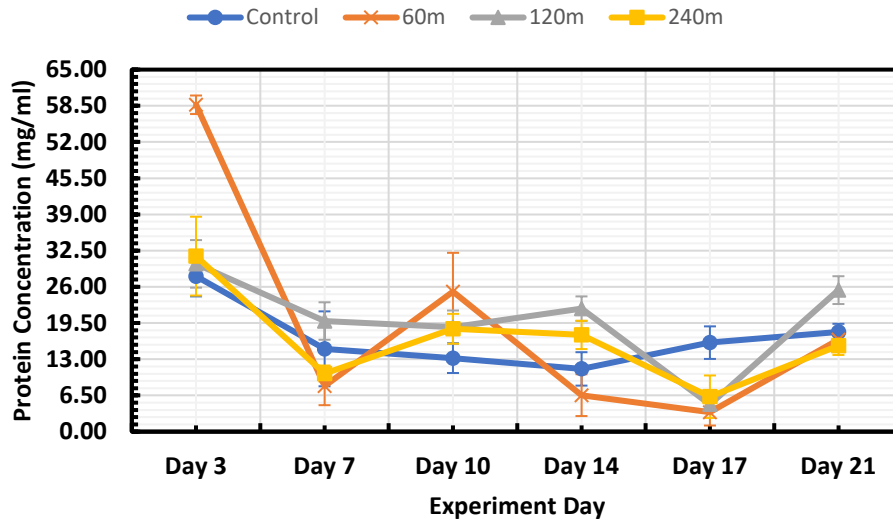


Figure 38. Timeline of extracted protein concentration in mg/ml for MilliQ + 100g lunar regolith exposures (Block 1).

Taking a look at Figure 38, we can still see the same pattern. Which seems to be related to the life cycle of *Chlorella V.* rather than the nutrition medium. A visible difference in overall protein concentration can be noticed. Where measured values are much lower than concentrations found in *Chlorella V.* cultivated in the other mediums. This makes it apparent that the lunar regolith is not providing adequate nutrition for the microalgae to produce protein. Exposed samples in general hold a higher average for protein concentration than the control except for the 240 minutes case, which tends to show that the EMF does have somewhat of an effect. Table 26 shows average values. The 60 minutes exposure has the highest protein concentration on Day 3 but tends to drop quickly to a very low value. Such a phenomena could be due to an adaptation response, as the low exposure sample is not exposed enough to become adapted. Otherwise, it could be an error in the measurement introduced by the NanoDrop One instrument.

Table 26. Averaged values for protein concentrations over the timeline of the experiment for each exposure.

Exposure	Average
0 m	16.86 mg/ml
60 m	19.77 mg/ml
120 m	20.19 mg/ml
240 m	16.58 mg/ml

EXPERIMENTAL BLOCK 2

This section lists results obtained in the second experimental block.

Growth as Optical Density Values

This subsection lists and discusses optical density values of growth data obtained from the second experimental block and compares them to the first block. Optical density measurements are listed for the cases of BBM nutrition medium, BBM + 100g lunar regolith nutrition medium, and MilliQ + 100g lunar regolith nutrition medium in Table 27, Table 28, and Table 29, respectively. Error measurements provided in tables resemble standard deviation obtained from three measurements of the same value. Graphs visually interpreting the data are shown for the cases of BBM, BBM + 100g lunar regolith, and MilliQ + 100g lunar regolith nutrition mediums, in Figure 39, Figure 40, and Figure 41, respectively.

Table 27. Optical Density Measurements for *Chlorella V.* growth in BBM only (Block 2).

Exposure	Day 1	Day 7	Day 16	Day 21
0 m	0.134 ± 0.017	0.186 ± 0.045	0.151 ± 0.016	0.124 ± 0.012
60 m	0.130 ± 0.022	0.171 ± 0.044	0.172 ± 0.014	0.191 ± 0.031
120 m	0.167 ± 0.032	0.239 ± 0.035	0.122 ± 0.006	0.189 ± 0.032
240 m	0.174 ± 0.044	0.164 ± 0.004	0.145 ± 0.010	0.147 ± 0.020

Table 28. Optical Density Measurements for *Chlorella V.* growth in BBM + 100g lunar regolith (Block 2).

Exposure	Day 1	Day 7	Day 16	Day 21
0 m	0.116 ± 0.003	0.158 ± 0.030	0.114 ± 0.011	0.121 ± 0.017
60 m	0.134 ± 0.011	0.169 ± 0.046	0.091 ± 0.002	0.140 ± 0.013
120 m	0.147 ± 0.017	0.148 ± 0.020	0.115 ± 0.001	0.093 ± 0.006
240 m	0.114 ± 0.009	0.142 ± 0.009	0.102 ± 0.014	0.103 ± 0.013

Table 29. Optical Density Measurements for *Chlorella V.* growth in MilliQ + 100g lunar regolith (Block 2).

Exposure	Day 1	Day 7	Day 16	Day 21
0 m	0.179 ± 0.031	0.201 ± 0.015	0.164 ± 0.021	0.179 ± 0.029
60 m	0.172 ± 0.033	0.240 ± 0.029	0.214 ± 0.022	0.179 ± 0.018
120 m	0.162 ± 0.028	0.218 ± 0.018	0.165 ± 0.026	0.129 ± 0.022
240 m	0.182 ± 0.022	0.151 ± 0.013	0.152 ± 0.029	0.167 ± 0.001

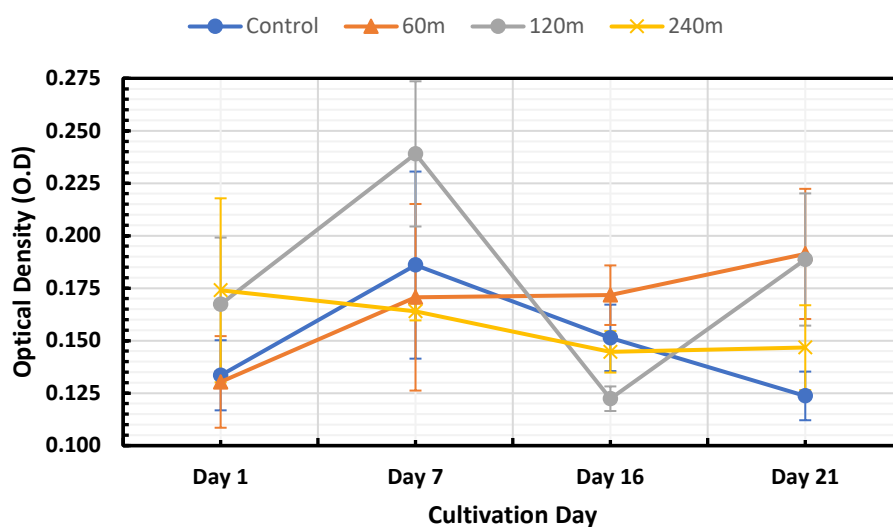


Figure 39. Measured Optical Density timeline for *Chlorella V.* exposures growth in BBM (Block 2).

Comparing block 2 growth in BBM shown in Figure 39 with block 1, we do find quite a difference. First, measured optical density values for the different exposures vary. The 240 minutes has the highest peak value in block 2, whereas control had the highest value for block 1. Moreover, the 60 minutes exposure takes an upward trend over the timeline of the experiment, however, it is fairly constant, and eventually decreases in block 1. The 240 minutes exposure sample takes a downward trend in block 2 compared to an increasing then decreasing trend in block 1. The control sample, however, is very similar in its pattern to how it was in block 1, despite being lower in value. Having many differences might not refute the possibility of magnetic field effects, but rather states the possibility of so. Other factors related to determining the growth of the *Chlorella V.* Microalgae could be in play, such as the current phase of cell growth the microalgae is currently in.

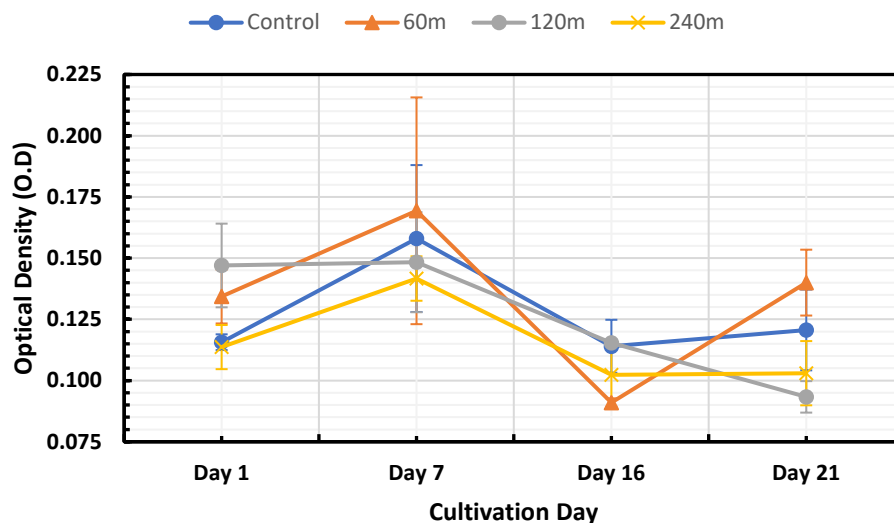


Figure 40. Measured Optical Density timeline for *Chlorella V.* exposures growth in BBM + 100g lunar regolith (Block 2)

For the block 2 experiment with the 100-gram lunar regolith augmented BBM, data trends are very consistent. As shown in Figure 40, lines expressing different exposures are in proximity and follow the same pattern. However, of the exposed samples only the 60 minutes exposure holds highest peak on Day 7, in comparison to both 60- and 120- minutes exposures at Day 9 in block 1. The magnetic field does not seem to hold too much of an effect as the disparity between measurements of the different exposure times is not exceptionally large.

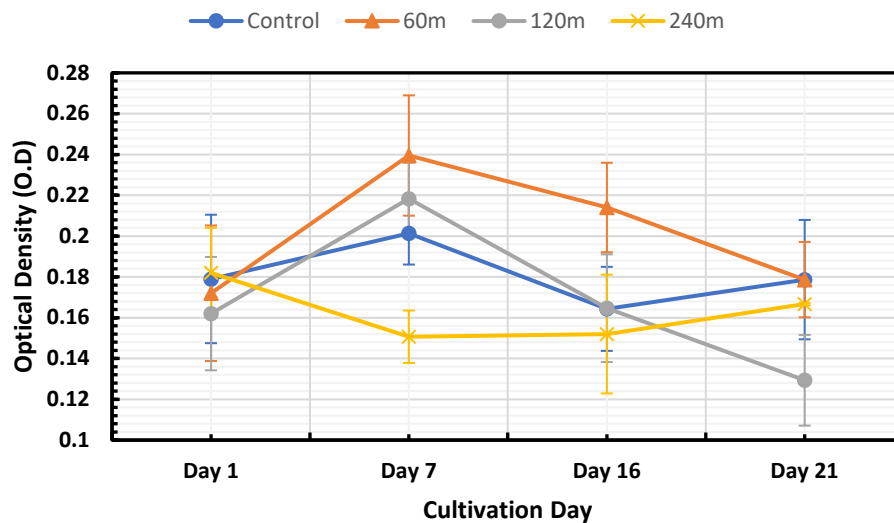


Figure 41. Measured Optical Density timeline for *Chlorella V.* exposures growth in MilliQ + 100g lunar regolith (Block 2).

A large difference between block 1 and block 2 exists in the case of MilliQ Water augmented with 100-gram lunar regolith medium. For the previous block, all samples were decreasing in optical density, thus showing a decrease in growth for all exposure samples. The current block shows an increase in optical density, which indicates microalgae growth from Day 1

to Day 7. The growth starts decreasing again after Day 7. Nonetheless, the 240 minutes exposure sample starts decreasing from Day 1 until Day 7 and stays consistent around an optical density range after that. It seems that the EMF in this case enhances growth for low exposure times until a certain point, then it introduces a stress response the higher the exposure time. Which is similar to effects seen in the previous block.

Effects on Beta-Carotene

Results are discussed and compared with the first experimental block in this section. Results are tabulated in Table 30 for the case of BBM as a nutrition medium, where Table 31, and Table 32 provide data for BBM + 100g, and MilliQ + 100g as mediums, respectively. Error measurements provided in tables resemble standard deviation obtained from three measurements of the same value. Figure 42, Figure 43, and Figure 44 represent the data for each respective nutrition medium graphically.

Table 30. Extracted Beta-Carotene Optical Density Measurements for *Chlorella V.* growth in BBM only (Block 2 - Blanked with Hexane).

Exposure	Day 3	Day 7	Day 10	Day 14	Day 17	Day 21
0 m	0.028 ± 0.001	0.009 ± 0.001	0.012 ± 0.001	0.021 ± 0.001	0.024 ± 0.000	0.016 ± 0.001
60 m	0.023 ± 0.001	0.019 ± 0.001	0.023 ± 0.001	0.013 ± 0.001	0.020 ± 0.002	0.013 ± 0.000
120 m	0.036 ± 0.000	0.022 ± 0.000	0.014 ± 0.001	0.009 ± 0.001	0.013 ± 0.000	0.011 ± 0.000
240 m	0.036 ± 0.001	0.018 ± 0.000	0.021 ± 0.000	0.009 ± 0.001	0.014 ± 0.000	0.010 ± 0.000

Table 31. Extracted Beta-Carotene Optical Density Measurements for *Chlorella V.* growth in BBM + 100g lunar regolith (Block 2 - Blanked with Hexane).

Exposure	Day 3	Day 7	Day 10	Day 14	Day 17	Day 21
0 m	0.015 ± 0.001	0.009 ± 0.001	0.017 ± 0.001	0.009 ± 0.001	0.008 ± 0.000	0.010 ± 0.001
60 m	0.010 ± 0.000	0.010 ± 0.001	0.020 ± 0.000	0.008 ± 0.000	0.002 ± 0.001	0.008 ± 0.002
120 m	0.011 ± 0.000	0.008 ± 0.001	0.018 ± 0.000	0.008 ± 0.000	0.006 ± 0.001	0.006 ± 0.001
240 m	0.011 ± 0.000	0.009 ± 0.000	0.018 ± 0.001	0.007 ± 0.000	0.006 ± 0.001	0.006 ± 0.001

Table 32. Extracted Beta-Carotene Optical Density Measurements for *Chlorella V.* growth in MilliQ + 100g lunar regolith (Block 2 - Blanked with Hexane).

Exposure	Day 3	Day 7	Day 10	Day 14	Day 17	Day 21
0 m	0.021 ± 0.001	0.035 ± 0.001	0.031 ± 0.001	0.014 ± 0.001	0.007 ± 0.001	0.012 ± 0.001
60 m	0.026 ± 0.001	0.032 ± 0.000	0.024 ± 0.001	0.015 ± 0.000	0.010 ± 0.000	0.013 ± 0.001
120 m	0.022 ± 0.001	0.017 ± 0.001	0.035 ± 0.001	0.022 ± 0.000	0.011 ± 0.001	0.015 ± 0.001
240 m	0.026 ± 0.000	0.017 ± 0.001	0.029 ± 0.001	0.032 ± 0.000	0.009 ± 0.001	0.013 ± 0.000

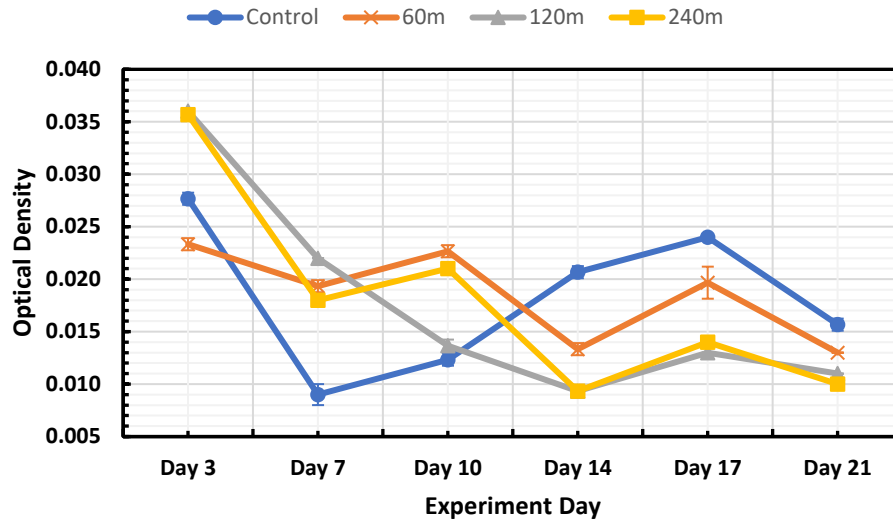


Figure 42. Measured Optical Density timeline for extracted Beta-carotene from exposures in BBM (Block 2).

The first difference between the data graphically shown in Figure 42 for block 2 and data shown in Figure 30 for block 1 is the decreasing beta-carotene concentration for the control exposure from Day 3 to Day 7. The opposite is happening in block 1, as the concentration of the pigment is increasing in this range. Moreover, the total range between Day 3 to Day 14 seems to be flipped between block 1 and block 2. After Day 14, both graphs agree with the same trend of increase in beta-carotene and eventually decreasing in Day 21. Other exposures are also having the same opposite effect, but between Day 3 and Day 7 only. They tend to be more consistent between the blocks from Day 7 upwards. The 120 minutes exposure does not have the same spurt of growth on Day 10 as in block 1, and the 240 minutes exposure has the spurt of growth in this block where it kept only decreasing in block 1. The 60 minutes sample is the only exposure that is consistent throughout the experiment between both blocks. The control samples in this block, however, have higher beta-carotene concentration than the 60 minutes samples.

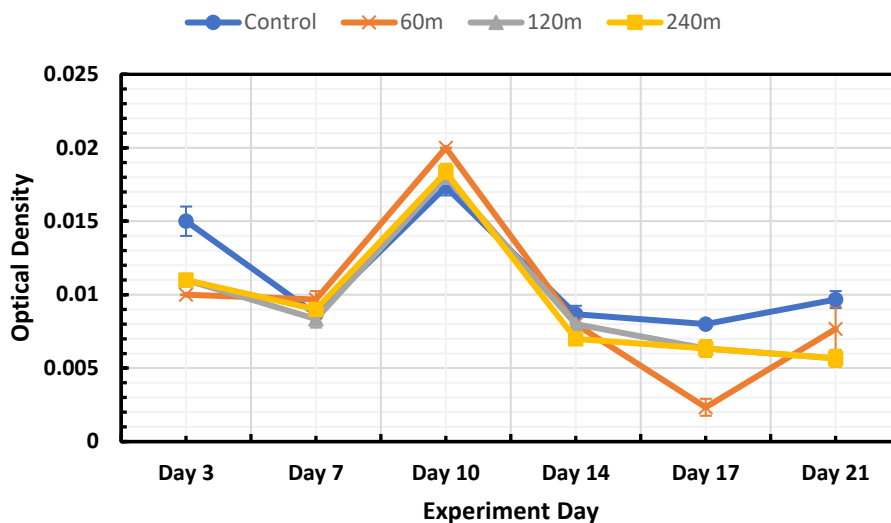


Figure 43. Measured Optical Density timeline for extracted Beta-carotene from exposures in BBM + 100g lunar regolith (Block 2).

The graph of beta-carotene concentration illustrated by Figure 43 for BBM augmented with 100 grams of lunar regolith shows tremendous closeness in measurements for all exposure samples. This is only indicative of the lack of any effects introduced by the magnetic field, as all exposures tend to have the same measurements as seen with the control. The initial and later parts of the graph have a slight deviation, but this could be attributed to slight errors in the extraction process, the instrument, or human measurement error.

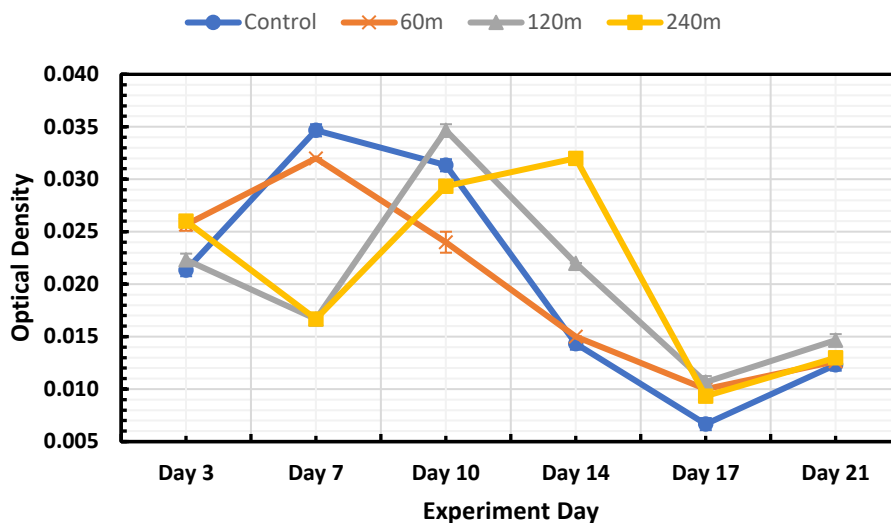


Figure 44. Measured Optical Density timeline for extracted Beta-carotene from exposures in MilliQ + 100g lunar regolith (Block 2).

The case of MilliQ water augmented with 100 grams of lunar regolith is peculiar, as it seems to provide a shift in how the data is describing the beta-carotene concentration trend from block 1 to block 2. In the first block Beta-carotene concentration is decreasing from Day 3 to Day 10, whereas in block 2 data shows either a direct increasing trend, or a slight decrease followed by an increase in concentration. The concentration decrease does not start happening later until between Day 10 to Day 17. The increase shown in block 1 to happen from Day 10 to Day 21, does not seem to start happening until Day 17, where the concentration of the pigment seems to start climbing. However, it is unknown if it will keep on increasing, we would be able to answer this question if there was more data measured beyond day 21 for block 2.

The delay in the decrease of concentration until Day 10 does not seem to be influenced by the magnetic field effects, as both blocks only differ by a shifted window. However, to have an increase initially refers to some kind of nutrient availability within the media. It could be possible

that the algae adapted faster than it would have for block 1 to the presence of the lunar regolith, but it is more likely that the diluted BBM in block 2 is of higher concentration than in block 1, hence the initial growth spurt.

Effects on Protein Concentration

In this subsection data is tabulated in Table 33, Table 34, and Table 35 for extracted protein optical density measurements of exposures cultivated in BBM, BBM + 100g lunar regolith, and MilliQ + 100g lunar regolith mediums, respectively. Figure 45, Figure 46, and Figure 47 represent the data visually, in the same order. Moreover, data in terms of protein concentration is listed in Table 36 for samples in BBM medium, Table 37 for samples in BBM + 100g lunar regolith medium, and Table 38 for samples in MilliQ + 100g lunar regolith medium. Figure 48, Figure 49, and Figure 50 present protein concentration data graphically, and in the same order. Figures representing protein concentration results are discussed in comparison to block 1, with attempts of finding similar patterns and data trends. Error measurements provided in tables resemble standard deviation obtained from three measurements of the same value.

Table 33. Extracted Protein Optical Density Measurements for *Chlorella V.* growth in BBM only (Blanked with NaOH).

Exposure	Day 3	Day 7	Day 10	Day 14	Day 17
0 m	0.54 ± 0.02	0.40 ± 0.04	0.47 ± 0.02	0.46 ± 0.04	0.49 ± 0.04
60 m	0.42 ± 0.06	0.55 ± 0.03	0.44 ± 0.03	0.49 ± 0.03	0.52 ± 0.02
120 m	0.40 ± 0.05	0.48 ± 0.01	0.50 ± 0.03	0.57 ± 0.03	0.55 ± 0.03
240 m	0.52 ± 0.04	0.48 ± 0.03	0.40 ± 0.02	0.54 ± 0.03	0.63 ± 0.02

Table 34. Extracted Protein Optical Density Measurements for *Chlorella V.* growth in BBM + 100g lunar regolith (Blanked with NaOH).

Exposure	Day 3	Day 7	Day 10	Day 14	Day 17
0 m	0.39 ± 0.04	0.46 ± 0.03	0.49 ± 0.05	0.50 ± 0.05	0.44 ± 0.03
60 m	0.47 ± 0.03	0.47 ± 0.02	0.53 ± 0.01	0.54 ± 0.03	0.44 ± 0.02
120 m	0.47 ± 0.06	0.76 ± 0.05	0.44 ± 0.03	0.53 ± 0.04	0.48 ± 0.03
240 m	0.57 ± 0.03	0.51 ± 0.05	0.34 ± 0.03	0.50 ± 0.01	0.44 ± 0.05

Table 35. Extracted Protein Optical Density Measurements for *Chlorella V.* growth in MilliQ + 100g lunar regolith (Blanked with NaOH).

Exposure	Day 3	Day 7	Day 10	Day 14	Day 17
0 m	0.48 ± 0.10	0.50 ± 0.07	0.41 ± 0.04	0.62 ± 0.02	0.55 ± 0.03
60 m	0.60 ± 0.03	0.47 ± 0.05	0.42 ± 0.01	0.45 ± 0.03	0.47 ± 0.03
120 m	0.50 ± 0.04	0.37 ± 0.04	0.42 ± 0.02	0.50 ± 0.03	0.46 ± 0.06
240 m	0.54 ± 0.04	0.54 ± 0.04	0.38 ± 0.04	0.50 ± 0.03	0.44 ± 0.03

Table 36. Extracted Protein Concentration Measurements for *Chlorella V.* growth in BBM only (Blanked with NaOH - Block 2).

Exposure	Day 3	Day 7	Day 10	Day 14	Day 17
0 m	19.03 ± 1.27	6.83 ± 3.36	13.21 ± 1.73	12.10 ± 3.63	14.59 ± 3.00
60 m	8.49 ± 5.35	19.31 ± 2.09	10.16 ± 2.67	14.59 ± 2.50	17.37 ± 1.73
120 m	7.10 ± 3.81	13.76 ± 0.83	15.70 ± 2.09	21.25 ± 2.20	19.31 ± 2.67
240 m	17.09 ± 3.00	13.76 ± 2.20	7.10 ± 1.66	18.47 ± 2.54	26.24 ± 1.66

Table 37. Extracted Protein Concentration Measurements for *Chlorella V.* growth in BBM + 100g lunar regolith (Blanked with NaOH - Block 2).

Exposure	Day 3	Day 7	Day 10	Day 14	Day 17
0 m	6.27 ± 3.63	12.37 ± 2.54	14.87 ± 3.93	15.70 ± 4.19	10.43 ± 2.88
60 m	12.93 ± 2.88	13.21 ± 1.73	17.92 ± 0.83	19.03 ± 2.09	10.71 ± 1.27
120 m	12.93 ± 4.63	37.33 ± 3.75	10.71 ± 2.40	17.92 ± 3.00	13.76 ± 2.20
240 m	21.53 ± 2.40	16.26 ± 4.32	2.11 ± 2.88	15.42 ± 0.83	10.71 ± 3.75

Table 38. Extracted Protein Concentration Measurements for *Chlorella V.* growth in MilliQ + 100g lunar regolith (Blanked with NaOH - Block 2).

Exposure	Day 3	Day 7	Day 10	Day 14	Day 17
0 m	13.48 ± 7.99	15.15 ± 5.84	8.21 ± 3.36	25.68 ± 1.27	19.31 ± 2.54
60 m	23.47 ± 2.67	13.21 ± 3.84	9.05 ± 0.96	10.99 ± 2.09	13.21 ± 2.40
120 m	15.42 ± 3.33	4.33 ± 3.36	8.77 ± 1.66	15.70 ± 2.09	11.82 ± 4.58
240 m	18.47 ± 2.92	18.75 ± 3.00	5.44 ± 3.33	15.42 ± 2.20	10.71 ± 2.54

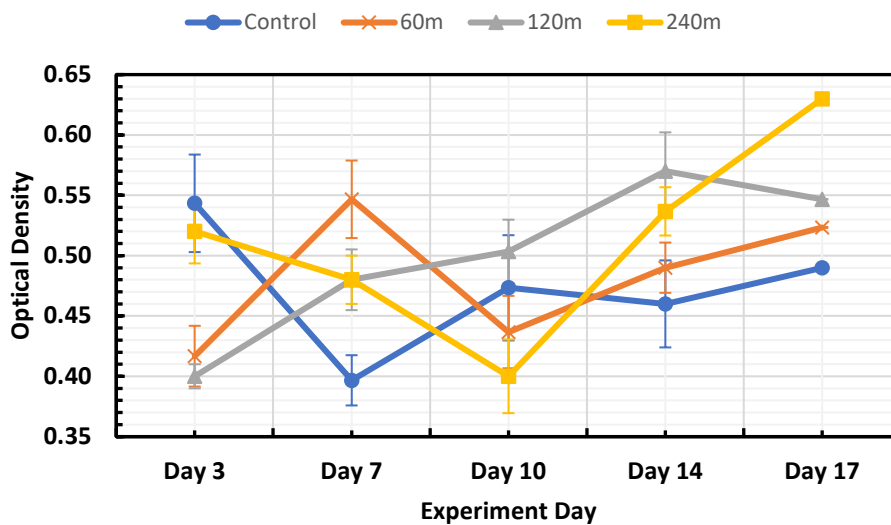


Figure 45. Measured Optical Density timeline for extracted Protein from exposures in BBM (Block 2).

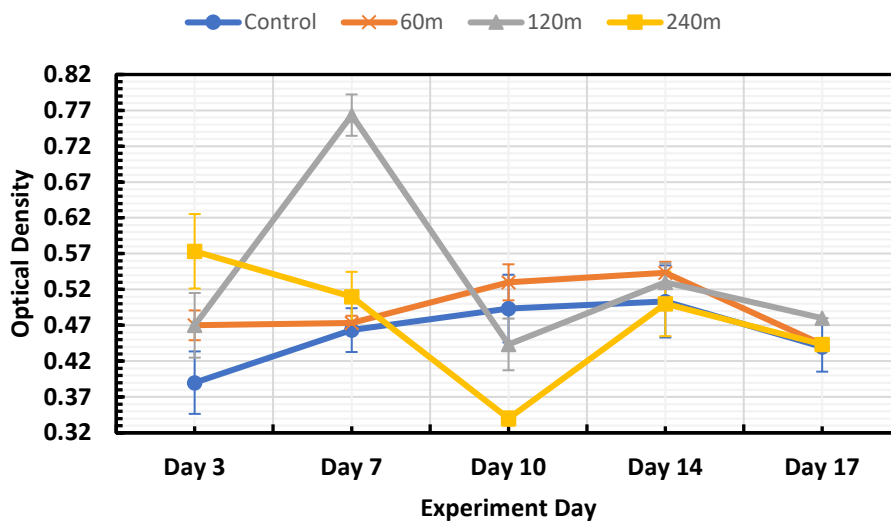


Figure 46. Measured Optical Density timeline for extracted Protein from exposures in BBM + 100g lunar regolith (Block 2).

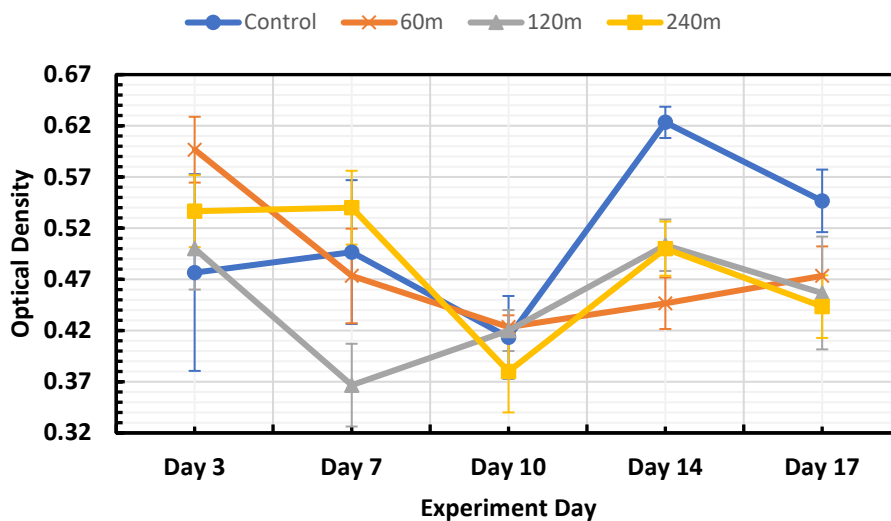


Figure 47. Measured Optical Density timeline for extracted Protein from exposures in MilliQ + 100g lunar regolith (Block 2).

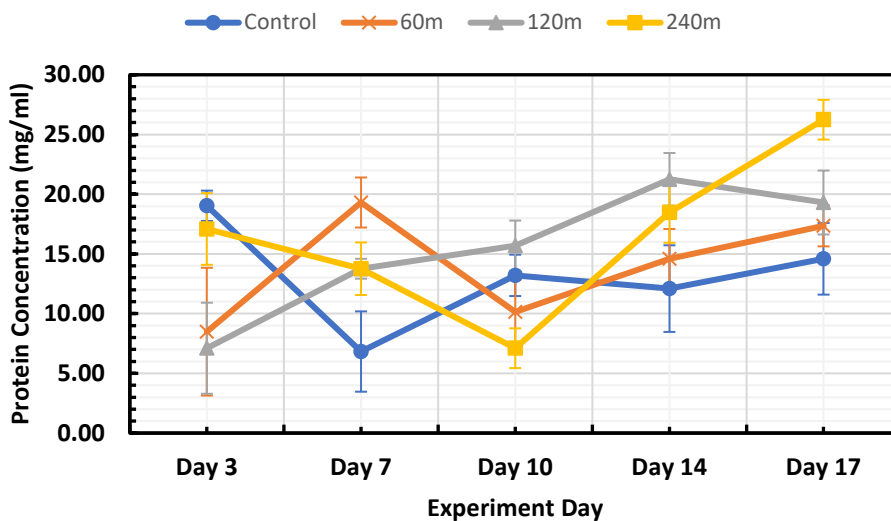


Figure 48. Timeline of extracted protein concentration in mg/ml for BBM only exposures (Block 2).

Block 2 measurements of protein concentration only went up until Day 17 as we were not able to measure protein concentration at Day 21 due to having insufficient Bradford Assay. Having

data points from Day 3 up until Day 17 constitutes enough data to show the behavior of microalgae in terms of protein production.

For the BBM nutrient, the current block's data trend seems to be shifted in comparison to what is seen in block 1. Investigating Figure 48 and Figure 36, we could see that block 2 is shifted to the left. Nonetheless, the same conclusion can be reached in that the EMF pushes the microalgae to produce more protein concentrations. However, higher exposures tend to peak at protein concentrations later in the experiment, whereas in earlier phases, the lower exposure (60 minutes samples) dominates. The control protein concentrations sits at an intermediate level between other exposures. The 240 minutes exposure has an always increasing slope for protein concentration, compared to the fluctuating protein concentration produced by the same exposure for block 1.

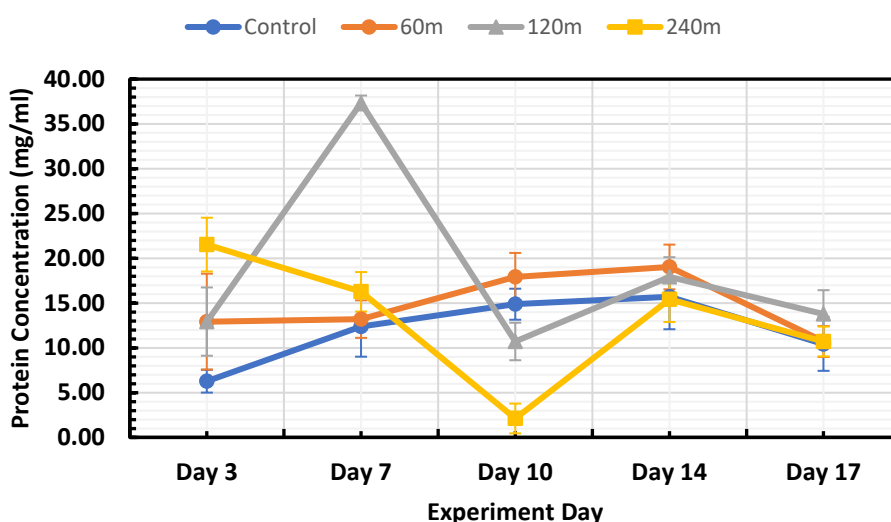


Figure 49. Timeline of extracted protein concentration in mg/ml for BBM + 100g lunar regolith exposures (Block 2).

Protein concentration for BBM augmented with 100 grams of lunar regolith shows increasing protein concentrations for the 60 minutes exposure, and control. Rather than a fluctuating curve, both of these exposures are increasing in concentration smoothly. It looks like higher exposure samples are affected by the EMF. The 240 minutes samples start higher but keep dipping until Day 10 then they start increasing again. The 120 minutes samples on the other hand, start lower, peak to a very high value on Day 7, and then decrease until Day 10, for which it starts increasing again. All exposures including control eventually reach a similar level of protein concentration at Day 14 and onward.

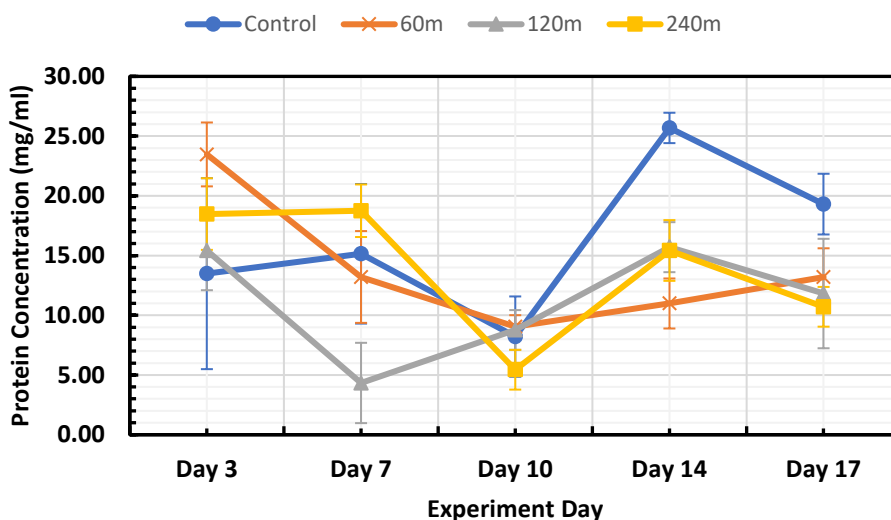


Figure 50. Timeline of extracted protein concentration in mg/ml for MilliQ + 100g lunar regolith exposures (Block 2).

Expecting decreasing protein concentration for all samples in the case of the MilliQ augmented with 100 grams of lunar regolith nutrition medium, this expectation is not entirely

fulfilled for block 2. Exposures of 60 minutes, and 240 minutes have such a trend, yet this is not seen in the control nor in the case of the 120 minutes exposure. It is normal to see some fluctuations in the curves as shown in the graph in Figure 50, however, an upwards increasing trend seems to be peculiar in comparison to block 1, and the previous indicators of the incapability of lunar regolith to adequately support the microalgae.

An interesting pattern noticed in the case of the MilliQ nutrition medium, is that both the control and the 240 minutes exposure increase initially until Day 7, decrease on Day 10, and increase again on Day 14, then decrease eventually. The 240 minutes curve, however, does not exceed its previous peak value, which results in an overall decreasing curve. This does not hold true for control, which is increasing on average.

BLOCKING AND STATISTICAL ANALYSIS

To provide a comprehensive understanding of the experiment, it is important to consider results from both experimental blocks. The aim for having multiple blocks in the first place was to isolate unexplained variance and induce a randomized set of runs following the Design of Experiments (DOE) methodology. Additionally, the use of blocking is intended to find factors interactions and confirm any findings to hold across multiple randomized repetitions of the experiment. While the nature of this experiment does not entirely conform due to full randomization not being possible, and the impracticality of a split-plot design, in addition to violating principles of DOE, it could still be studied through this approach. This section provides tabulated results and figures extracted from analyzing data using StatEase360 statistics software.

The main reason for which this experiment does not conform to DOE is due to its dependency on the factor of time. In DOE, a completely randomized design is required. All factors are randomizable, and could be either easy, or hard to change, the latter requiring a split-plot analysis, which offers two levels of randomization and is outside the scope of this thesis. Time cannot be considered a factor in this regard, as it cannot be randomized into a specified sequence of runs. To overcome this issue, one way to model our experiment is to consider each day to be a separate experiment, with the randomized factors of exposure time and nutrition medium, thus eliminating the dependency on cultivation time. The following data resembles our analysis results taken from the software:

Protein Concentration ANOVA

Table 39. ANOVA for Protein Concentration on Day 3.

Source	Sum of Squares	DoF	Mean Square	F-value	p-value
Block	2.80	1	2.80		
Model	3.45	8	0.4315	6.17	< 0.0001
A-Exposure Time	0.3758	1	0.3758	5.38	0.0237
B-Nutrition Medium	2.24	2	1.12	16.06	< 0.0001
AB	0.1767	2	0.0884	1.26	0.2896
A²	0.1012	1	0.1012	1.45	0.2334
A²B	0.5542	2	0.2771	3.97	0.0240
Residual	4.33	62	0.0699		
Lack of Fit	2.88	14	0.2058	6.81	< 0.0001
Pure Error	1.45	48	0.0302		
Cor Total	10.58	71			

Factor Coding: Actual

Response: R1

-----95% CI Bands

- B1 BBM
- ▲ B2 BBM + 100g
- ◆ B3 MilliQ + 100g

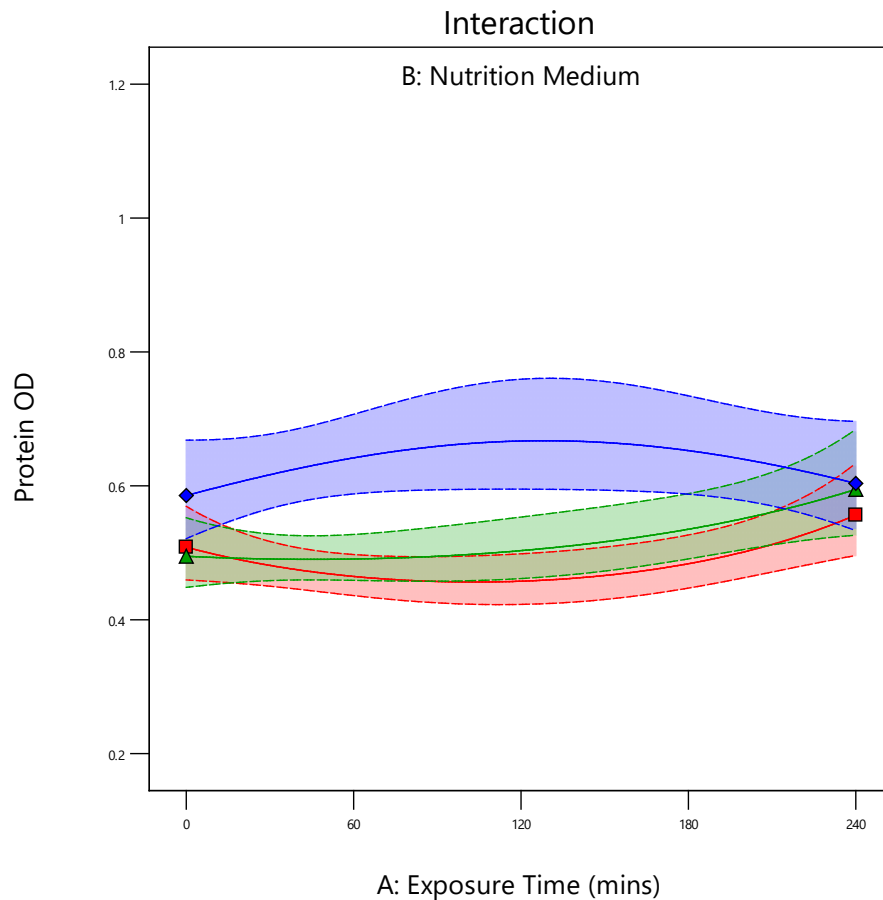


Figure 51. Interactions between factors for protein concentration analysis on Day 3.

Table 40. ANOVA for Protein Concentration on Day 7.

Source	Sum of Squares	DoF	Mean Square	F-value	p-value
Block	0.0115	1	0.0115		
Model	0.1742	8	0.0218	2.60	0.0160
A-Exposure Time	0.0229	1	0.0229	2.73	0.1034
B-Nutrition Medium	0.0208	2	0.0104	1.25	0.2949
AB	0.0243	2	0.0122	1.45	0.2416
A²	0.0411	1	0.0411	4.91	0.0304
A²B	0.0651	2	0.0325	3.89	0.0256
Residual	0.5187	62	0.0084		
Lack of Fit	0.4381	14	0.0313	18.62	< 0.0001
Pure Error	0.0807	48	0.0017		
Cor Total	0.7044	71			

Factor Coding: Actual
Response: R1
 -----95% CI Bands

- B1 BBM
- ▲ B2 BBM + 100g
- ◆ B3 MilliQ + 100g

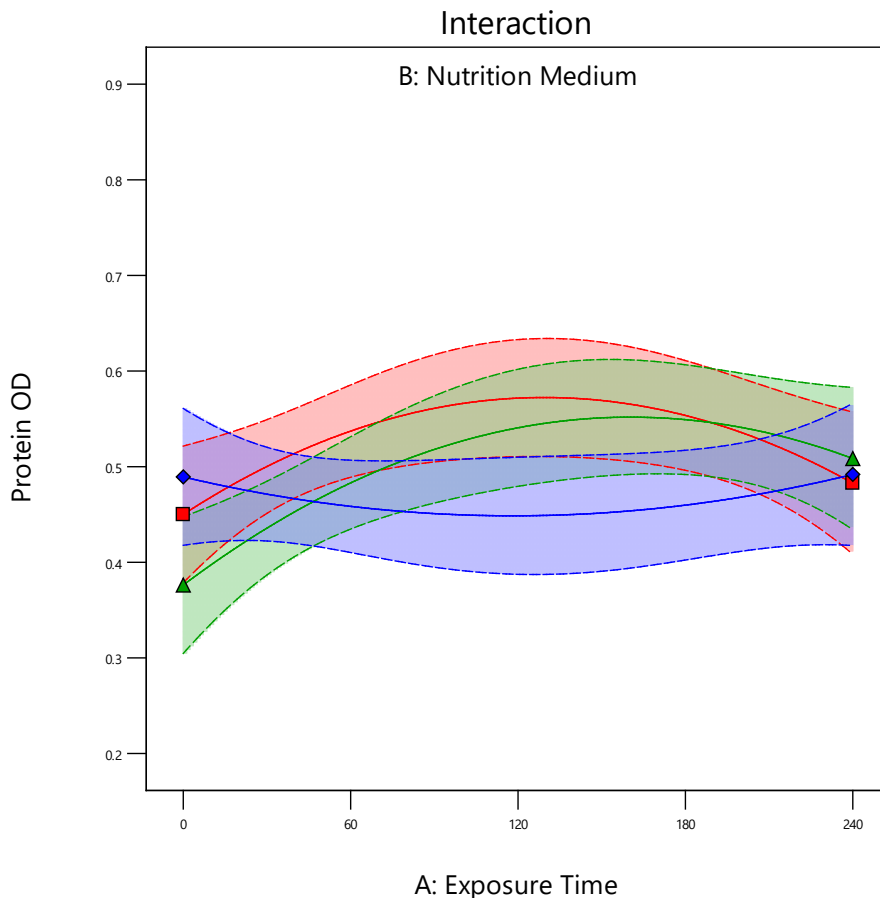


Figure 52. Interactions between factors for protein concentration analysis on Day 7.

Table 41. ANOVA for Protein Concentration on Day 10.

Source	Sum of Squares	DoF	Mean Square	F-value	p-value
Block	0.0512	1	0.0512		
Model	0.0958	11	0.0087	1.96	0.0494
A-Exposure Time	0.0027	1	0.0027	0.6129	0.4368
B-Nutrition Medium	0.0100	2	0.0050	1.12	0.3326
AB	0.0006	2	0.0003	0.0686	0.9338
A²	0.0032	1	0.0032	0.7209	0.3993
A²B	0.0085	2	0.0042	0.9508	0.3923
A³	0.0024	1	0.0024	0.5401	0.4653
A³B	0.0684	2	0.0342	7.70	0.0011
Residual	0.2622	59	0.0044		
Lack of Fit	0.1987	11	0.0181	13.64	< 0.0001
Pure Error	0.0635	48	0.0013		
Cor Total	0.4092	71			

Factor Coding: Actual
Response: R1
 -----95% CI Bands

- B1 BBM
- ▲ B2 BBM + 100g
- ◆ B3 MilliQ + 100g

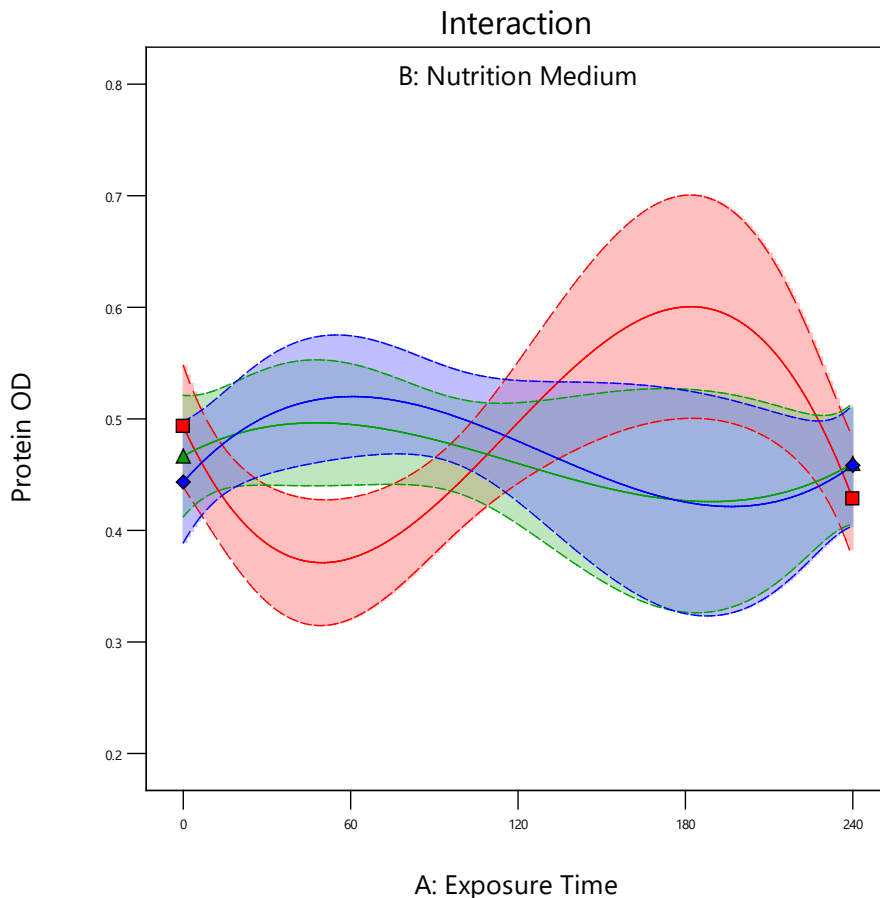


Figure 53. Interactions between factors for protein concentration analysis on Day 10.

Table 42. ANOVA for Protein Concentration on Day 14.

Source	Sum of Squares	DoF	Mean Square	F-value	p-value
Block	0.2059	1	0.2059		
Model	0.1258	11	0.0114	3.69	0.0005
A-Exposure Time	0.0003	1	0.0003	0.1060	0.7459
B-Nutrition Medium	0.0569	2	0.0285	9.17	0.0003
AB	0.0027	2	0.0014	0.4378	0.6475
A²	0.0010	1	0.0010	0.3283	0.5688
A²B	0.0115	2	0.0058	1.86	0.1649
A³	0.0162	1	0.0162	5.22	0.0260
A³B	0.0372	2	0.0186	5.99	0.0043
Residual	0.1830	59	0.0031		
Lack of Fit	0.1330	11	0.0121	11.63	< 0.0001
Pure Error	0.0499	48	0.0010		
Cor Total	0.5147	71			

Factor Coding: Actual
Response: R1
 -----95% CI Bands

■ B1 BBM
 ▲ B2 BBM + 100g
 ◆ B3 MilliQ + 100g

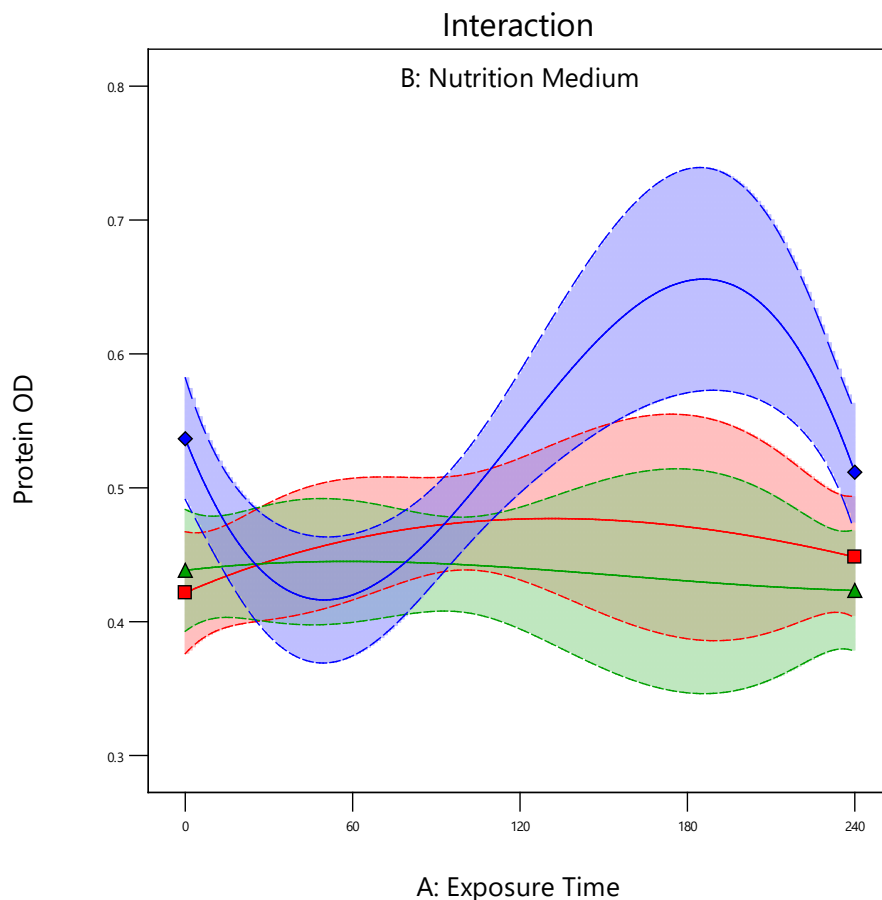


Figure 54. Interactions between factors for protein concentration analysis on Day 14.

Table 43. ANOVA for Protein Concentration on Day 17.

Source	Sum of Squares	DoF	Mean Square	F-value	p-value
Block	0.0003	1	0.0003		
Model	0.2007	8	0.0251	8.35	< 0.0001
A-Exposure Time	0.0038	1	0.0038	1.28	0.2626
B-Nutrition Medium	0.1281	2	0.0641	21.33	< 0.0001
AB	0.0385	2	0.0192	6.40	0.0030
A²	0.0020	1	0.0020	0.6577	0.4205
A²B	0.0283	2	0.0141	4.71	0.0125
Residual	0.1862	62	0.0030		
Lack of Fit	0.1331	14	0.0095	8.60	< 0.0001
Pure Error	0.0531	48	0.0011		
Cor Total	0.3872	71			

Factor Coding: Actual
Response: R1
 -----95% CI Bands

■ B1 BBM
 ▲ B2 BBM + 100g
 ◆ B3 MilliQ + 100g

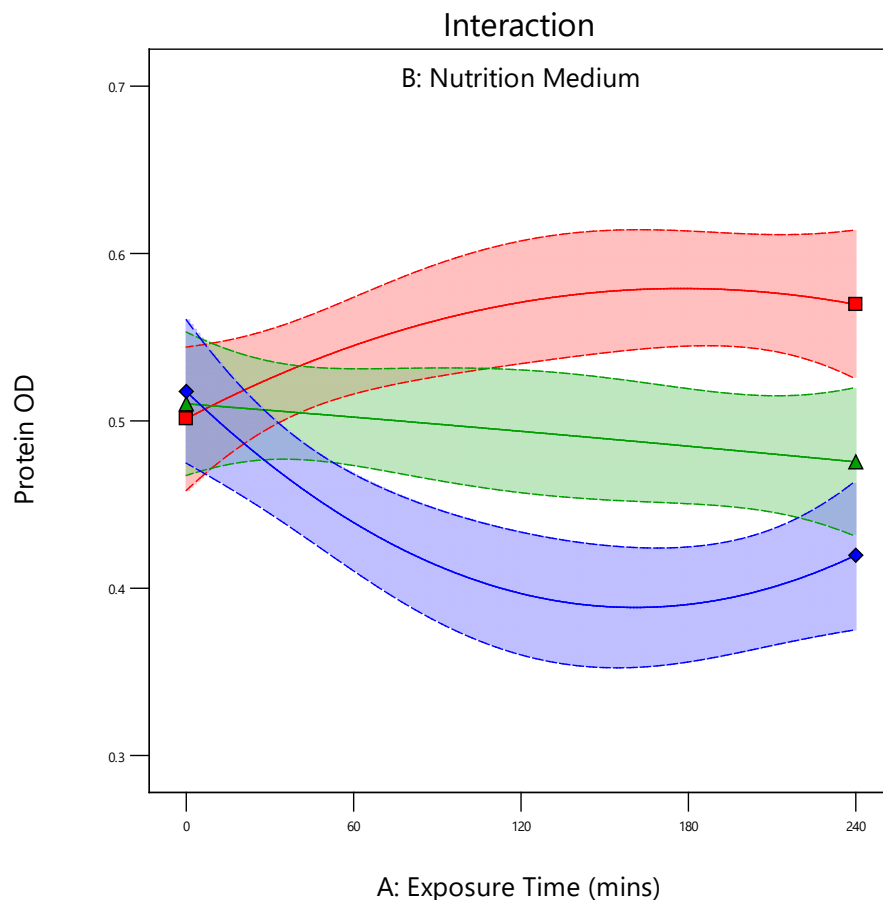


Figure 55. Interactions between factors for protein concentration analysis on Day 17.

Following up with the ANOVA for each measurement day, starting with Day 3 for protein concentration analysis as shown in Table 39, both exposure time and nutrition medium are of high significance based on their p-values. There does not appear to be linear interactions between the two factors; however, for the most fitting model, the square of the exposure time has significant interaction with the nutrition medium. This indicates the higher weight of the medium factor in determining protein concentration. It also shows that a higher exposure time is needed to provide a changing effect in protein concentration for a provided medium. Figure 51 illustrates this interaction between the factors and shows the peak value to be in MilliQ + 100g regolith

medium at the 120 minutes exposure time according to the fitting model, although it does not correctly match actual measurements. Main effects, and interaction effects, however, tend to partially resemble the changes in protein concentration shown in the figures of block 1 and block 2.

In Day 7, the ANOVA shows a change in the significance of the main factors, as none of them are of high significance. Neither is their linear interaction. Yet the square of the exposure time is significant, accompanied by the interaction of the square of the exposure time with the nutrition medium. This still shows that although exposure times are significant, they are not as influential as the medium. According to the fitted model shown in Figure 52, MilliQ medium is of lowest effect, followed by both regular BBM and BBM augmented with 100 grams of lunar regolith.

The significance of main effects and linear interactions tends to decrease and become insignificant at Day 10. A cubed exposure time interaction with the nutrition medium is the only significant interaction. Which could provide a clue on why most protein measurements tend to peak or hit lowest values on this day. The model graph shown in Figure 53 provides an indicator towards some of the complex relationships seen in earlier data figures. This figure, however, shows that both BBM and MilliQ + 100g regolith mediums are superior on this day at different exposure times. The 60 minutes exposure provides the highest protein concentration with MilliQ based medium. Exposure ranges from 120 to 240 minutes provide the highest protein concentration with BBM.

The ANOVA of Day 14 points towards significance in the nutrition medium factor again, in compliance with the hypothesized idea mentioned earlier of the seemingly increased nutrients exhaustion. Referring to protein concentrations graphs, all mediums dip on Day 14. A cubed exposure time factor is significant for the model, showing that much change is required by the exposure time for a change in protein concentration. Both BBM and BBM + 100g mediums tend to overlap in terms of expected response over a continuous range of exposure time as shown in Figure 54. However, the MilliQ + 100g medium tends to peak between 120 minutes, and 240 minutes exposure.

Day 17 shows a continuous case of significance of the nutrition medium. Additionally, the linear interaction between nutrition medium and magnetic field follow the same proposed idea of increased or decreased nutrition exhaustion based on how much exposure the samples have had. Higher power interactions between the two factors exist yet are not as important as the linear interactions. Exposure time ranges upward of 60 minutes with BBM as a medium seem to enhance protein concentration the most. The same exposure time range provides lowest protein concentration if coupled with MilliQ augmented with 100 grams of lunar regolith as a medium. These results are illustrated by Figure 55.

Beta-Carotene Concentration ANOVA

Table 44. ANOVA for Beta-Carotene Concentration on Day 3.

Source	Sum of Squares	DoF	Mean Square	F-value	p-value
Block	0.0419	1	0.0419		
Model	0.2265	5	0.0453	0.7358	0.5993
A-Exposure Time	0.0011	1	0.0011	0.0173	0.8958
B-Nutrition Medium	0.2115	2	0.1058	1.72	0.1875
AB	0.0139	2	0.0070	0.1129	0.8934
Residual	4.00	65	0.0616		
Lack of Fit	3.99	17	0.2349	1299.19	< 0.0001
Pure Error	0.0087	48	0.0002		
Cor Total	4.27	71			

Factor Coding: Actual
Response: R1
 -----95% CI Bands

- B1 BBM
- ▲ B2 BBM + 100g
- ◆ B3 MilliQ + 100g

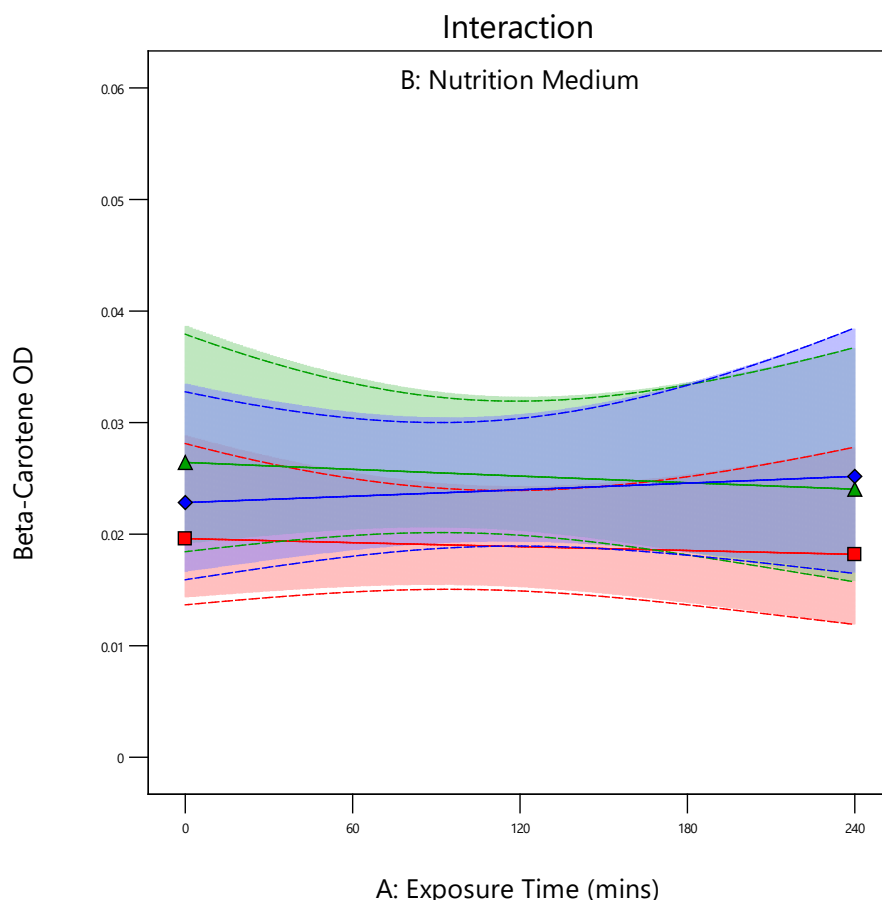


Figure 56. Interactions between factors for Beta-Carotene concentration analysis on Day 3.

Table 45. ANOVA for Beta-Carotene Concentration on Day 7.

Source	Sum of Squares	DoF	Mean Square	F-value	p-value
Block	0.0020	1	0.0020		
Model	0.0020	5	0.0004	4.43	0.0016
A-Exposure time	0.0003	1	0.0003	3.23	0.0770
B-Nutrition Medium	0.0012	2	0.0006	6.71	0.0022
AB	0.0005	2	0.0002	2.75	0.0712
Residual	0.0058	65	0.0001		
Lack of Fit	0.0058	17	0.0003	724.47	< 0.0001
Pure Error	0.0000	48	4.722E-07		
Cor Total	0.0098	71			

Factor Coding: Actual
Response: R1
 -----95% CI Bands

- B1 BBM
- ▲ B2 BBM + 100g
- ◆ B3 MilliQ + 100g

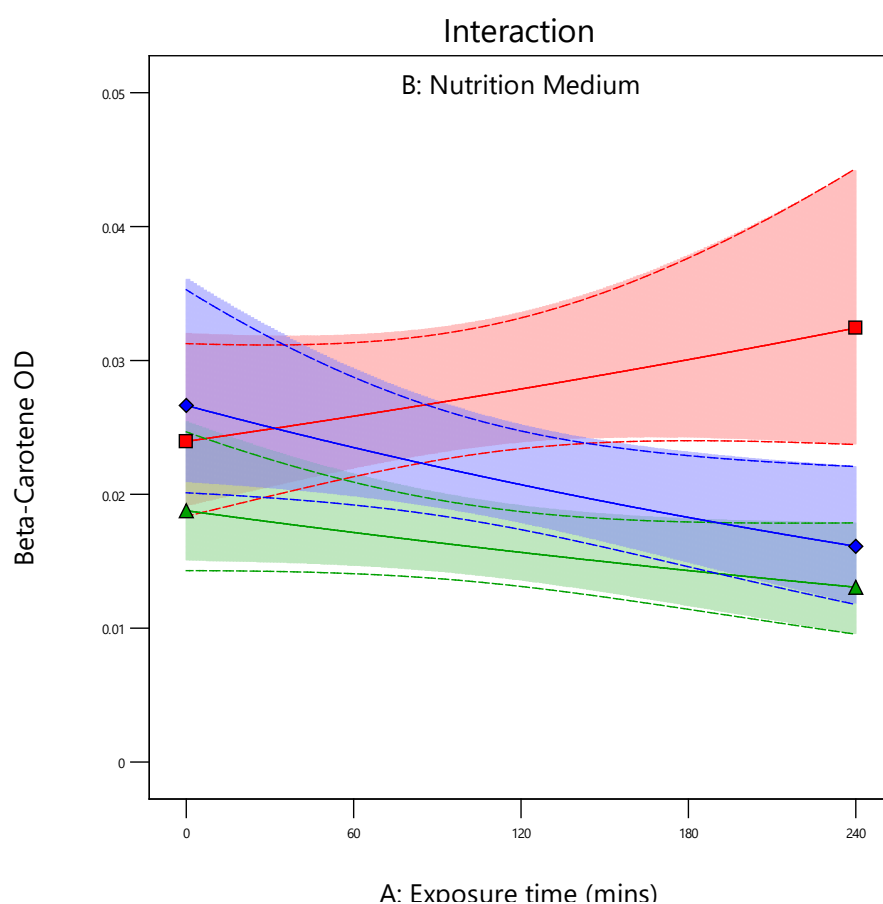


Figure 57. Interactions between factors for Beta-Carotene concentration analysis on Day 7.

Table 46. ANOVA for Beta-Carotene Concentration on Day 10.

Source	Sum of Squares	DoF	Mean Square	F-value	p-value
Block	0.0012	1	0.0012		
Model	0.0017	5	0.0003	2.43	0.0440
A-Exposure time	0.0001	1	0.0001	1.03	0.3145
B-Nutrition Medium	0.0015	2	0.0008	5.45	0.0065
AB	0.0000	2	0.0000	0.1221	0.8853
Residual	0.0091	65	0.0001		
Lack of Fit	0.0091	17	0.0005	2574.10	< 0.0001
Pure Error	0.0000	48	2.083E-07		
Cor Total	0.0120	71			

Factor Coding: Actual
Response: R1
 -----95% CI Bands

- B1 BBM
- ▲ B2 BBM + 100g
- ◆ B3 MilliQ + 100g

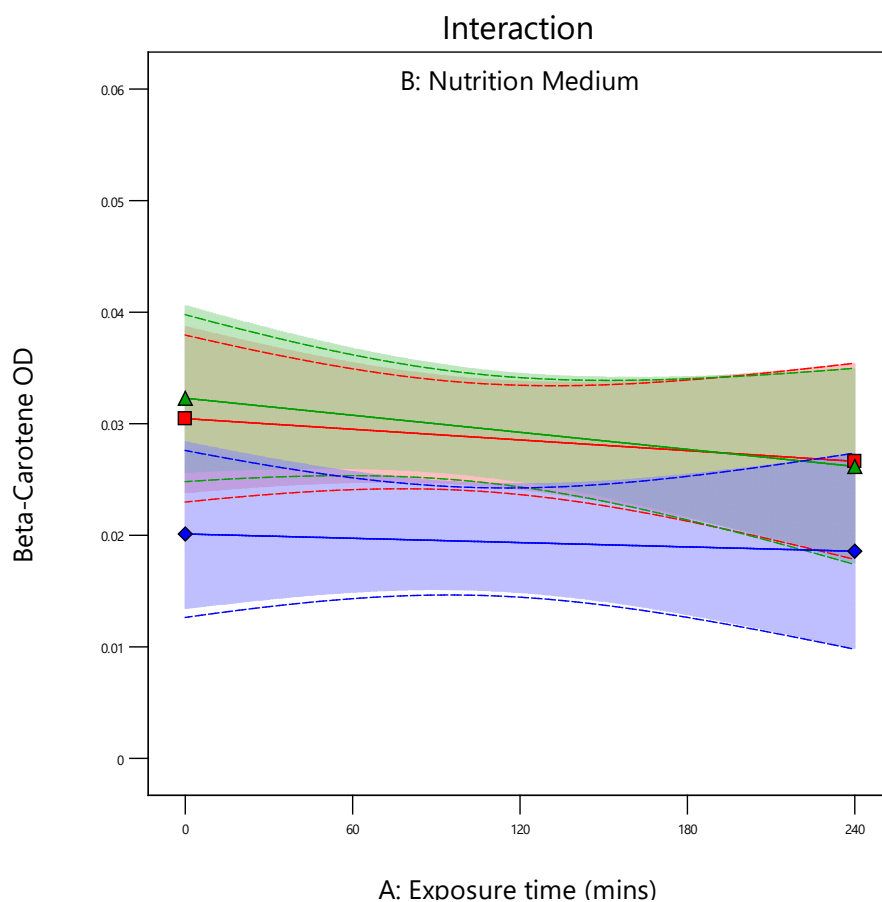


Figure 58. Interactions between factors for Beta-Carotene concentration analysis on Day 10.

Table 47. ANOVA for Beta-Carotene Concentration on Day 14.

Source	Sum of Squares	DoF	Mean Square	F-value	p-value
Block	0.0000	1	0.0000		
Model	0.0010	6	0.0002	5.91	< 0.0001
A-Exposure Time	0.0001	1	0.0001	3.30	0.0740
B-Nutrition Medium	0.0002	2	0.0001	3.84	0.0266
AB	0.0005	2	0.0003	9.39	0.0003
A ²	0.0002	1	0.0002	5.70	0.0199
Residual	0.0018	64	0.0000		
Lack of Fit	0.0017	16	0.0001	98.42	< 0.0001
Pure Error	0.0001	48	1.097E-06		
Cor Total	0.0028	71			

Factor Coding: Actual
Response: R1
 -----95% CI Bands

- B1 BBM
- ▲ B2 BBM + 100g
- ◆ B3 MilliQ + 100g

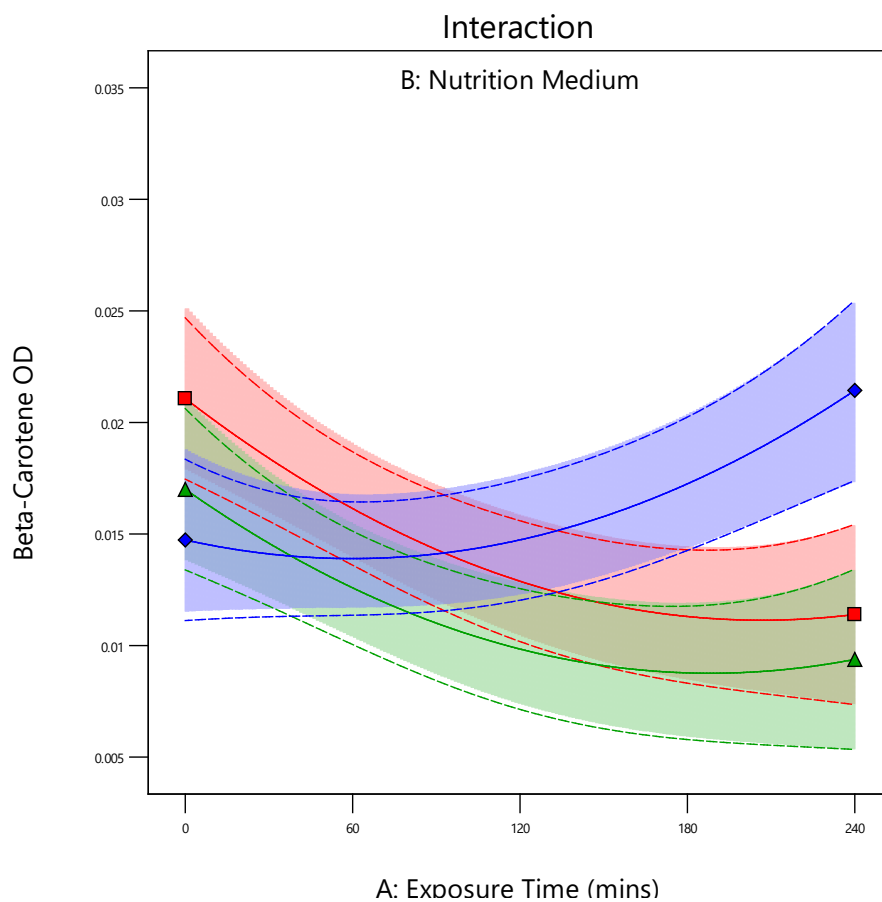


Figure 59. Interactions between factors for Beta-Carotene concentration analysis on Day 14.

Table 48. ANOVA for Beta-Carotene Concentration on Day 17.

Source	Sum of Squares	DoF	Mean Square	F-value	p-value
Block	0.0002	1	0.0002		
Model	0.0020	8	0.0002	17.98	< 0.0001
A-Exposure Time	0.0007	1	0.0007	48.24	< 0.0001
B-Nutrition Medium	0.0007	2	0.0003	23.75	< 0.0001
AB	0.0003	2	0.0002	11.00	< 0.0001
A ²	0.0002	1	0.0002	14.19	0.0004
A ² B	0.0002	2	0.0001	5.94	0.0043
Residual	0.0009	62	0.0000		
Lack of Fit	0.0008	14	0.0001	149.20	< 0.0001
Pure Error	0.0000	48	4.028E-07		
Cor Total	0.0031	71			

Factor Coding: Actual
Response: R1
 -----95% CI Bands

- B1 BBM
- ▲ B2 BBM + 100g
- ◆ B3 MilliQ + 100g

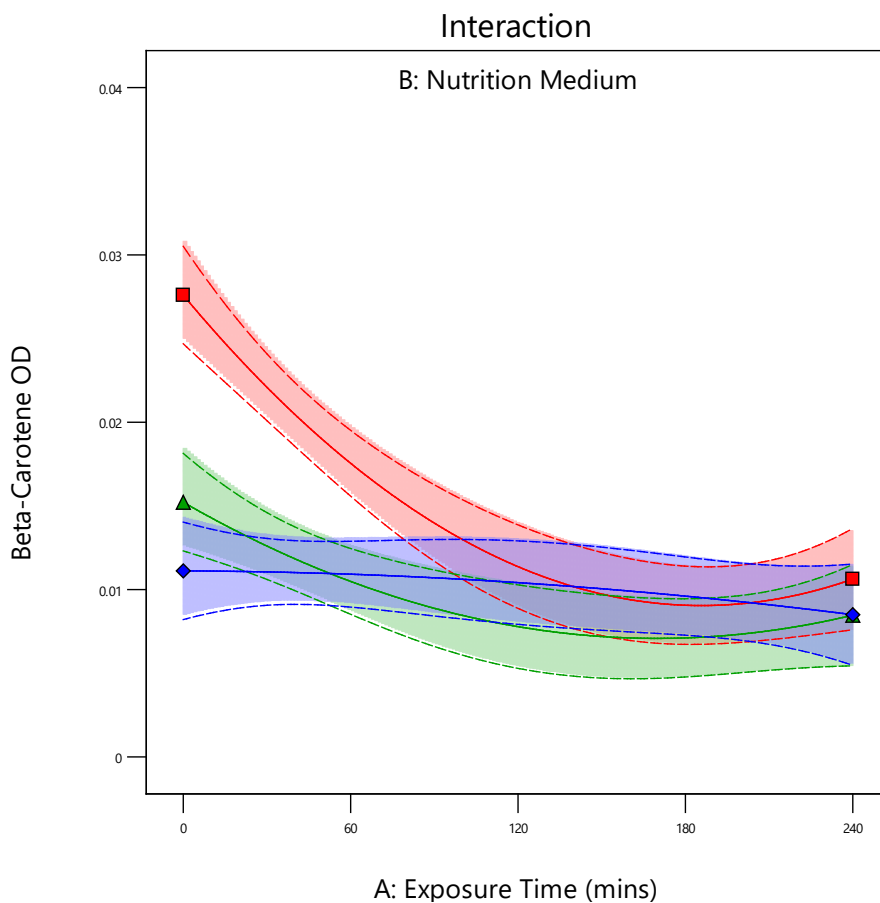


Figure 60. Interactions between factors for Beta-Carotene concentration analysis on Day 17.

Table 49. ANOVA for Beta-Carotene Concentration on Day 21.

Source	Sum of Squares	DoF	Mean Square	F-value	p-value
Block	0.0001	1	0.0001		
Model	0.0012	5	0.0002	16.93	< 0.0001
A-Exposure Time	0.0009	1	0.0009	65.99	< 0.0001
B-Nutrition Medium	0.0001	2	0.0001	3.79	0.0279
AB	0.0002	2	0.0001	5.53	0.0060
Residual	0.0009	65	0.0000		
Lack of Fit	0.0009	17	0.0001	168.32	< 0.0001
Pure Error	0.0000	48	3.194E-07		
Cor Total	0.0022	71			

Factor Coding: Actual
Response: R1
 -----95% CI Bands

- B1 BBM
- ▲ B2 BBM + 100g
- ◆ B3 MilliQ + 100g

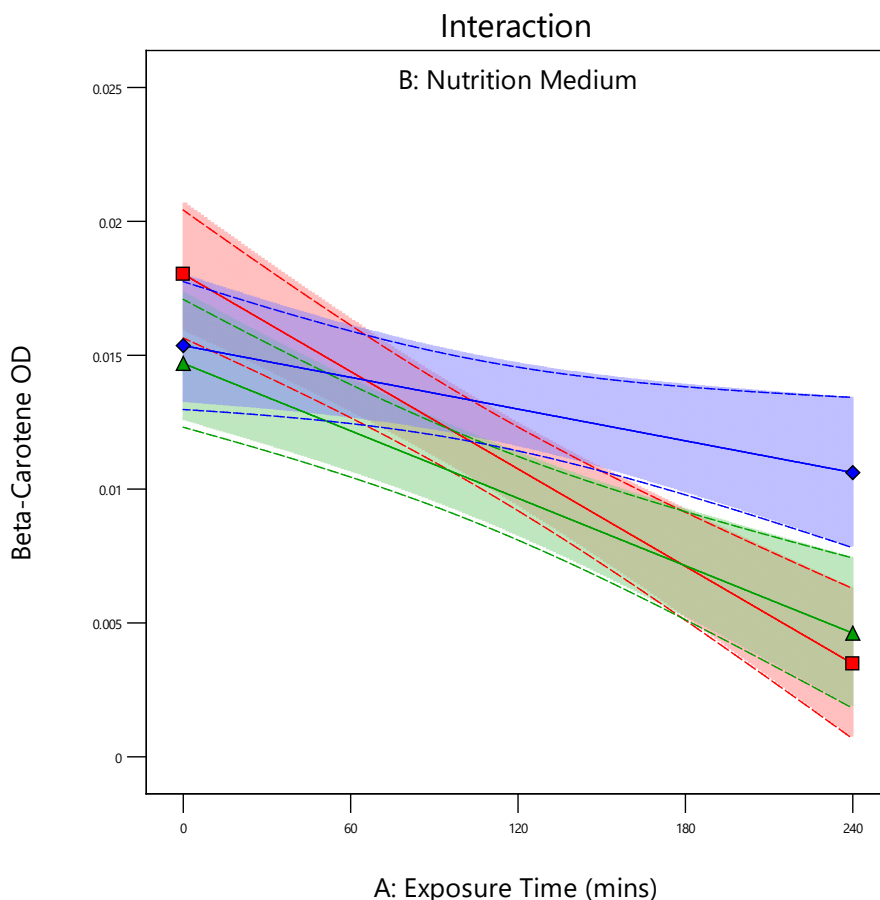


Figure 61. Interactions between factors for Beta-Carotene concentration analysis on Day 21.

In investigation of ANOVA results on Day 3 which are shown in

Table 44, there does not appear to be any significant factors affecting Beta-Carotene concentration. This indicates that for different exposure times, under different mediums, and for both blocks, the beta-carotene measured concentrations would still not be affected. Such a conclusion is expected in the initial days of the experiment. However, when starting to investigate ANOVA for Day 7 shown in Table 45 the nutrition medium started becoming a significant factor. This is logically expected, as the microalgae is growing and producing beta-carotene, it needs to extract nutrients from the medium. Based on the fitted model described by the graph in Figure 57, BBM medium is superior in terms of beta-carotene concentration measured for exposures upward of 120 minutes. Below 120 minutes exposure time, other nutrition mediums seem to be able to do as well in terms of pigment concentration based on the fitted model. In Day 10 ANOVA results in Table 46 show that the nutrient medium is still a significant factor, although it is noticed that the p-value for this factor is increasing.

A linear interaction between the nutrient medium and exposure time factors starts happening at Day 14, as supported by the values in the ANOVA shown in Table 47, despite having only the nutrient medium as a significant factor. This means that changing exposure times will not affect the beta carotene concentration if the medium was constant. Changing the medium itself would contribute to different yields of beta-carotene concentration. Different exposure times with different mediums would affect the beta-carotene concentration. Now, due to the proximity of the different exposure curves for beta-carotene concentration drawn from our measurements earlier in the results section, we can identify that these significance results hold true, as this close proximity resembles similar values of beta-carotene concentrations for the

different exposure times. Nonetheless, following Figure 59 for the fitted model at Day 14, it seems that the MilliQ medium at highest exposure time of 240 minutes, or no exposure with BBM medium would produce highest Beta-Carotene content.

Exceedingly high significance of the main factors, linear interactions, and higher power interactions in beta-carotene concentration is found to happen at Day 17 according to ANOVA in Table 48. Which is expected during a more advanced phase in the timeline of the growth of the microalgae. Figure 60 shows that the BBM resembles the best medium for growth for exposure times up to 60 minutes. Main factors are still significant in Day 21 ANOVA shown in Table 49, with linear interaction significant as well. However, according to the fitted model curve, all mediums tend to contribute to a similar amount of beta-carotene concentration, yet it seems that beyond the 60 minutes exposure time, the MilliQ augmented with 100 grams of lunar regolith medium will provide for higher beta-carotene concentrations than other mediums despite the resulting beta-carotene eventually having a lower concentration than pigment produced with no exposure.

Global ANOVA Model

The following section displays a global model of all factors including cultivation day. Although cultivation day is not a randomized factor. However, this approach shows the beta-carotene and protein concentration change over the cultivation period. Tables provided only show highly significant terms as provided by the ANOVA.

Table 50. ANOVA for Beta-Carotene Concentration in Global Model.

Source	Sum of Squares	DoF	Mean Square	F-value	p-value
Block	0.6857	1	0.6857		
Model	9.96	52	0.1915	4.52	< 0.0001
A-Cultivation Day	3.02	1	3.02	71.24	< 0.0001
B-exposure	0.4446	1	0.4446	10.48	0.0013
C-medium	0.5308	2	0.2654	6.26	0.0022
AB	0.2165	1	0.2165	5.11	0.0246
AC	0.5262	2	0.2631	6.20	0.0023
A ²	1.30	1	1.30	30.57	< 0.0001
A ³ C	0.4783	2	0.2392	5.64	0.0039
A ⁴	0.5040	1	0.5040	11.89	0.0006
A ⁴ C	0.8345	2	0.4173	9.84	< 0.0001
Residual	12.98	306	0.0424		
Lack of Fit	12.86	66	0.1949	403.19	< 0.0001
Pure Error	0.1160	240	0.0005		
Cor Total	23.62	359			

Table 51. Fit Summary Statistics of Global Beta-Carotene Concentration Model.

Statistic	Value	Statistic	Value
Std. Dev.	0.2059	R ²	0.4342
Mean	-1.78	Adjusted R ²	0.3380
C.V. %	11.55	Predicted R ²	0.2124
		Adeq Precision	10.3582

Factor Coding: Actual

Response: BetaC

0.002 0.053

Actual Factor:

C = BBM

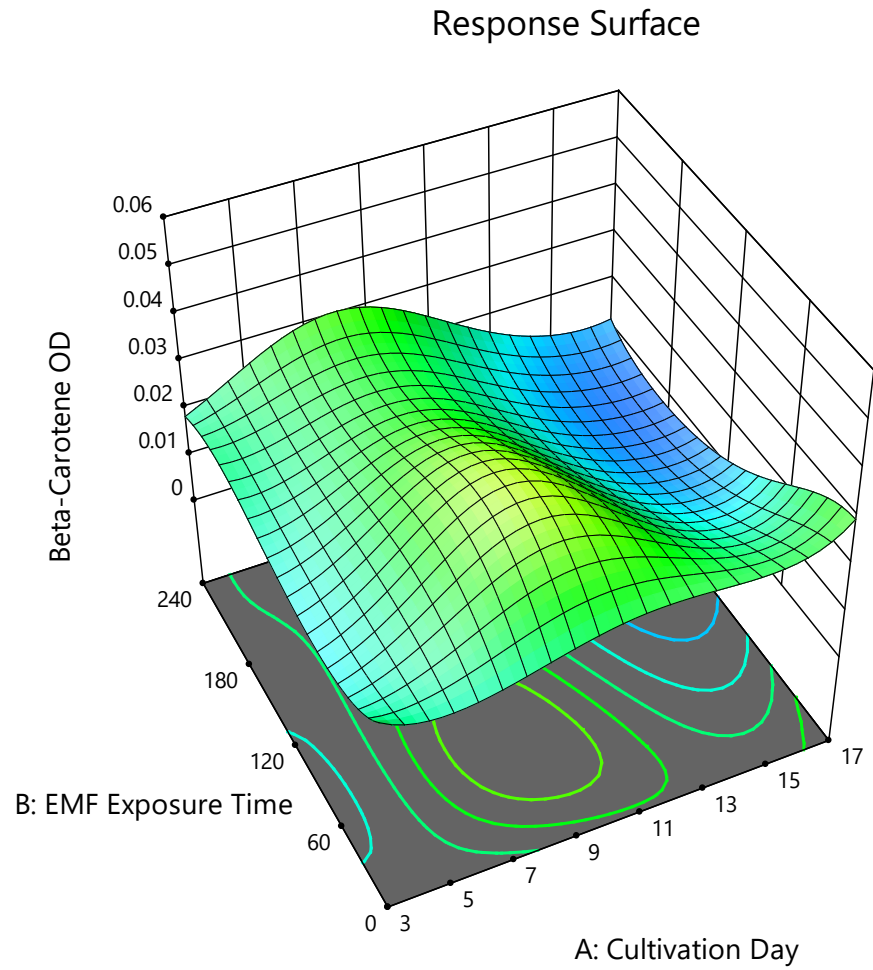


Figure 62. Global Model Response Surface for Beta-Carotene Concentration in BBM Medium.

Factor Coding: Actual

Response: BetaC

0.002 0.053

Actual Factor:

C = BBM + 100g

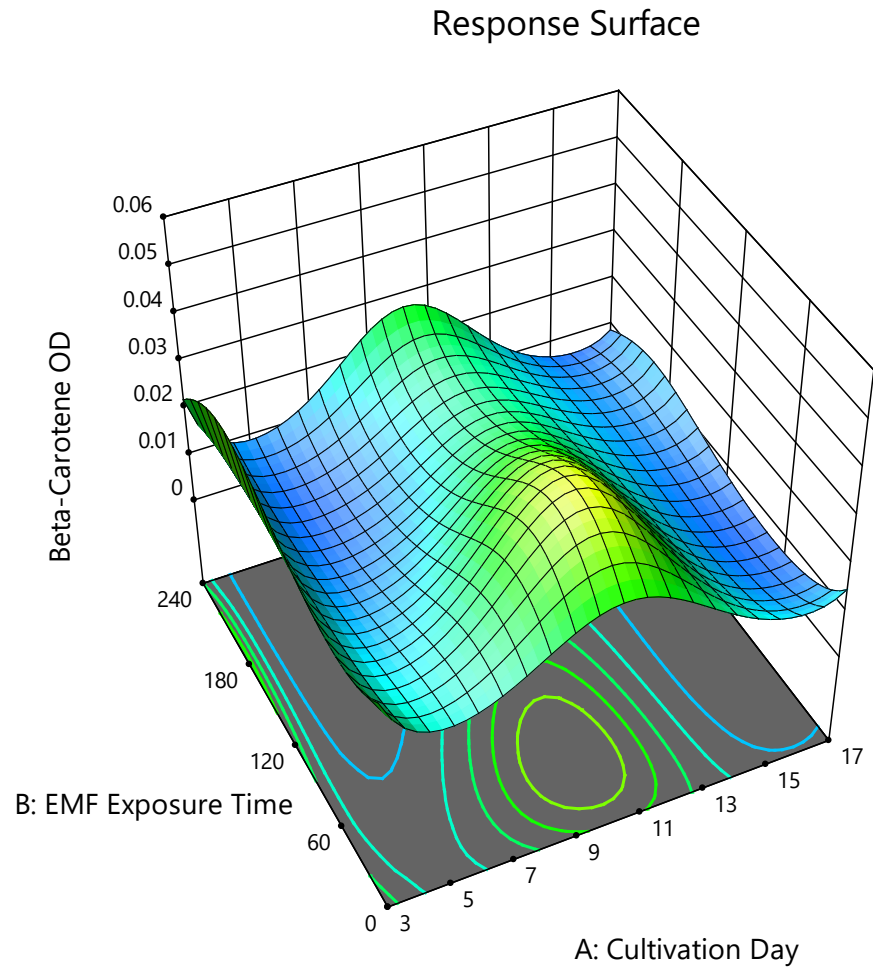


Figure 63. Global Model Response Surface for Beta-Carotene Concentration in BBM + 100g Medium.

Factor Coding: Actual

Response: BetaC

0.002 0.053

Actual Factor:

C = MilliQ + 100g

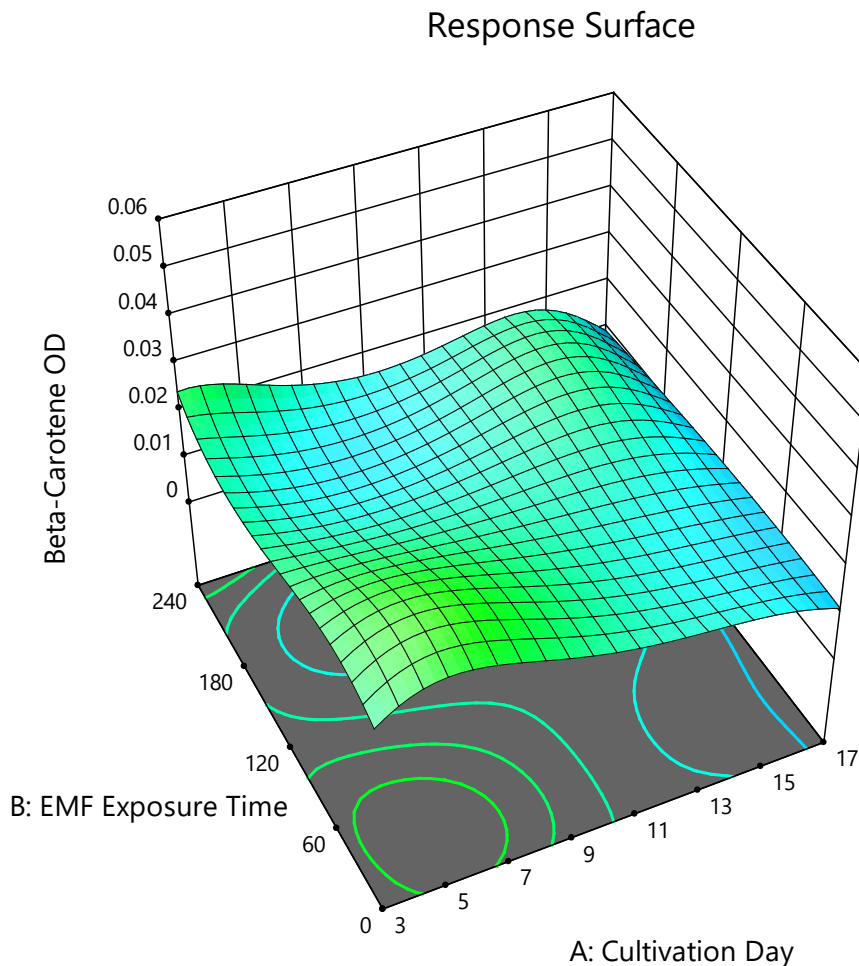


Figure 64. Global Model Response Surface for Beta-Carotene Concentration in MilliQ + 100g Medium.

Assessing the ANOVA of the global model for Beta-Carotene as provided by Table 50, it is very clear that the cultivation day resembles the most significant factor, with the caveat that we are violating DOE rules of randomization. This significance follows along with how the beta-carotene concentration is correlated with the phase of growth of the microalgae, and how at different days, the concentration fluctuates based on the interaction between this factor of cultivation day, and other factors of nutrition medium, and exposure time, resembling the role

and effect of either of these factors at different phases. This could be noticed by following the response surfaces shown in Figure 62, Figure 63, and Figure 64.

Along the cultivation day axis of all these surfaces, there always exists a fluctuation pattern that extends over all the surface despite the exposure time and nutrition medium. In all mediums, the concentration tends to peak, or dip around day 9, regardless of exposure time. If one is to follow the surface along the exposure time axis, there would still be a continuous maxima for the case of BBM in Figure 62 and BBM + 100g in Figure 63 and minima for the case of MilliQ + 100g in Figure 64 around day 9.

The fit summary statistics for the Beta-Carotene global model in Table 51 provide us with an insight on model adequacy for the Beta-Carotene global model. Per calculated values, the resulting R^2 statistic is low, which points towards the large effect of the error term relative to the total sum of squares. Hence, the considerable value of the error compared to the block and model terms. Similarly, for adjusted R^2 the value tends to be even lower, and not in equivalence with the R^2 statistic, this is due to the large degrees of freedom resembling the residual error term compared to a single degree of freedom for block and 52 degrees of freedom for the model. The predicted R^2 term is lowest and would resemble an unreliable model to predict future points. In summary, these results indicate promise for the model to explore data trends and the initial nature of effects of the nutrition medium and magnetic field on microalgae, but one that suggests further work is required. Nonetheless, the adequate precision statistic is higher than four, indicating adequate responses of the concentration values relative to the measurement noise present.

Table 52. ANOVA for Protein Concentration in Global Model.

Source	Sum of Squares	DoF	Mean Square	F-value	p-value
Block	0.0005	1	0.0005		
Model	0.8365	52	0.0161	2.74	< 0.0001
A-Cultivation Day	0.0868	1	0.0868	14.79	0.0001
B-exposure	0.0082	1	0.0082	1.40	0.2382
C-medium	0.0664	2	0.0332	5.66	0.0038
A ²	0.1710	1	0.1710	29.15	< 0.0001
A ² B ²	0.0287	1	0.0287	4.90	0.0277
A ³ C	0.0943	2	0.0471	8.04	0.0004
A ² B ³	0.0579	1	0.0579	9.86	0.0019
AB ³ C	0.0523	2	0.0262	4.46	0.0123
Residual	1.79	306	0.0059		
Lack of Fit	1.38	66	0.0209	12.05	< 0.0001
Pure Error	0.4161	240	0.0017		
Cor Total	2.63	359			

Table 53. Fit Summary Statistics of Global Protein Concentration Model.

Statistic	Value	Statistic	Value
Std. Dev.	0.0766	R ²	0.3179
Mean	-0.3158	Adjusted R ²	0.2020
C.V. %	24.25	Predicted R ²	0.0603
		Adeq Precision	10.5731

Factor Coding: Actual

Response: Protein

0.25 1.04

Actual Factor:

C = BBM

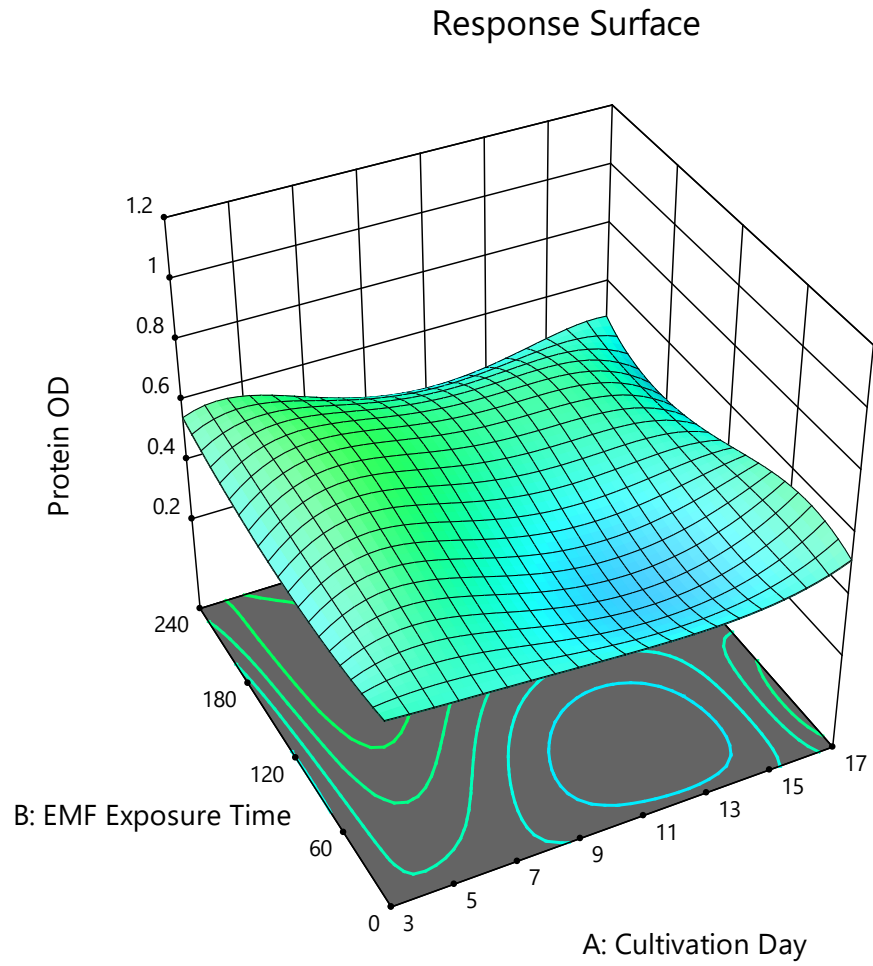


Figure 65. Global Model Response Surface for Protein Concentration in BBM Medium.

Factor Coding: Actual

Response: Protein

0.25 1.04

Actual Factor:

C = BBM + 100g

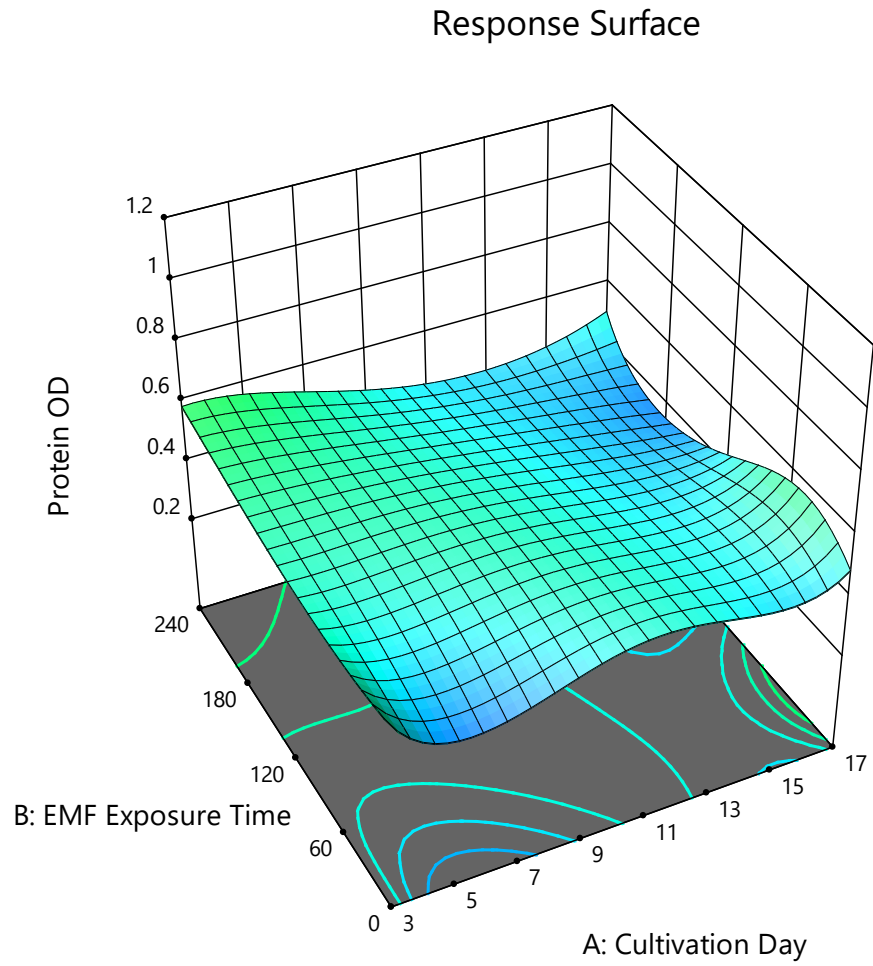


Figure 66. Global Model Response Surface for Protein Concentration in BBM + 100g Medium.

Factor Coding: Actual

Response: Protein

0.25 1.04

Actual Factor:

C = MilliQ + 100g

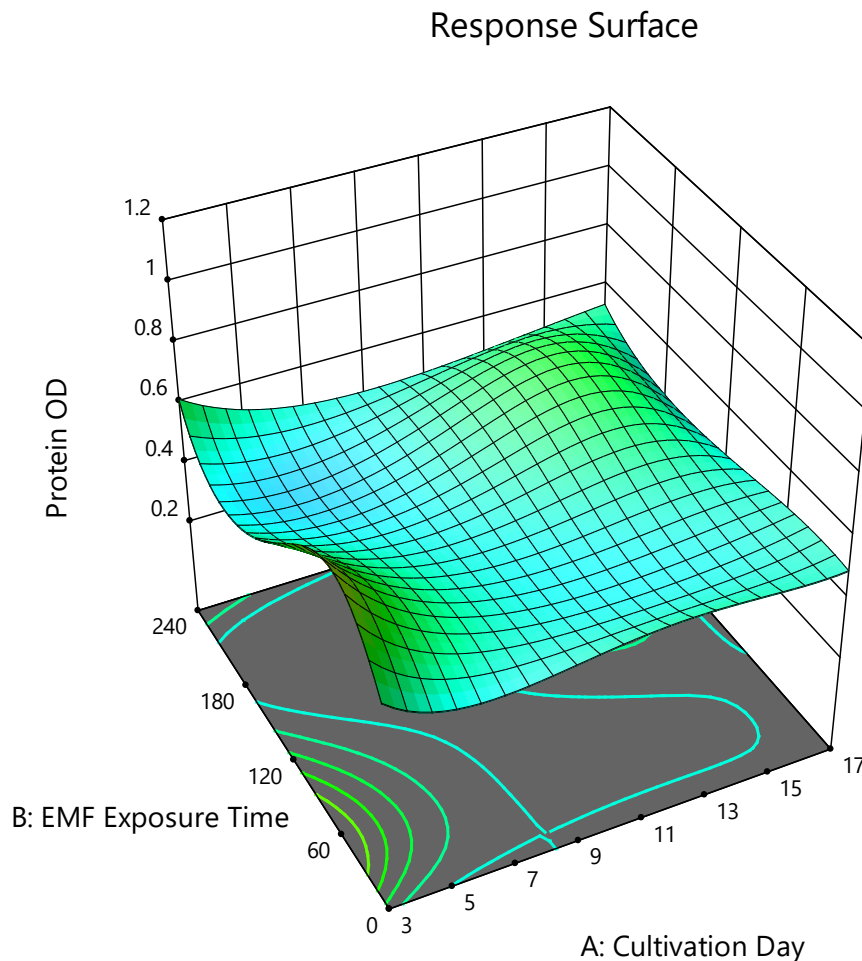


Figure 67. Global Model Response Surface for Protein Concentration in MilliQ + 100g Medium.

Similar to what is seen in ANOVA for Beta-Carotene, similar significance can be seen in the ANOVA of protein shown in Table 52, where the cultivation day factor has the highest significance. However, exposure time by itself is not significant as a main effect compared to how it is in the case of Beta-Carotene, and despite being highly significant in many higher order interaction terms.

Response surfaces shown in Figure 65, Figure 66, and Figure 67 possess close characteristics to the surfaces shown for the beta-carotene model. This infers the same

correlation between protein concentration and the growth phase of microalgae. Moreover, the concentration still fluctuates depending on the interactions with the other factors of nutrition medium and exposure time. However, in the case of protein, there are differences between different mediums for which days the concentration peaks or dips. For BBM the concentration peaks between day 7 to day 11, where it peaks between day 9 to day 13 in the case of BBM + 100g, and dips between day 7 to 13 in the case of MilliQ + 100g.

The global protein concentration model does not represent the actual system in the best way according to its fit summary statistics, shown in Table 53. The calculated R^2 value is low, and according to this value, the error term makes up around 70% of the total sum of squares of the system. Additionally, the adjusted R^2 is lower, similar to what is seen in the Beta-Carotene global model, as the degrees of freedom are heavily weighted towards the residuals in comparison to the block and total sum of squares. This model is also not predictive of any points, as the predicted R^2 value is extremely low being close to zero. The adequate precision however is higher than four, which allows us to navigate the design space, and identifies the current model to be a valid representation of actual responses rather than overpowered with noise.

CHAPTER V

CONCLUSIONS AND FUTURE WORK

The aim of this research was to investigate the effects introduced by the lunar environment on biological entities such as the *Chlorella vulgaris* microalgae, for the purpose of understanding the capabilities of such an environment in supporting life.

Factors of lunar regolith as a nutrient medium and its small magnetic field are selected as representatives of the lunar environment. After performing the experiments in multiple blocks, it could definitely be noticed the discrepancy in some of measured elements between both blocks, indicating an inconsistent result from varying both factors. However, these factors were still of effect on the microalgae.

Investigating the graphs resulting from data measured in the lab showed that the presence of the microalgae in an EMF similar to that of the moon can result in both enhancing and stressing effects, yet the mechanism for determining which is which is still ambiguous. ANOVA on protein, and beta-carotene showed the existence of factor interactions between EMF exposure time, and nutrient medium, which could explain the variability in response. However, this might not be accurate as accompanying regression models were not of high fit. Moreover, it was obvious that the presence of the lunar regolith by itself as a nutrient medium does not have the capability to provide nutrients to the microalgae. In some measurements, pigments and bioactive compounds seemed to thrive in the medium with MilliQ water and lunar regolith only. Peculiarly, the presence of the regolith augmented to another nutrient medium such as BBM provided for enhancements of growth in microalgae samples from some exposure periods.

Overall, this work proved that both factors do indeed produce effects, and it showed the extent of these effects through the reported results of optical density of growth, beta-carotene, and protein concentration.

In terms of future work, higher granularity in measurement days should be attempted, which would provide for smoother curves and consideration of any intermediate changes. Also, further investigations with the microscope are suggested to identify physical changes occurring on the micro level, which would help in determining the nature of responses obtained. Moreover, the initial experimental culture of microalgae should not only be selected based on the optical density of growth, but rather the actual cellular growth state by inspecting the cells again under the microscope. Additionally, multiple rounds of protein extraction with Sodium Hydroxide (NaOH) should be repeated for the same biomass to release all protein present to the supernatant. Similarly, multiple rounds of Beta-Carotene extraction should be repeated with Potassium Hydroxide (KOH) and with Hexane.

For this research, the use of the design of experiment approach does not constitute the best tool for statistically analyzing the results due to the presence of the factor of cultivation time, which cannot be randomized. Therefore, a different statistical tool should be chosen. An extra block was intended to be done for this research; however, running out of Bradford assay deemed this attempt unreachable within the time limit for submitting my work.

Repeating this research with better laboratory equipment is recommended. Measuring the Beta-carotene optical density with the Unico spectrophotometer lacked the precision required to provide more sensitive readings for some samples. Additionally, another

spectrophotometer should be used to measure the protein concentration than the NanoDrop One, as it is deemed to not be fully accurate at some concentrations by the scientific community.

In conclusion, this work needs to be augmented with a multitude of additional experiments to be able to accurately determine the exact effects on protein and beta-carotene, including an additional block of the same nature of the ones done in this experiment. It can show that very high protein and beta-carotene concentrations could still exist with the presence of an EMF and lunar regolith in the medium. However, a different experimental design using better laboratory equipment could cater for results of better statistical significance.

REFERENCES

- [1] "Artemis - NASA." Accessed: Apr. 06, 2024. [Online]. Available: <https://www.nasa.gov/feature/artemis/>
- [2] M. Ragan, "On the delineation and higher-level classification of algae," *Eur. J. Phycol.*, vol. 33, no. 1, pp. 1–15, Feb. 1998, doi: 10.1080/09670269810001736483.
- [3] K. Heimann and R. Huerlimann, "Chapter 3 - Microalgal Classification: Major Classes and Genera of Commercial Microalgal Species," in *Handbook of Marine Microalgae*, S.-K. Kim, Ed., Boston: Academic Press, 2015, pp. 25–41. doi: 10.1016/B978-0-12-800776-1.00003-0.
- [4] G. W. Maneveldt and D. W. Keats, "Chromista," in *eLS*, 1st ed., John Wiley & Sons, Ltd, Ed., Wiley, 2003. doi: 10.1038/npg.els.0001960.
- [5] S. Hemaiswarya, R. Raja, R. Ravikumar, and I. Carvalho, "Microalgae taxonomy and breeding," *Biofuel Crops Prod. Physiol. Genet.*, pp. 44–53, Jun. 2013.
- [6] A. Richmond and Q. Hu, Eds., *Handbook of microalgal culture: applied phycology and Biotechnology*, Second edition. Chichester, West Sussex, UK: John Wiley & Sons, Ltd, 2013.
- [7] M. W. Beyerinck, *Culturversuche mit Zoochlorellen, Lichenengonidien und anderen niederen Algen*. 1890.
- [8] C. Safi, B. Zebib, O. Merah, P.-Y. Pontalier, and C. Vaca-Garcia, "Morphology, composition, production, processing and applications of *Chlorella vulgaris*: A review," *Renew. Sustain. Energy Rev.*, vol. 35, pp. 265–278, Jul. 2014, doi: 10.1016/j.rser.2014.04.007.
- [9] I. T. K. Ru, Y. Y. Sung, M. Jusoh, M. E. A. Wahid, and T. Nagappan, "Chlorella vulgaris: a perspective on its potential for combining high biomass with high value bioproducts," *Appl. Phycol.*, vol. 1, no. 1, pp. 2–11, Dec. 2020, doi: 10.1080/26388081.2020.1715256.
- [10] J. A. Coronado-Reyes, J. A. Salazar-Torres, B. Juárez-Campos, and J. C. González-Hernández, "*Chlorella vulgaris*, a microalgae important to be used in Biotechnology: a review," *Food Sci. Technol.*, vol. 42, p. e37320, Nov. 2020, doi: 10.1590/fst.37320.
- [11] G. Detrell, "Chlorella Vulgaris Photobioreactor for Oxygen and Food Production on a Moon Base—Potential and Challenges," *Front. Astron. Space Sci.*, vol. 8, 2021, Accessed: Apr. 30, 2023. [Online]. Available: <https://www.frontiersin.org/articles/10.3389/fspas.2021.700579>
- [12] T. Niederwieser, P. Kociolek, and D. Klaus, "A review of algal research in space," *Acta Astronaut.*, vol. 146, pp. 359–367, May 2018, doi: 10.1016/j.actaastro.2018.03.026.
- [13] N. M. Sisakyan, O. G. Gazenko, and V. V. Antipov, "Satellite biological experiments--major results and problems," *Life Sci. Space Res.*, vol. 3, pp. 185–205, 1965.
- [14] É. N. Vaulina, I. D. Anikeeva, I. G. Gubareva, and G. A. Shtraukh, "Influence of Space-Flight Factors aboard 'Zond' Automatic Stations on Survival and Mutability of *Chlorella* Cells," *Cosm. Res.*, vol. 9, p. 865, Nov. 1971.

- [15] E. N. Vaulina and E. V. Moskvitin, "[Experiment with Chlorella on 'Zond'-8 automatic station]," *Kosm. Biol. Aviakosm. Med.*, vol. 9, no. 3, pp. 81–82, 1975.
- [16] I. D. Anikeeva and É. N. Vaulina, "Influence of Space-Flight Factors aboard Soyuz-5 Satellite on Chlorella Cells," *Cosm. Res.*, vol. 9, p. 870, Nov. 1971.
- [17] T. B. Galkina and G. I. Meleshko, "Investigation of the physiological activity of chlorella after exposure to spaceflight factors aboard the 'Salyut' orbital station," *Kosm. Biol. Aviakosm. Med.*, vol. 9, pp. 25–30, 1975.
- [18] E. V. Moskvitin and E. N. Vaulina, "[Experiment with a physiologically active culture of Chlorella on 'Soiuz-9' spacecraft]," *Kosm. Biol. Aviakosm. Med.*, vol. 9, no. 3, pp. 7–10, 1975.
- [19] E. V. Moskvitin and E. N. Vaulina, "EFFECT OF DYNAMIC FACTORS OF SPACE FLIGHTS ON THE GREEN ALGA *Chlorella vulgaris*," in *Life Sciences and Space Research*, P. H. A. Sneath, Ed., Pergamon, 1974, pp. 113–118. doi: 10.1016/B978-0-08-021783-3.50019-2.
- [20] G. Detrell *et al.*, "PBR@LSR: the Algae-based Photobioreactor Experiment at the ISS – Operations and Results," Jul. 2020, Accessed: Oct. 12, 2023. [Online]. Available: <https://ttu-ir.tdl.org/handle/2346/86331>
- [21] J. Myers, "Use of algae for support of the human in space," *Life Sci. Space Res.*, vol. 2, pp. 323–336, 1964.
- [22] M. Yamamoto, M. Fujishita, A. Hirata, and S. Kawano, "Regeneration and maturation of daughter cell walls in the autospore-forming green alga *Chlorella vulgaris* (Chlorophyta, Trebouxiophyceae)," *J. Plant Res.*, vol. 117, no. 4, pp. 257–264, Aug. 2004, doi: 10.1007/s10265-004-0154-6.
- [23] A. M. Illman, A. H. Scragg, and S. W. Shales, "Increase in *Chlorella* strains calorific values when grown in low nitrogen medium," *Enzyme Microb. Technol.*, vol. 27, no. 8, pp. 631–635, Nov. 2000, doi: 10.1016/S0141-0229(00)00266-0.
- [24] M. Yamamoto, I. Kurihara, and S. Kawano, "Late type of daughter cell wall synthesis in one of the Chlorellaceae, *Parachlorella kessleri* (Chlorophyta, Trebouxiophyceae)," *Planta*, vol. 221, no. 6, pp. 766–775, Aug. 2005, doi: 10.1007/s00425-005-1486-8.
- [25] I. Maruyama, T. Nakao, I. Shigeno, Y. Ando, and K. Hirayama, "Application of unicellular algae *Chlorella vulgaris* for the mass-culture of marine rotifer *Brachionus*," *Hydrobiologia*, vol. 358, no. 1/3, pp. 133–138, 1997, doi: 10.1023/A:1003116003184.
- [26] J. Masojídek, K. Ranglová, G. E. Lakatos, A. M. Silva Benavides, and G. Torzillo, "Variables Governing Photosynthesis and Growth in Microalgae Mass Cultures," *Processes*, vol. 9, no. 5, Art. no. 5, May 2021, doi: 10.3390/pr9050820.
- [27] G. Markou, D. Vandamme, and K. Muylaert, "Microalgal and cyanobacterial cultivation: The supply of nutrients," *Water Res.*, vol. 65, pp. 186–202, Nov. 2014, doi: 10.1016/j.watres.2014.07.025.
- [28] J. Masojídek, G. Torzillo, and M. Koblížek, "Photosynthesis in Microalgae," in *Handbook of Microalgal Culture*, 1st ed., A. Richmond and Q. Hu, Eds., Wiley, 2013, pp. 21–36. doi: 10.1002/9781118567166.ch2.

- [29] “8.2 The Light-Dependent Reactions of Photosynthesis - Biology | OpenStax.” Accessed: Oct. 22, 2023. [Online]. Available: <https://openstax.org/books/biology/pages/8-2-the-light-dependent-reactions-of-photosynthesis>
- [30] Daisy Dobrijevic, “Earth’s magnetic field: Explained,” Space.com. Accessed: Apr. 07, 2024. [Online]. Available: <https://www.space.com/earths-magnetic-field-explained>
- [31] “Earth’s Magnetic Field: Origin, Structure, and Impact on Humanity,” Earth.com. Accessed: Apr. 07, 2024. [Online]. Available: <https://www.earth.com/earthpedia-articles/earths-magnetic-field-origin-structure-and-impact-on-humanity/>
- [32] “An Overview of the Earth’s Magnetic Field.” Accessed: Apr. 07, 2024. [Online]. Available: <https://geomag.bgs.ac.uk/education/earthmag.html>
- [33] X. Luo, H. Zhang, and J. Zhang, “The influence of a static magnetic field on a *Chlorella vulgaris* - *Bacillus licheniformis* consortium and its sewage treatment effect,” *J. Environ. Manage.*, vol. 295, p. 112969, Oct. 2021, doi: 10.1016/j.jenvman.2021.112969.
- [34] X. Luo, H. Zhang, Q. Li, and J. Zhang, “Effects of static magnetic field on *Chlorella vulgaris*: growth and extracellular polysaccharide (EPS) production,” *J. Appl. Phycol.*, vol. 32, no. 5, pp. 2819–2828, Oct. 2020, doi: 10.1007/s10811-020-02164-7.
- [35] J. R. Newman and R. C. Watson, “Preliminary observations on the control of algal growth by magnetic treatment of water,” in *Biology, Ecology and Management of Aquatic Plants*, J. Caffrey, P. R. F. Barrett, M. T. Ferreira, I. S. Moreira, K. J. Murphy, and P. M. Wade, Eds., in *Developments in Hydrobiology*. Dordrecht: Springer Netherlands, 1999, pp. 319–322. doi: 10.1007/978-94-017-0922-4_47.
- [36] K. M. Deamici *et al.*, “Microalgae Cultivated under Magnetic Field Action: Insights of an Environmentally Sustainable Approach,” *Sustainability*, vol. 14, no. 20, Art. no. 20, Jan. 2022, doi: 10.3390/su142013291.
- [37] C. Verseux, M. Baqué, K. Lehto, J.-P. P. de Vera, L. J. Rothschild, and D. Billi, “Sustainable life support on Mars – the potential roles of cyanobacteria,” *Int. J. Astrobiol.*, vol. 15, no. 1, pp. 65–92, Jan. 2016, doi: 10.1017/S147355041500021X.
- [38] M. Baqué, C. Verseux, U. Böttger, E. Rabbow, J.-P. P. de Vera, and D. Billi, “Preservation of Biomarkers from Cyanobacteria Mixed with Mars-Like Regolith Under Simulated Martian Atmosphere and UV Flux,” *Orig. Life Evol. Biospheres*, vol. 46, no. 2, pp. 289–310, Jun. 2016, doi: 10.1007/s11084-015-9467-9.
- [39] D. W. Ming and D. L. Henninger, “Use of lunar regolith as a substrate for plant growth,” *Adv. Space Res.*, vol. 14, no. 11, pp. 435–443, Nov. 1994, doi: 10.1016/0273-1177(94)90333-6.
- [40] A. Ellery, “Supplementing Closed Ecological Life Support Systems with In-Situ Resources on the Moon,” *Life*, vol. 11, no. 8, Art. no. 8, Aug. 2021, doi: 10.3390/life11080770.
- [41] F. B. Salisbury, “Chapter 5 Growing Crops for Space Explorers on the Moon, Mars, or in Space,” in *Advances in Space Biology and Medicine*, vol. 7, S. L. Bontinc, Ed., Elsevier, 1999, pp. 131–162. doi: 10.1016/S1569-2574(08)60009-X.

- [42] A.-L. Paul, S. M. Elardo, and R. Ferl, "Plants grown in Apollo lunar regolith present stress-associated transcriptomes that inform prospects for lunar exploration," *Commun. Biol.*, vol. 5, no. 1, pp. 1–9, May 2022, doi: 10.1038/s42003-022-03334-8.
- [43] L. G. Duri *et al.*, "The Potential for Lunar and Martian Regolith Simulants to Sustain Plant Growth: A Multidisciplinary Overview," *Front. Astron. Space Sci.*, vol. 8, 2022, Accessed: May 09, 2023. [Online]. Available: <https://www.frontiersin.org/articles/10.3389/fspas.2021.747821>
- [44] G. W. W. Wamelink, J. Y. Frissel, W. H. J. Krijnen, M. R. Verwoert, and P. W. Goedhart, "Can Plants Grow on Mars and the Moon: A Growth Experiment on Mars and Moon Soil Simulants," *PLoS ONE*, vol. 9, no. 8, p. e103138, Aug. 2014, doi: 10.1371/journal.pone.0103138.
- [45] D. C. Montgomery, *Design and Analysis of Experiments*, Tenth edition. Hoboken, NJ: Wiley, 2020.
- [46] T. A. Aragaw and A. Asmare, "Experimental Identifications of Fresh Water Microalgae Species and Investigating the Media and PH Effect on the Productions of Microalgae," vol. 5, pp. 124–131, Feb. 2017.
- [47] H. W. Bischoff and H. C. Bold, *Some Soil Algae from Enchanted Rock and Related Algal Species*. in Phycological studies, no. IV. University of Texas, 1963. [Online]. Available: <https://books.google.com/books?id=xHHwAAAAMAAJ>
- [48] PhytoTech Labs, "Bold's Basal Medium (BBM)." Accessed: Sep. 11, 2023. [Online]. Available: <https://phytotechlab.com/bold-s-basal-medium-bbm.html>
- [49] PhytoTech Labs, "B1675 Bold's Basal Medium Product Information Sheet." Accessed: Nov. 08, 2023. [Online]. Available: <https://phytotechlab.com/mwdownloads/download/link/id/52>
- [50] R. Serra-Maia, O. Bernard, A. Gonçalves, S. Bensalem, and F. Lopes, "Influence of temperature on *Chlorella vulgaris* growth and mortality rates in a photobioreactor," *Algal Res.*, vol. 18, pp. 352–359, Sep. 2016, doi: 10.1016/j.algal.2016.06.016.
- [51] N. G. Muñoz, O. G. A. Vives, H. C. Sariol, R. M. P. Silva, and A. J. Capote, "Temperature of the mixed culture of *Chlorella vulgaris* to open sky: incidence in biomass concentration," *Tecnol. Quím.*, vol. 39, no. 3, pp. 580–591.
- [52] S. L. Meng *et al.*, "Interaction Effects of Temperature, Light, Nutrients, and pH on Growth and Competition of *Chlorella vulgaris* and *Anabaena* sp. Strain PCC," *Front. Environ. Sci.*, vol. 9, Jul. 2021, doi: 10.3389/fenvs.2021.690191.
- [53] L. M. Cycil *et al.*, "Investigating the Growth of Algae Under Low Atmospheric Pressures for Potential Food and Oxygen Production on Mars," *Front. Microbiol.*, vol. 12, 2021, Accessed: May 01, 2023. [Online]. Available: <https://www.frontiersin.org/articles/10.3389/fmicb.2021.733244>
- [54] N. Rajendran, "Cultivation and Chemical Composition of Microalgae *Chlorella Vulgaris* and its Antibacterial Activity against Human Pathogens Abbreviations," Dec. 2018.
- [55] R. M. Brown, D. A. Larson, and H. C. Bold, "Airborne Algae: Their Abundance and Heterogeneity," *Science*, vol. 143, no. 3606, pp. 583–585, Feb. 1964, doi: 10.1126/science.143.3606.583.
- [56] UNICO, "UNICO 1100 Series Spectrophotometer Service Manual."

- [57] Thermo Fisher Scientific Inc., “NanoDrop One User Guide.” Thermo Fisher Scientific Inc. Accessed: Mar. 17, 2024. [Online]. Available: https://assets.thermofisher.com/TFS-Assets/MSD/manuals/nanodrop-one-c-user-guide-EN_20211102.pdf
- [58] “NanoDrop Spectrophotometer Resources - US.” Accessed: Mar. 17, 2024. [Online]. Available: <https://www.thermofisher.com/us/en/home/industrial/spectroscopy-elemental-isotope-analysis/molecular-spectroscopy/uv-vis-spectrophotometry/instruments/nanodrop/resources.html>
- [59] Micro Magnetics, “Triaxial Helmholtz Coil with Controller System Hardware Manual.”
- [60] M. D’Este, D. De Francisci, and I. Angelidaki, “Novel protocol for lutein extraction from microalga *Chlorella vulgaris*,” *Biochem. Eng. J.*, vol. 127, pp. 175–179, Nov. 2017, doi: 10.1016/j.bej.2017.06.019.
- [61] H. Zheng, J. Yin, Z. Gao, H. Huang, X. Ji, and C. Dou, “Disruption of *Chlorella vulgaris* Cells for the Release of Biodiesel-Producing Lipids: A Comparison of Grinding, Ultrasonication, Bead Milling, Enzymatic Lysis, and Microwaves,” *Appl. Biochem. Biotechnol.*, vol. 164, no. 7, pp. 1215–1224, Aug. 2011, doi: 10.1007/s12010-011-9207-1.
- [62] J. Wang, X. Hu, J. Chen, T. Wang, X. Huang, and G. Chen, “The Extraction of β -Carotene from Microalgae for Testing Their Health Benefits,” *Foods*, vol. 11, no. 4, p. 502, Feb. 2022, doi: 10.3390/foods11040502.
- [63] J. Bazarnova, Y. Smyatskaya, A. Shlykova, A. Balabaev, and S. Đurović, “Obtaining Fat-Soluble Pigments—Carotenoids from the Biomass of *Chlorella* Microalgae,” *Appl. Sci.*, vol. 12, no. 7, Art. no. 7, Jan. 2022, doi: 10.3390/app12073246.
- [64] R. Hajare, A. Ray, Shreya, C. Tharachand, M. N. Avadhani, and C. I. Selvaraj, “Extraction and quantification of antioxidant lutein from various plant sources,” *Int. J. Pharm. Sci. Rev. Res.*, vol. 22, pp. 152–157, Oct. 2013.
- [65] “ β -Carotene synthetic no. = 93 UV, powder 7235-40-7.” Accessed: Mar. 26, 2024. [Online]. Available: <http://www.sigmaaldrich.com/>
- [66] M. M. Bradford, “A rapid and sensitive method for the quantitation of microgram quantities of protein utilizing the principle of protein-dye binding,” *Anal. Biochem.*, vol. 72, pp. 248–254, May 1976, doi: 10.1006/abio.1976.9999.
- [67] A. Andreeva *et al.*, “Production, Purification, and Study of the Amino Acid Composition of Microalgae Proteins,” *Molecules*, vol. 26, no. 9, Art. no. 9, Jan. 2021, doi: 10.3390/molecules26092767.
- [68] C. L. Kielkopf, W. Bauer, and I. L. Urbatsch, “Bradford Assay for Determining Protein Concentration,” *Cold Spring Harb. Protoc.*, vol. 2020, no. 4, p. pdb.prot102269, Apr. 2020, doi: 10.1101/pdb.prot102269.
- [69] “Bradford Assay for Protein.” Accessed: Mar. 26, 2024. [Online]. Available: <https://www.bio.umass.edu/micro/immunology/542igg/bradford.htm>
- [70] Thermo Fisher Scientific, “Pierce™ Bradford Protein Assay Kit User Guide.” Accessed: Mar. 26, 2024. [Online]. Available: https://assets.thermofisher.com/TFS-Assets/LSG/manuals/MAN0011181_Coomassie_Bradford_Protein_Asy_UG.pdf

- [71] "Protein determination by the Bradford method." Accessed: Mar. 26, 2024. [Online]. Available: <https://www.ruf.rice.edu/~bioslabs/methods/protein/bradford.html>
- [72] C. Proteomics, "Protocol for Bradford Protein Assay," Creative Proteomics. Accessed: Mar. 26, 2024. [Online]. Available: <https://www.creative-proteomics.com/resource/protocol-for-bradford-protein-assay.htm>
- [73] "Quantifying proteins using the Bradford method." Accessed: Mar. 26, 2024. [Online]. Available: <http://www.qiagen.com/us/knowledge-and-support/knowledge-hub/bench-guide/protein/protein-analysis/quantifying-proteins-using-the-bradford-method>
- [74] "Quick Start™ Bradford Protein Assay | Bio-Rad." Accessed: Mar. 26, 2024. [Online]. Available: <https://www.bio-rad.com/en-us/product/quick-start-bradford-protein-assay?ID=5ec149ee-0cd1-468b-8651-a2fe9de6944d>
- [75] Bio-Rad, "Quick Start™ Bradford Protein Assay Instruction Manual." Accessed: Mar. 26, 2024. [Online]. Available: <https://www.bio-rad.com/webroot/web/pdf/lsr/literature/4110065A.pdf>
- [76] Bio-Rad, "Quick Start™ Bradford Protein Assay Quick Guide." Accessed: Mar. 26, 2024. [Online]. Available: https://www.bio-rad.com/sites/default/files/webroot/web/pdf/lsr/literature/Bulletin_6835.pdf
- [77] "NanoDrop One/One^c Microvolume UV-Vis Spectrophotometers - US." Accessed: Sep. 01, 2023. [Online]. Available: <https://www.thermofisher.com/us/en/home/industrial/spectroscopy-elemental-isotope-analysis/molecular-spectroscopy/uv-vis-spectrophotometry/instruments/nanodrop/instruments/nanodro-one.html>
- [78] Sigma-Aldrich, "Bradford Reagent," Technical Bulletin B6916. Accessed: Mar. 26, 2024. [Online]. Available: <https://www.sigmaaldrich.com/deepweb/assets/sigmaaldrich/product/documents/165/479/b6916bulms.pdf>

VITA

Jerjes Philip Butros Abedrabbo

Mechanical & Aerospace Engineering Department
Old Dominion University
238 Kaufman Hall, Norfolk, VA, 23529

Jerjes Philip Butros Abedrabbo was born in Jerusalem in 1994. He has always been fascinated with space, especially after his Mom and Dad bought him a CD with an encyclopedia about space, and he carries the dream of becoming the first Astronaut of Palestinian roots. He lived in Jericho, West Bank, Palestine for most of his early years, attending Terra Sancta Elementary School. He later moved to Beit Sahour, West Bank, Palestine with his family. In 2010, he was chosen to participate in the U.S Department of State YES program as a foreign exchange student at North Bend High School, OR, where he spent the next 10 months and fell in love with the USA, graduating eventually with an Honor's. He went back to Palestine and finished his high school education with excellence and passed the country's standardized Tawjihi exam with a result ranking him in the top 10% in his city.

Carrying his dream of becoming an Astronaut, he did his Bachelor of Science in Mechatronics Engineering accompanied by a minor in Computer Science at Birzeit University, Ramallah, graduating in the top 5% in his class. After university, he joined Western Digital Corp. as a Software Engineer, and later joined Lightbits Labs as a Senior Software Engineer. He has upwards of five years of experience as a Software Engineer in embedded, storage, and low-level systems. In 2022, Jerjes was awarded the prestigious Fulbright Scholarship and was selected to pursue his Master of Science degree in Aerospace Engineering at Old Dominion University, VA, where he became the lead Flight Software and Hardware Engineer for the collaborative Old Dominion University – United States Coast Guard Academy CubeSat mission nicknamed SeaLion, supervised by his advisor Dr. Sharana Asundi, developing its embedded systems and flight software. On his path to his desired and destined goal of becoming an Astronaut, Jerjes will be starting his PhD in Aerospace Engineering at the University of Florida on a four-year full funded fellowship in August 2024, where he will be continuing his research in the field of Space and pursuing his enthusiasm for its mysteries.